



Optics III

Intersubband transitions and unipolar optoelectronic devices

Maria Tchernycheva

*Institut d'Electronique Fondamentale,
UMR CNRS 8622, University Paris-Sud XI, Orsay, France*

GaNEx Summer School on the physics and applications of nitrides,
23-28/06/2013, Montpellier, La Grande Motte, France

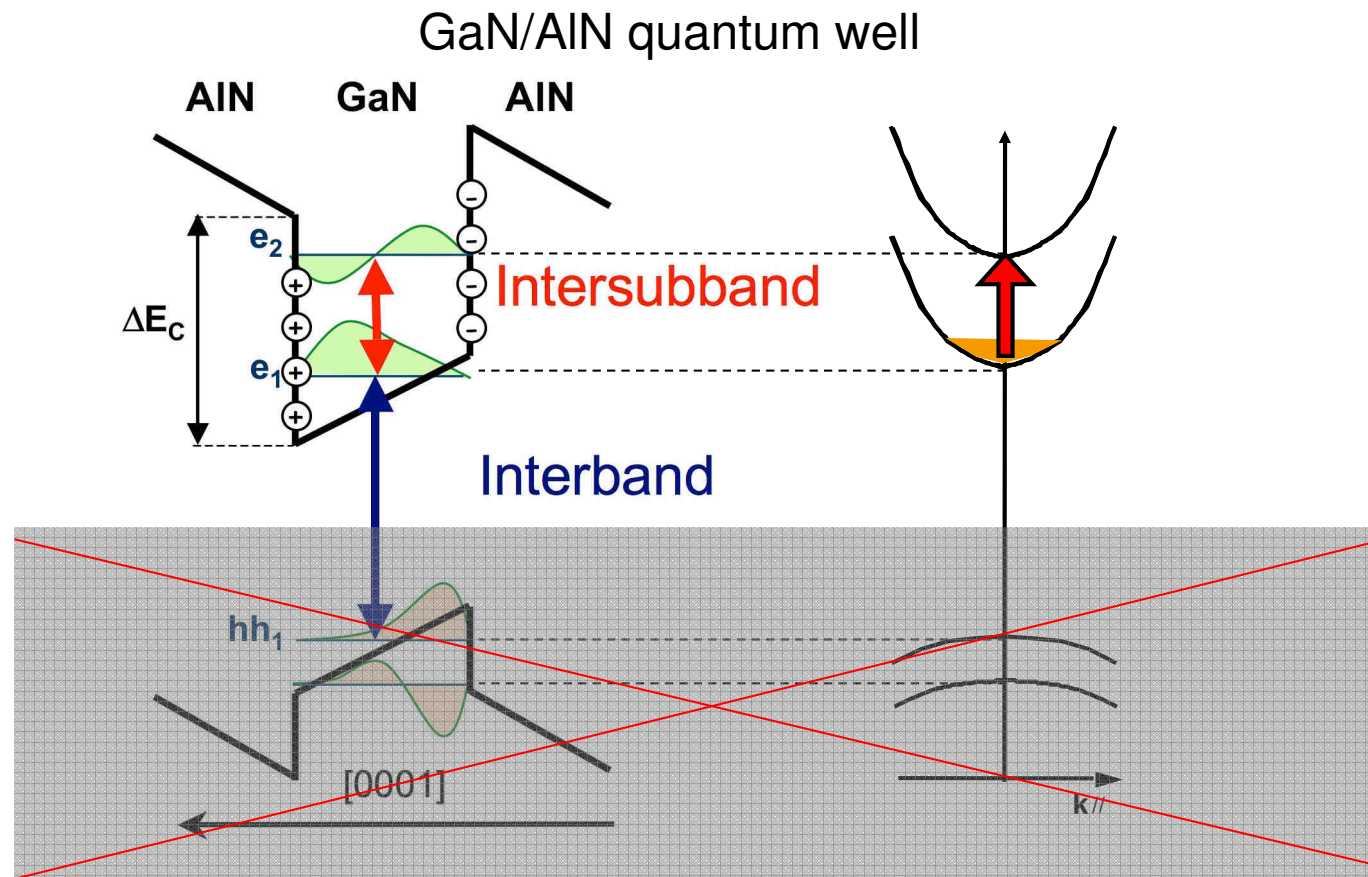


Outline

- Intersubband transitions in nitride heterostructures: theoretical aspects
 - General properties of ISB transitions
 - Modeling within the envelope function formalism
- Infrared spectroscopy of nitride quantum wells and quantum dots
- Nitride unipolar devices
 - Intersubband photodetectors
 - Intersubband light modulators
 - Intersubband light emitters
- Prospects for THz nitride lasers

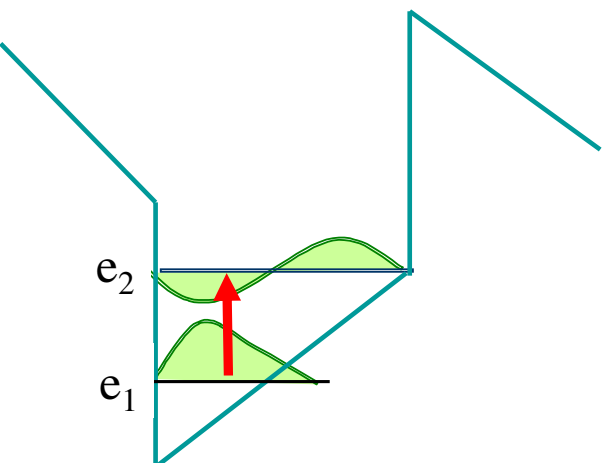
What are intersubband transitions?

- Intersubband transitions are transitions between quantum confined states in the conduction (valence) band of quantum wells, wires or dots
- Only one type of carriers (usually electrons)
- ISB wavelength is almost temperature-insensitive

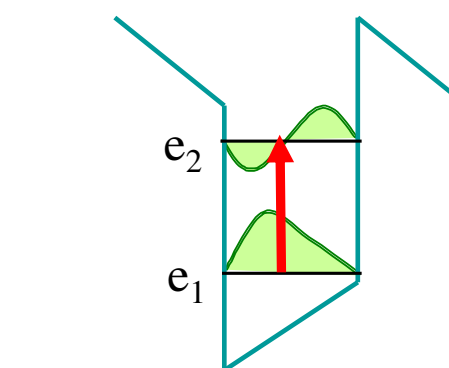


Wavelength tunability of ISB transitions

- Wavelength can be tuned by adjusting layer thickness – possibility to engineer the quantum confinement in order to make nitrides optically active at new wavelengths irrespective of their band gap
- ISB wavelength depends on the electric field (voltage tunable)
- Shortest wavelength is limited by the band discontinuity
- Large CB offset ~ 1.75 eV GaN/AlN \rightarrow ISB transition at $1.3 - 1.55 \mu\text{m}$
- But large effective mass ($m^* = 0.22m_0$) \rightarrow Narrow QWs are required



Large quantum well



Narrow quantum well

Intersubband selection rules

Wavefunction $F(r) = \sum_n \Psi_n(r) u_{n,k_0}(r)$

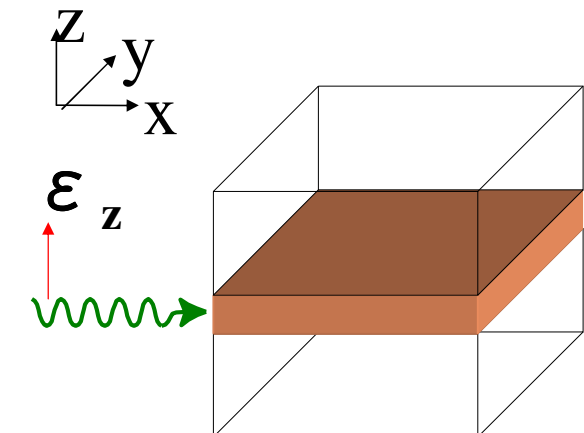
envelope function
slowly varying component

periodic part of the Bloch function
rapidly varying component

► Optical matrix element

$$\underbrace{\langle u_f | \vec{\epsilon} \cdot \vec{p} | u_i \rangle}_{\text{Interband term}} \langle \Psi_f | \Psi_i \rangle + \underbrace{\langle \Psi_f | \vec{\epsilon} \cdot \vec{p} | \Psi_i \rangle}_{\text{Intersubband term}} \delta_{if}$$

light polarization vector

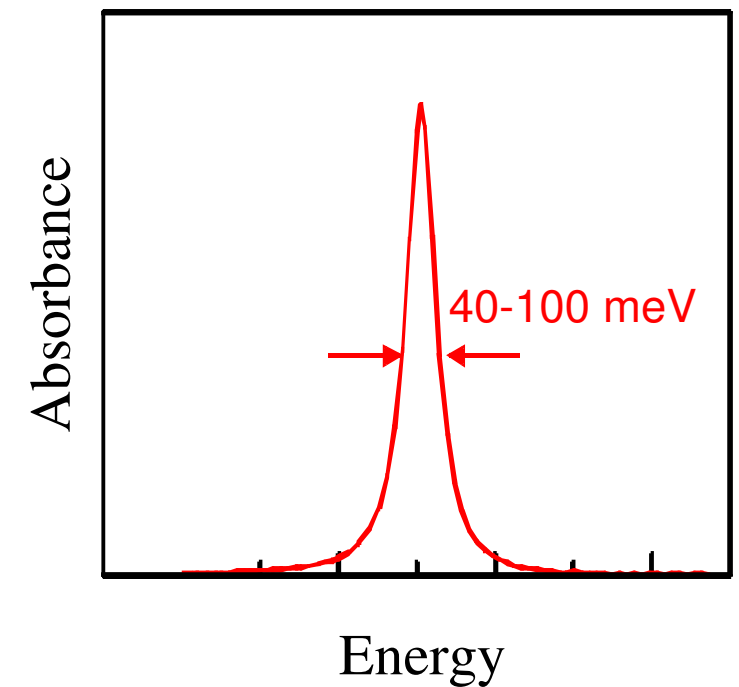
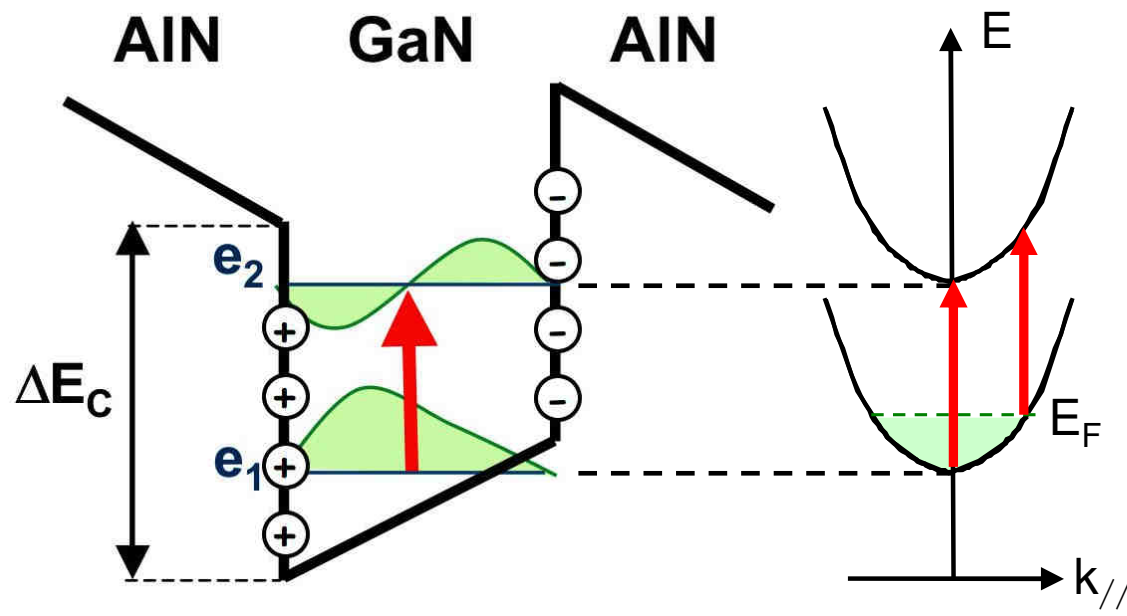


► ISB transition is allowed :

- if incident light has a polarization component along the confinement direction (TM for QWs)
- between states with opposite parity of envelope functions : $\Delta n = \pm 1, \pm 3, \text{etc.}$
- internal field breaks the symmetry → weak transitions for $\Delta n = \pm 2$

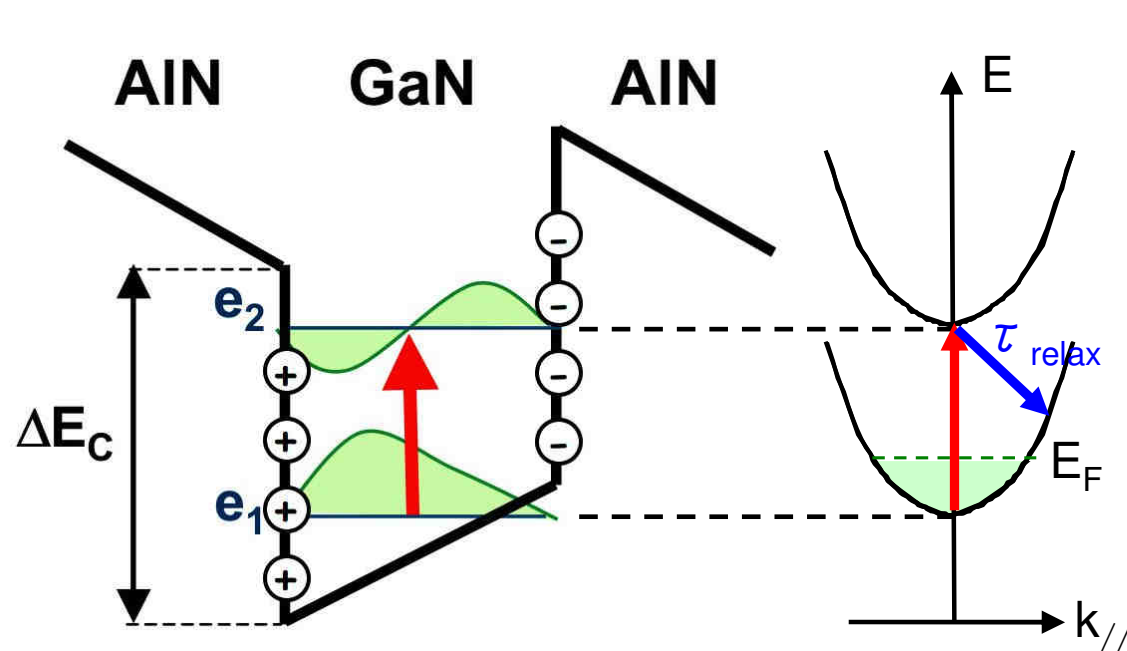
Properties of ISB transitions

- Resonant transitions (Lorenzian or Gaussian lineshape)
- Oscillator strength is large : optical dipole scales like enveloppe wavefunction extension $\vec{\mu}_{if} = e \langle \Psi_f | \vec{e} \cdot \vec{r} | \Psi_i \rangle$, for GaN/AlN QW $\mu_{12} \approx 0.25 eL$
- Absorption is controlled by doping, no absorption for undoped structure



Specific properties of ISB transitions in nitrides

- Enhanced electron-LO phonon interaction in nitrides
 - Very short absorption recovery time (0.15-0.4 ps)
- Prospects for ultra-fast ISB devices



Other features

- Remote lateral valleys ($>2\text{eV}$)
- Large LO-phonon energy: 92 meV
- Low dielectric constant

Comparison between intersubband and interband transitions in GaN/AlN QWs

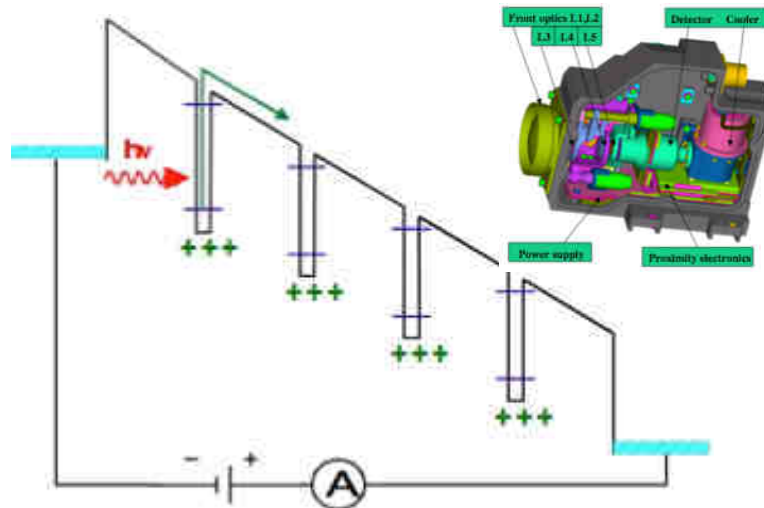
	Intersubband	Interband
Spectral range	Near-to-far IR	VIS – to - UV
Carriers	unipolar (only electrons)	bipolar (electrons and holes)
Relaxation time	0.15-0.4 ps	0.2 ns up to μ s
Temperature dependence	Almost none	Strong redshift : $E_g(T) \approx 70$ meV (4K – 300K)
Selection rules	$\Delta n = \pm 1, \pm 3, \dots$ ϵ_z (TM) No	$\Delta n = 0$ (neglecting field) $\epsilon_{x, y}$ for X_A (TE) Yes
Normal incidence		
Optical dipole	$0.25 e L_w$	several Å
Lineshape	Resonant	Staircase-like+excitonic resonance
Absorption	Doping required	Doping is not necessary

Why intersubband transitions ?

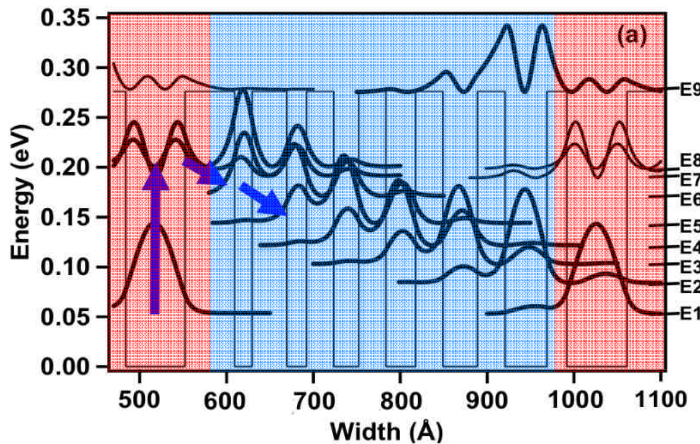
Intersubband control-by-design devices



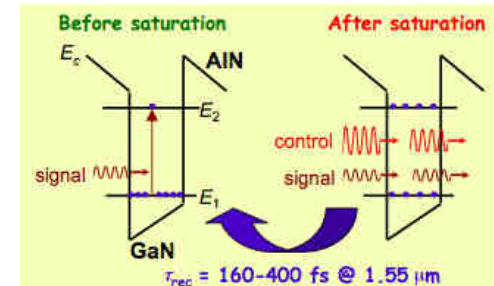
UNIVERSITÉ
PARIS-SUD 11



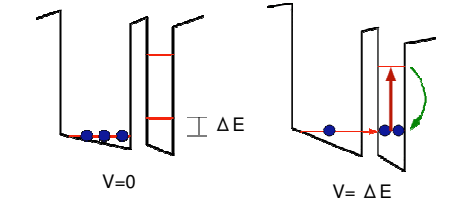
IR detectors (QWIPs or QDIPs)



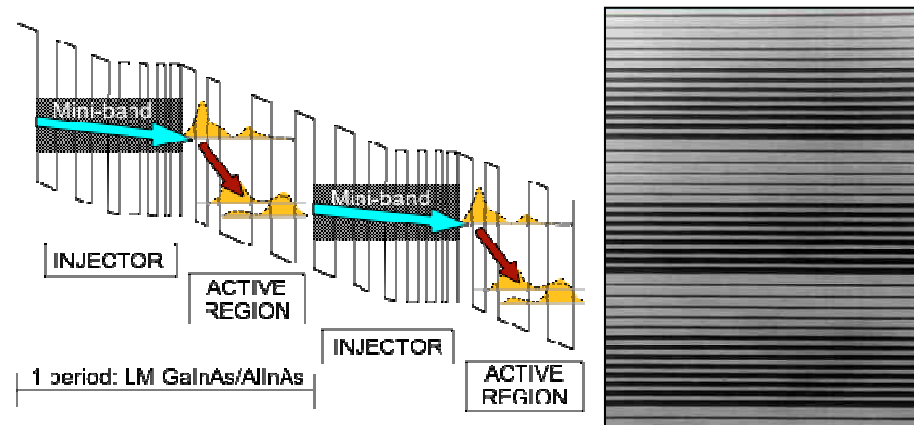
Quantum cascade detectors



All-optical switches

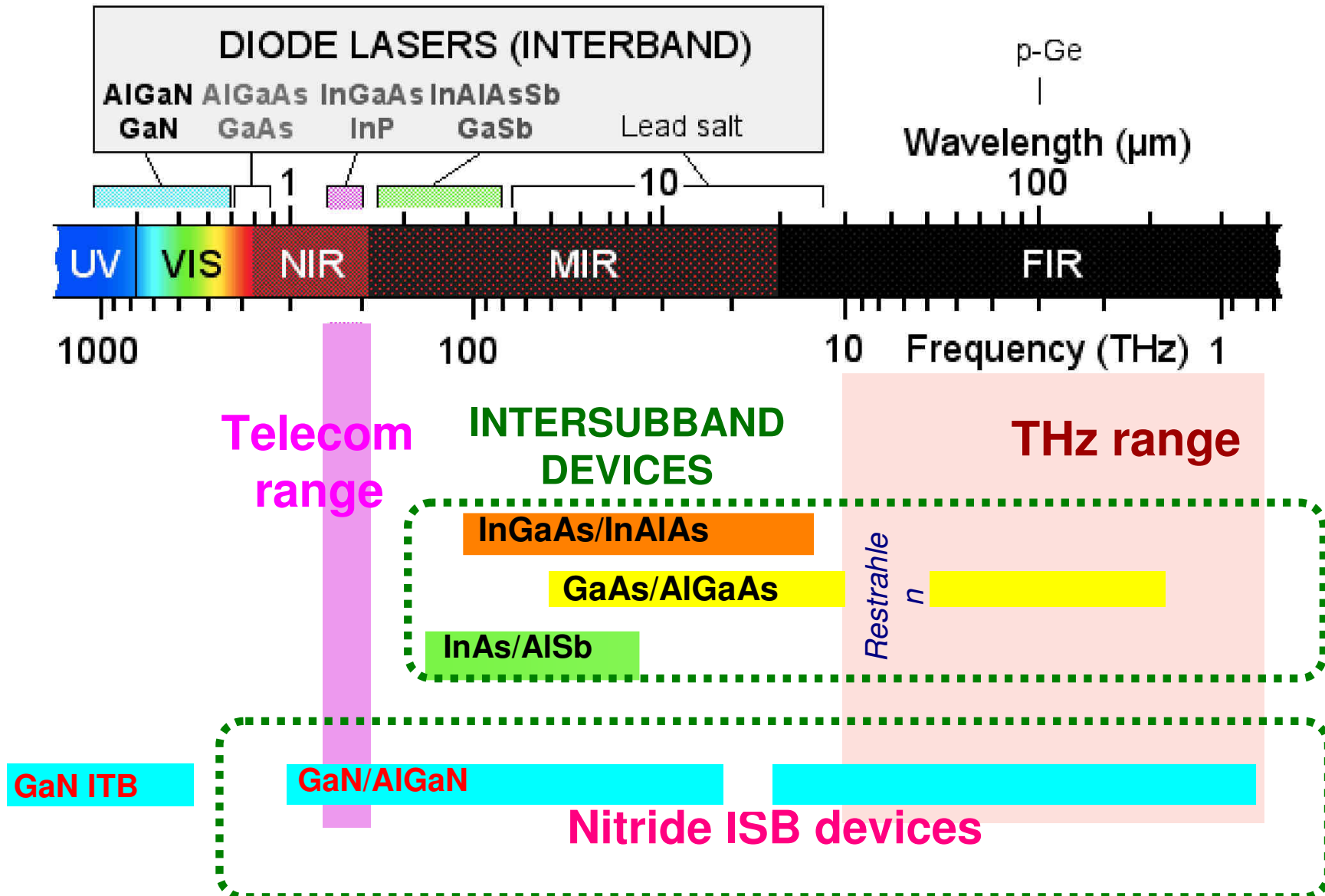


Electro-optical modulators



Quantum cascade lasers

Spectral domain for intersubband devices

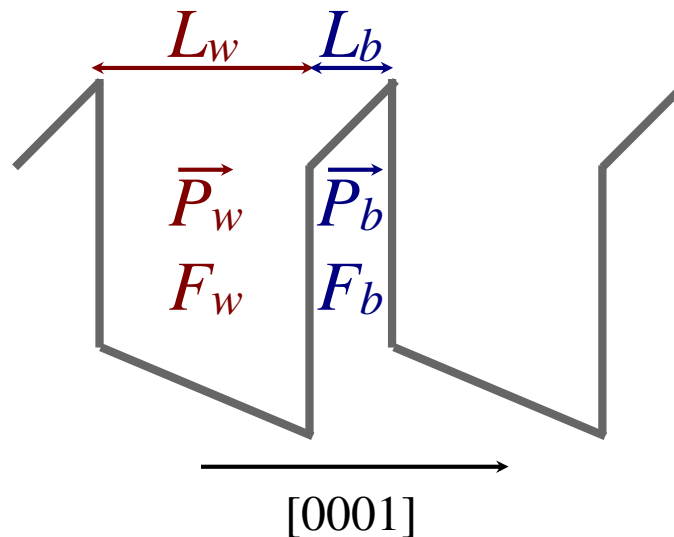


Calculation of the intersubband transition energy

Multiple GaN/AlGaN quantum wells

How to calculate the electric field?

Commonly used hypothesis of a periodic structure : zero potential drop at each period



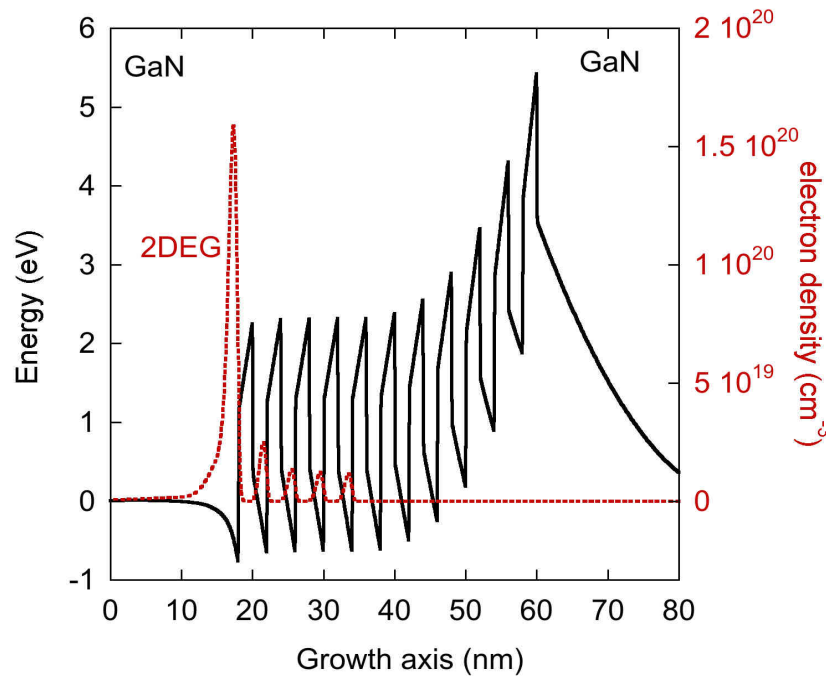
$$\begin{aligned} F_w &= \frac{P_b - P_w}{\epsilon_0} \frac{L_b}{L_b \epsilon_w + L_w \epsilon_b} \\ F_b &= - \frac{P_b - P_w}{\epsilon_0} \frac{L_w}{L_b \epsilon_w + L_w \epsilon_b} \end{aligned}$$

Electric field depends on

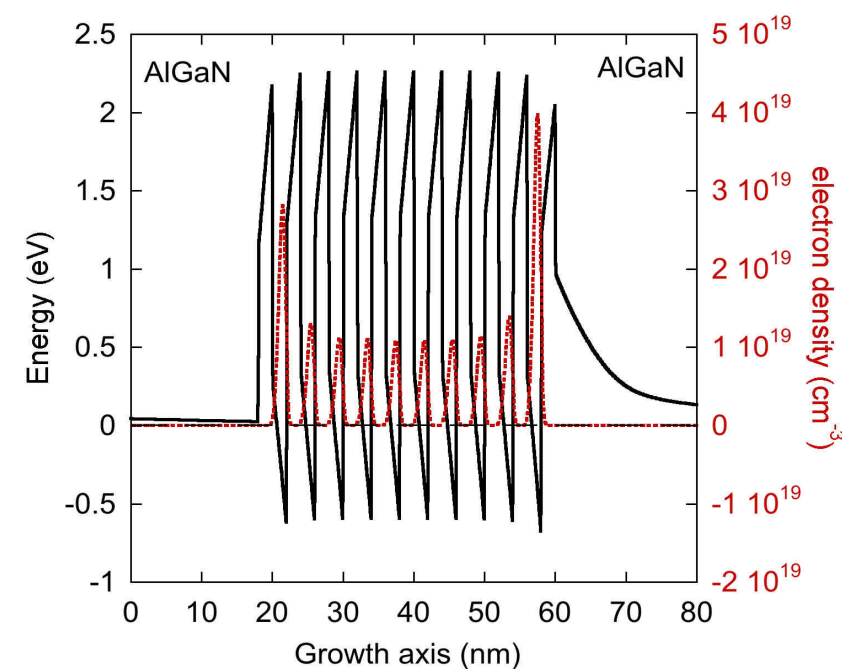
- ✓ Aluminium content in the barrier
- ✓ Barrier thickness
- ✓ Well thickness

Band bending

GaN/AlN doped QWs between doped GaN claddings



GaN/AlN doped QWs between doped AlGaN claddings



- Depletion region at the upper interface and a 2D electron gas at the lower interface.
- Inhomogeneous carrier concentration
- AlGaN claddings with Al content equal to the average Al concentration
- Homogeneous carrier concentration

Conduction band non-parabolicity

Calculation is restricted to a single GaN/AlN QW

Effective mass approximation

$$\left(-\frac{\hbar^2}{2m^*} \frac{d^2}{dz^2} + U_H(z) \right) \Psi(z) = E \Psi(z)$$

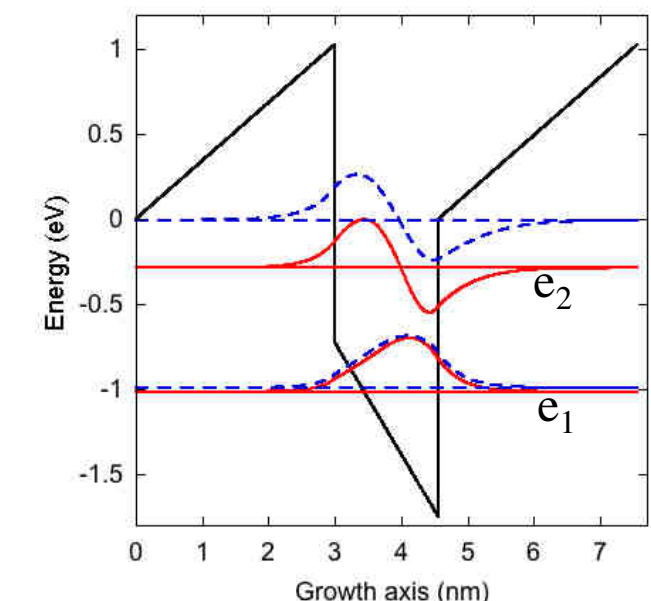
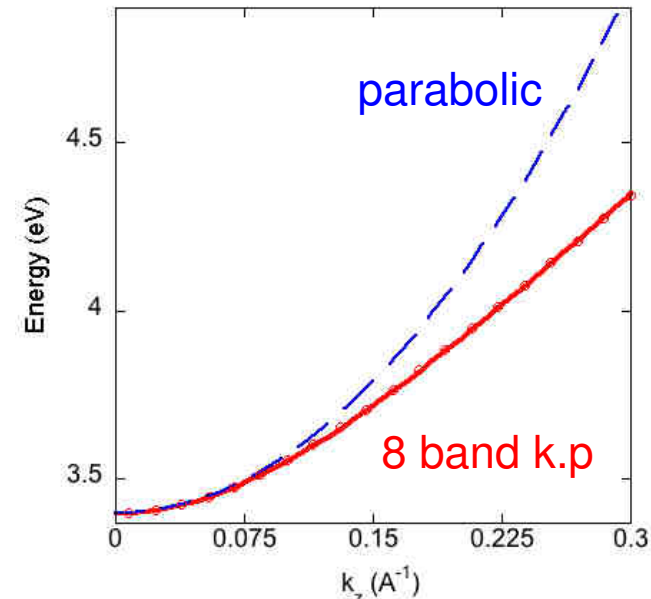
For ISB transition with high $e_1 - e_2$ energy non-parabolicity becomes significant

Non-parabolicity of the conduction band is taken into account using energy-dependent effective mass

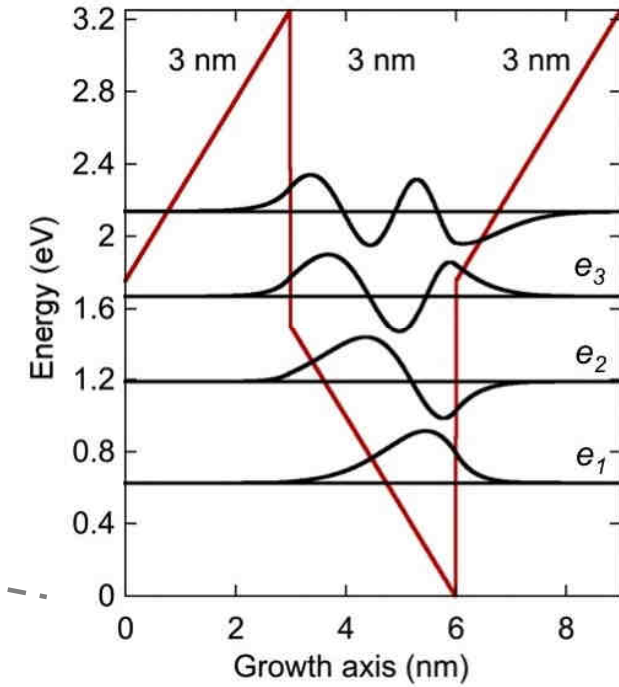
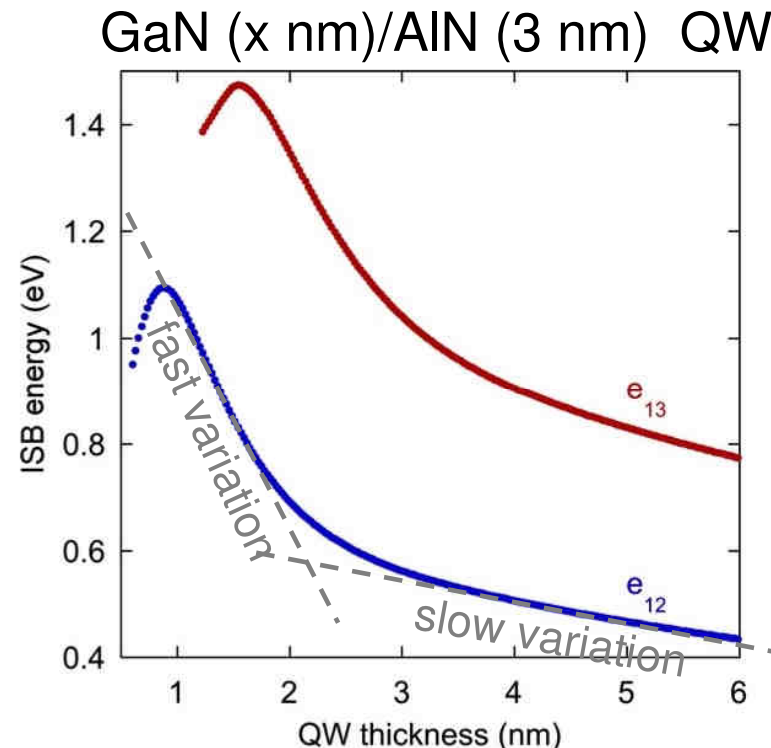
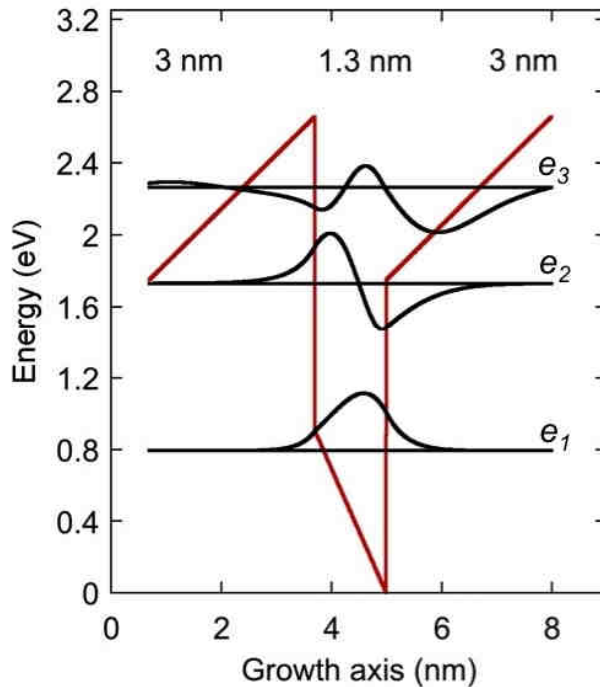
$$m^*(E) = 0.22m_0(1 + 0.068E + 0.003E^2)$$

E – energy from the bottom of the conduction band

Error for $e_1 - e_2$ energy can reach 25%



Dependence on the QW thickness



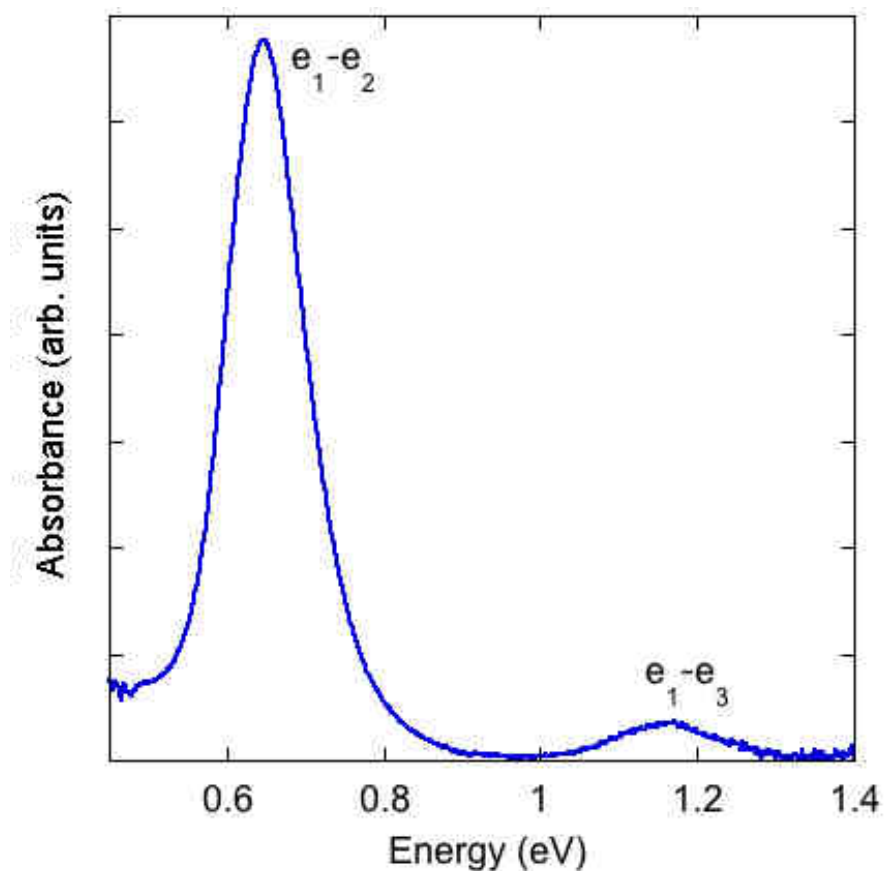
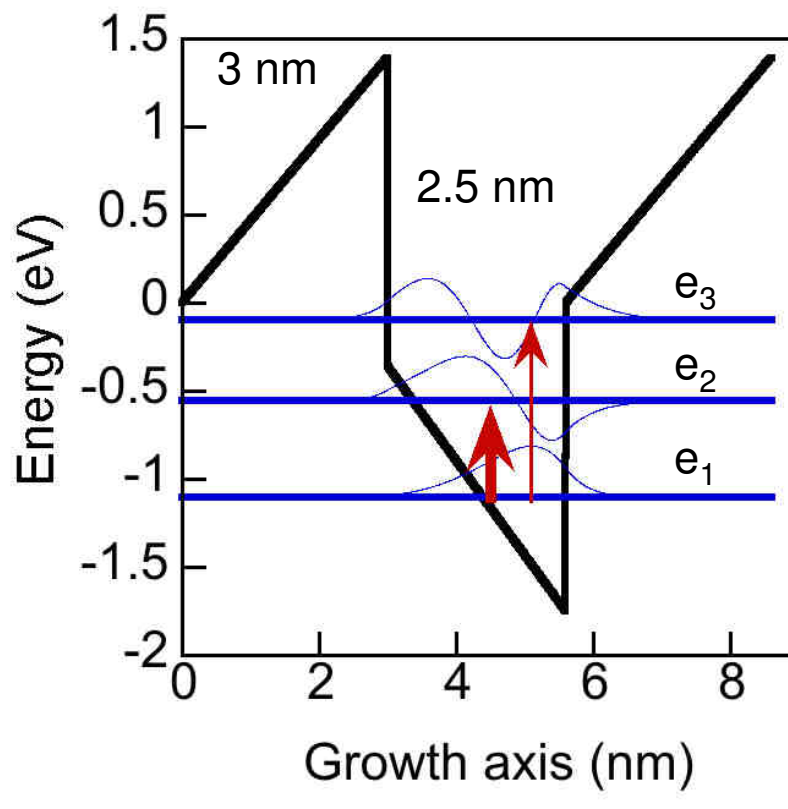
- Confinement by the QW interfaces, transition energy is determined by the well thickness
- Delocalization of e₂ state in the barriers for L_w<1 nm

- Confinement by the V-shaped potential, transition energy is determined by the magnitude of the internal field
- “Saturation” of the e₁-e₂ energy at ≈0.4 eV

Simulated ISB absorption spectrum

n-doped GaN/AlN 2.5 nm / 3 nm quantum well

- Strong e_1 - e_2 absorption, weak e_1 - e_3 absorption (5% of the e_1 - e_2 amplitude)
- Absorption magnitude **0.025%** for 1 QW doped at 10^{12} cm^{-2} ($2.5 \times 10^{19} \text{ cm}^{-3}$) for 1 pass at 30° angle in GaN



Strongly doped heterostructures

Solution of Schrödinger and Poisson equations

$$\begin{cases} \left(-\frac{\hbar^2}{2m^*} \frac{d^2}{dz^2} + U_H(z) + U_{SC}(z) \right) \Psi_i(z) = E_i \Psi_i(z) \\ \frac{d^2}{dz^2} U_{SC}(z) = \frac{e^2}{\varepsilon} (N_D^+(z) - \sum_i n_i^S |\Psi_i(z)|^2) \end{cases}$$

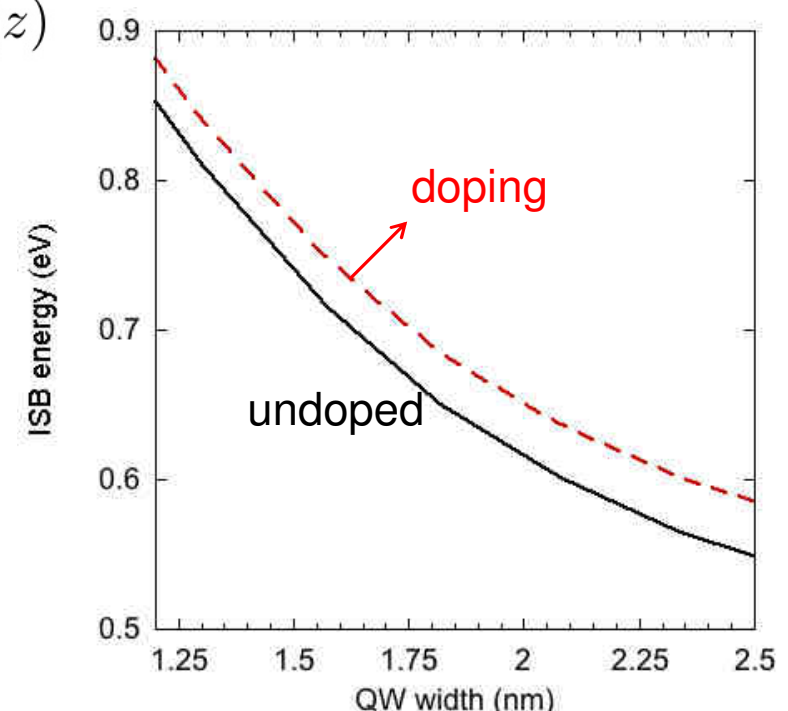
with surface carrier density

$$n_i^S = \frac{m^* k T}{\pi \hbar^2} \ln \left(1 + \exp \left(\frac{E_F - E_i}{k T} \right) \right)$$

Typical carrier concentration 10^{12} cm^{-2}

Doping induced effects :

- electric field screening (ISB redshift)
- depolarization shift (ISB blueshift)
- exchange interaction (ISB blueshift)

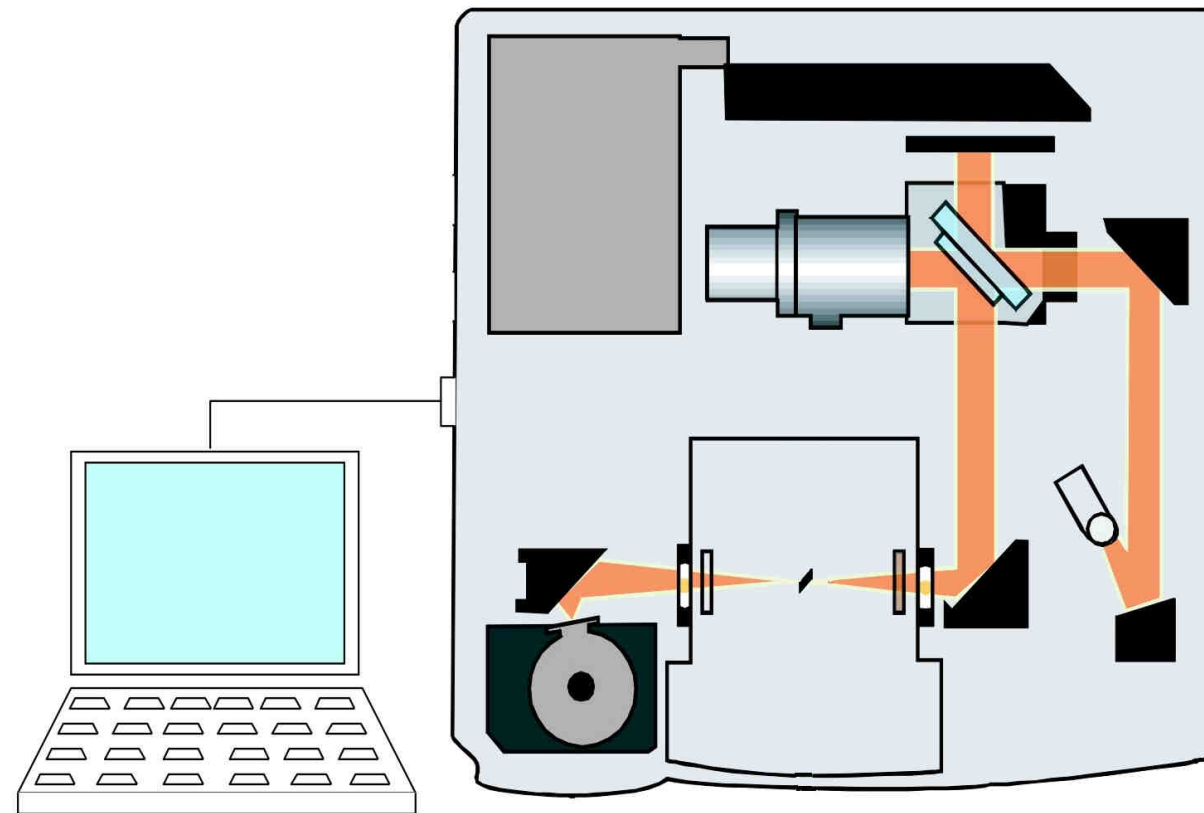


Resulting effect is a blueshift of the ISB transition with doping

Measurement of the intersubband absorption in GaN/AlN quantum wells and quantum dots

Detecting ISB absorption

- Main tool – Fourier Transform Infrared spectroscopy

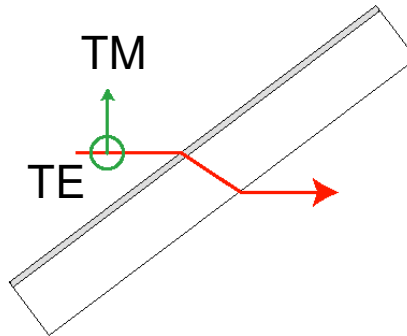


Light coupling geometry

- non-zero ϵ_z component is required to satisfy polarization selection rules
- For spectroscopy :

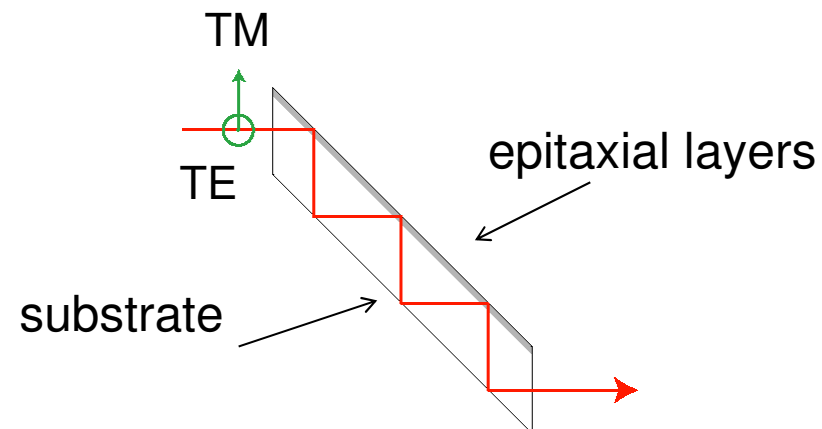
Brewster's angle

67° incidence in air
24° in GaN



Multipass waveguide

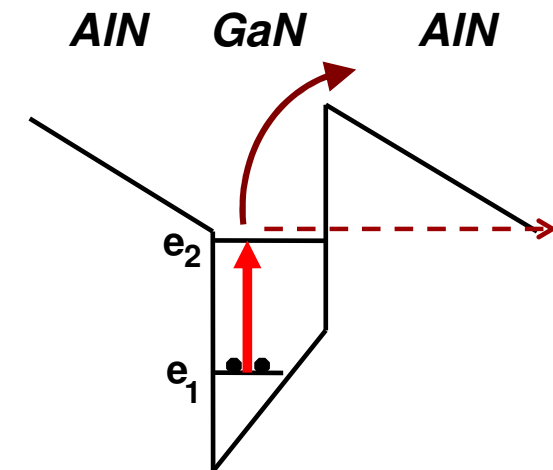
45° incidence in sapphire
31° in GaN



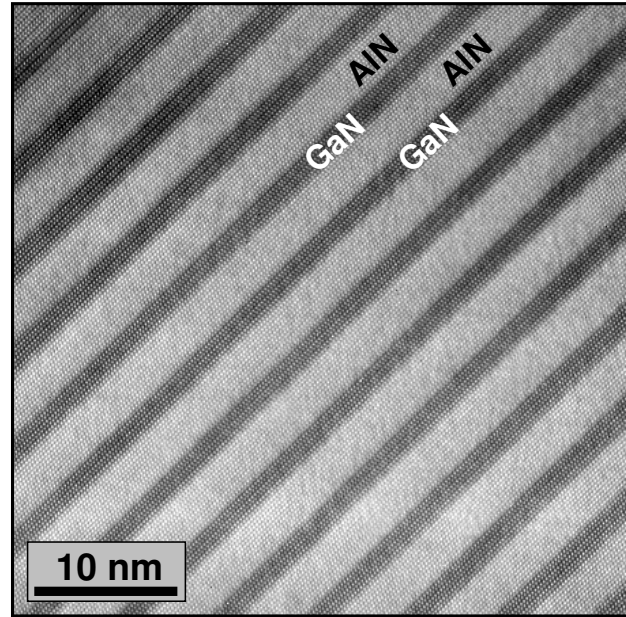
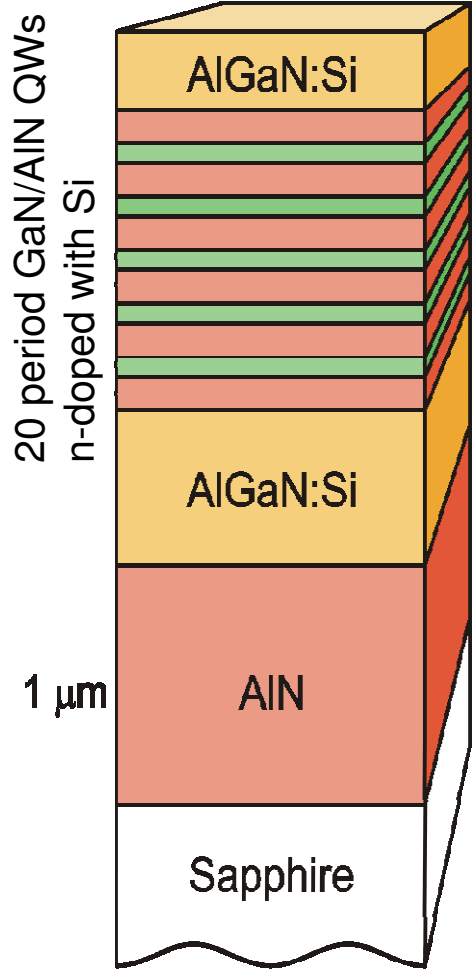
- For devices : waveguide configuration (pure TM) or normal incidence with a top grating (diffraction orders have a TM component)

Detecting ISB absorption

- IR transmission spectroscopy (bound-to-bound transition, possible only in doped samples)
- Photoinduced absorption spectroscopy (bound-to-bound transition, possible in both doped and undoped samples)
- Photocurrent spectroscopy (bound-to-continuum or bound-to-bound transition, possible only in doped samples)



Near infrared spectroscopy of GaN/AlN quantum wells

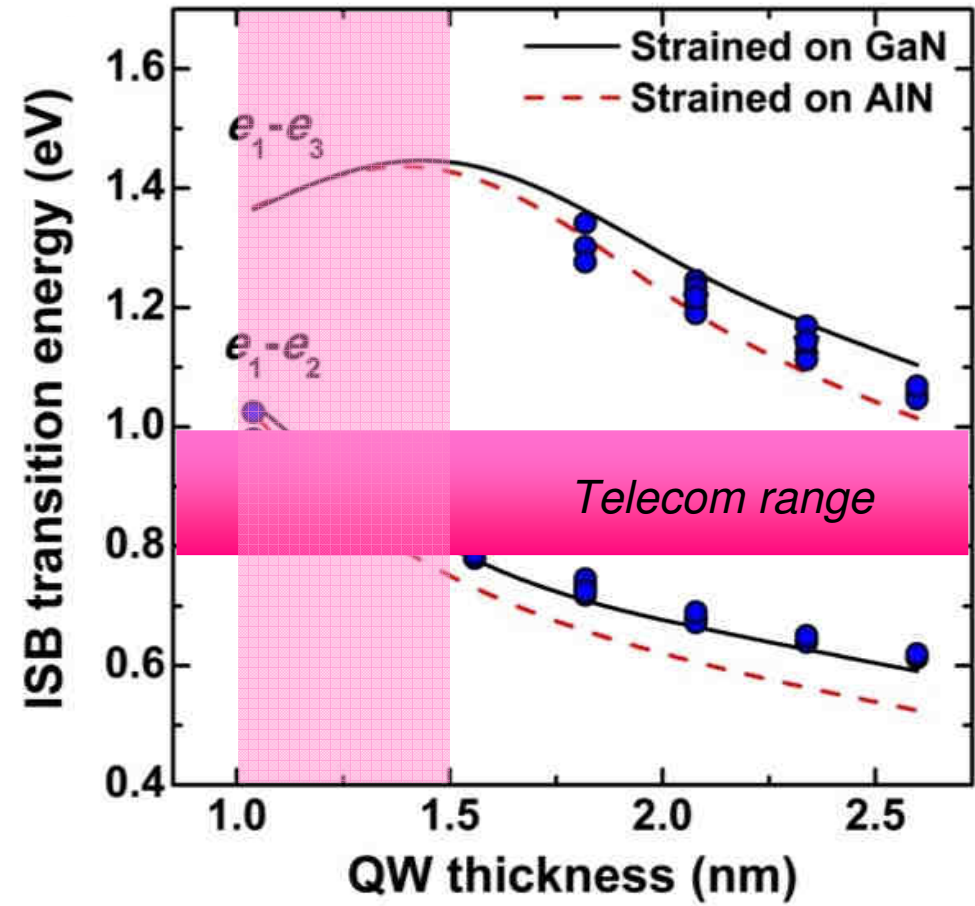
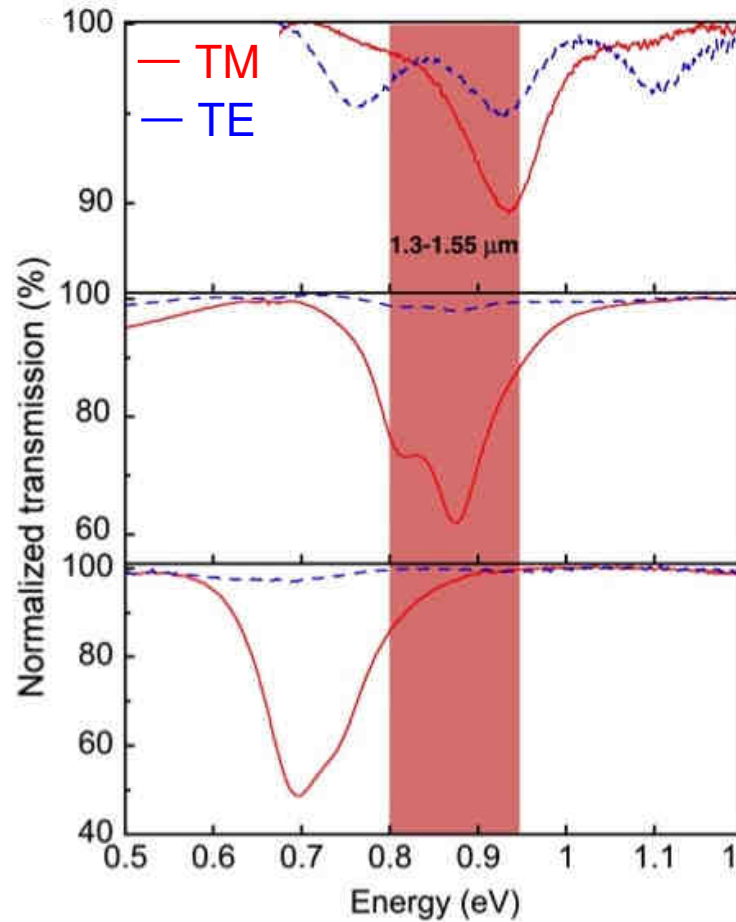


PA-MBE growth, TEM CEA-Grenoble

PA-MBE growth of GaN/AlN quantum wells

- ✓ Metal-rich conditions
- ✓ Low growth temperature ($\sim 720^\circ \text{ C}$) to prevent GaN/AlN interaction – abrupt and smooth GaN/AlN interfaces at the monolayer scale
- ✓ Low growth rate for thickness control
- ✓ AlN-on-sapphire substrates: crack-free growth (compressive strain)

Near infrared spectroscopy of GaN/AlN quantum wells



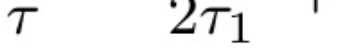
- ISB absorption in **1.3-1.55 μm** range for quantum wells with thickness **1-1.5 nm**
- Thickness control down to 1 atomic layer is required – MBE technique

ISB lineshape and broadening in GaN/AlN QWs

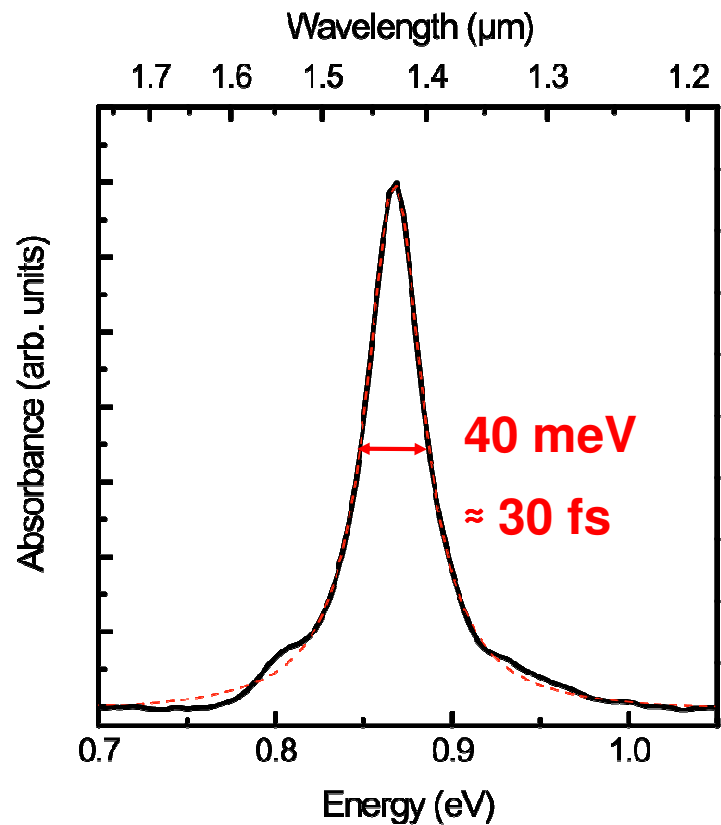
- Lorentzian shape or multi-peak lineshape
 - Typical ISB broadening at 0.8 eV is 40-70 meV (undoped) or 60-100 meV (doped)
 $\Delta E/E \approx 5\text{-}10\%$
 - Homogeneous broadening in a two-level system : Wavelength (μm)

1.7	1.6	1.5	1.4	1.3
-----	-----	-----	-----	-----

$$\Delta E = 2\hbar/\tau \quad \text{with} \quad \frac{1}{\tau} = \frac{1}{2\tau_1} + \frac{1}{\tau_2}$$

population relaxation  phase relaxation

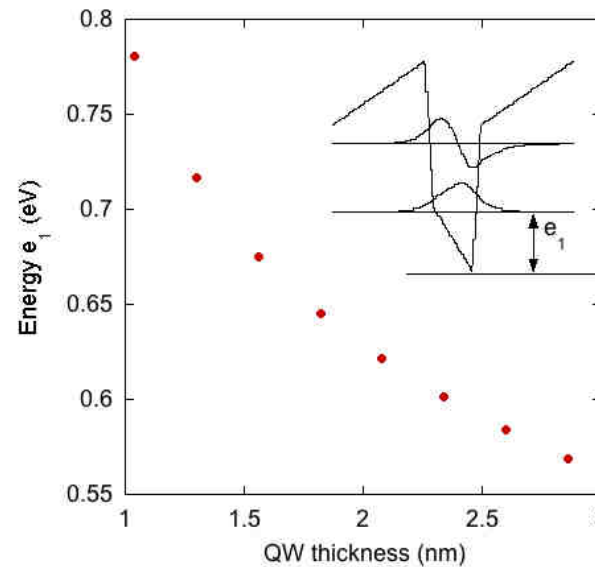
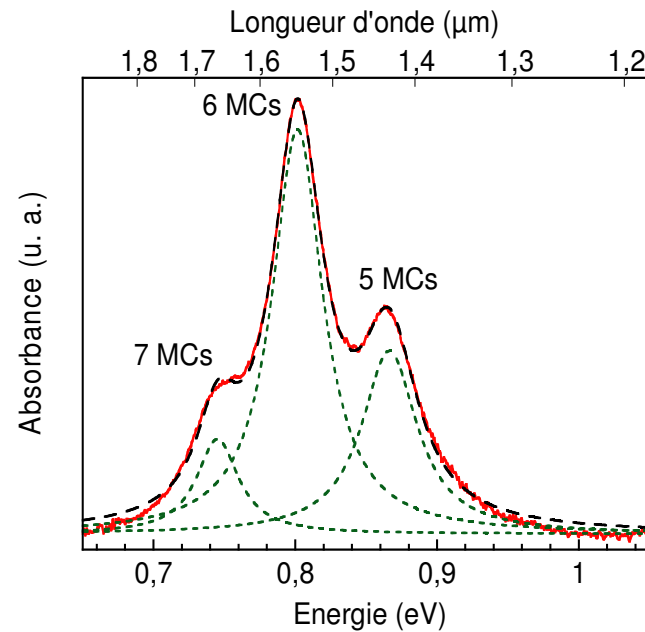
- GaN/AlN QWs intersubband relaxation 0.15-0.4 ps
 - Dephasing time is much shorter (tens of fs)
 - Processes responsible for relaxation :
 - electron - LO-photon interaction
 - electron-electron interaction (for doped QWs)
 - electron-impurity interaction (for QWs doped above $5 \times 10^{19} \text{ cm}^{-3}$)



*F. Julien et al., PSS 204, 1987
(2007)*

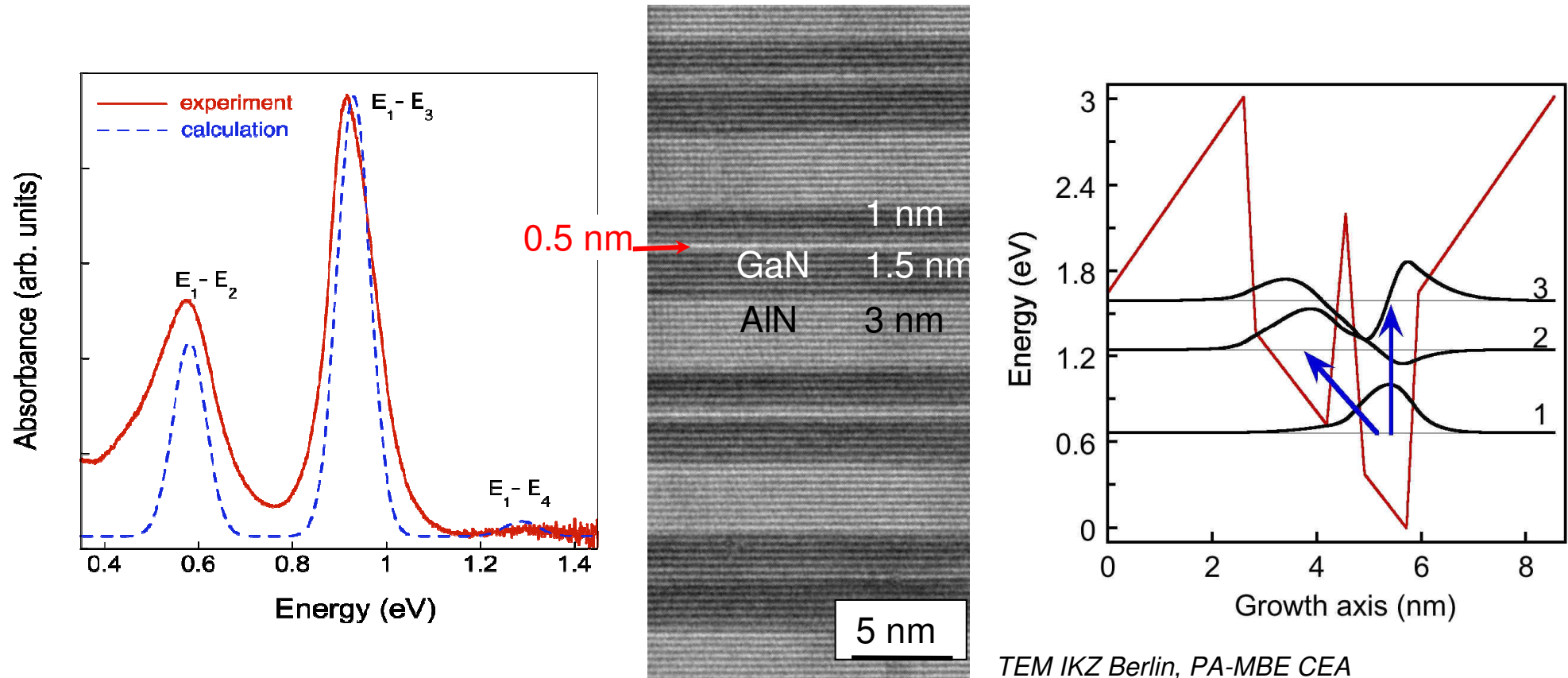
N. Suzuki, et N. Iizuka, Jpn. J. Appl. Phys. 37, L369 (1998)

Origine of the multi-peak ISB lineshape



- Narrow QWs (< 2nm) : 1 ML thickness fluctuation induces a large energy shift > 25 meV
- Carrier localization at room temperature
- The peaks correspond to QWs with a well thickness equal to an integer number of monolayers
- Different from GaAs/AlGaAs system, where large QWs are used and the ML fluctuation induces a small spectral shift resulting in an inhomogeneous broadening

ISB transitions in coupled quantum wells



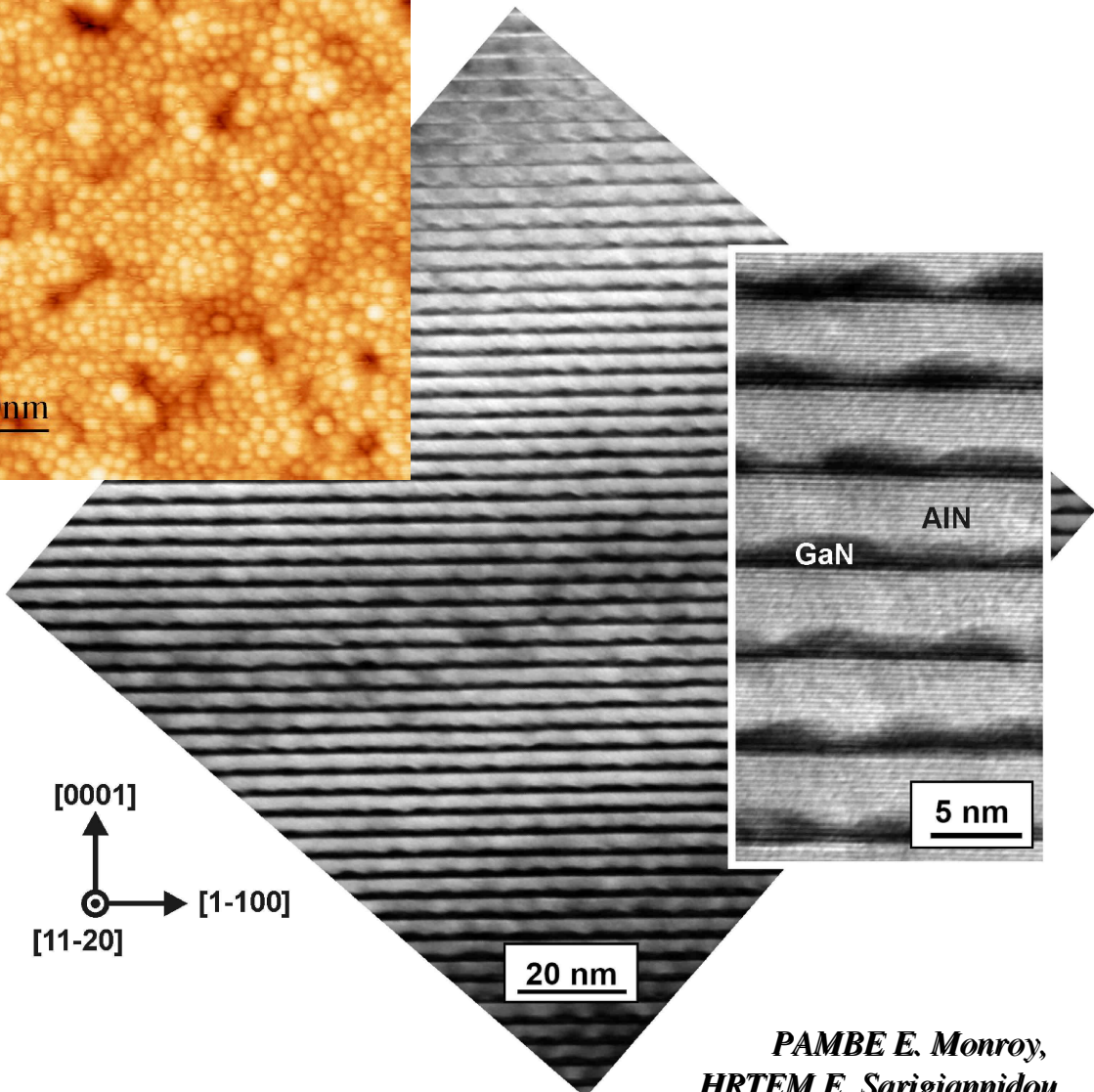
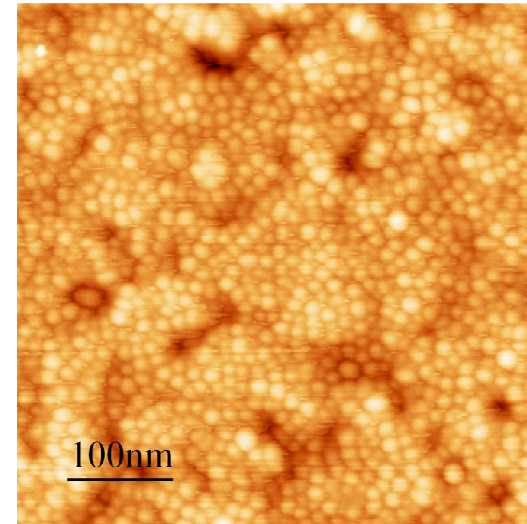
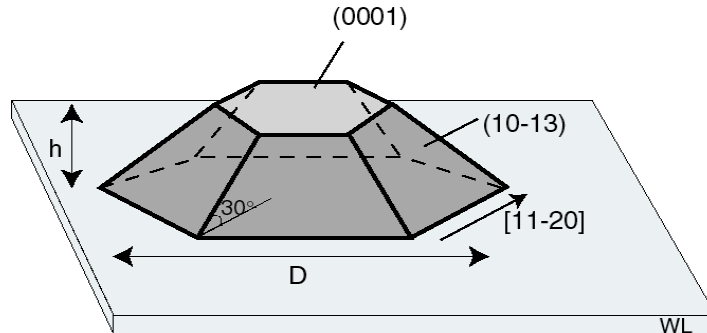
TEM IKZ Berlin, PA-MBE CEA

- Intersubband absorption e_1-e_2 and e_1-e_3 between the ground state and the excited states delocalized in two quantum wells
- Transition energy depends on the applied electric field

GaN/AlN quantum dots

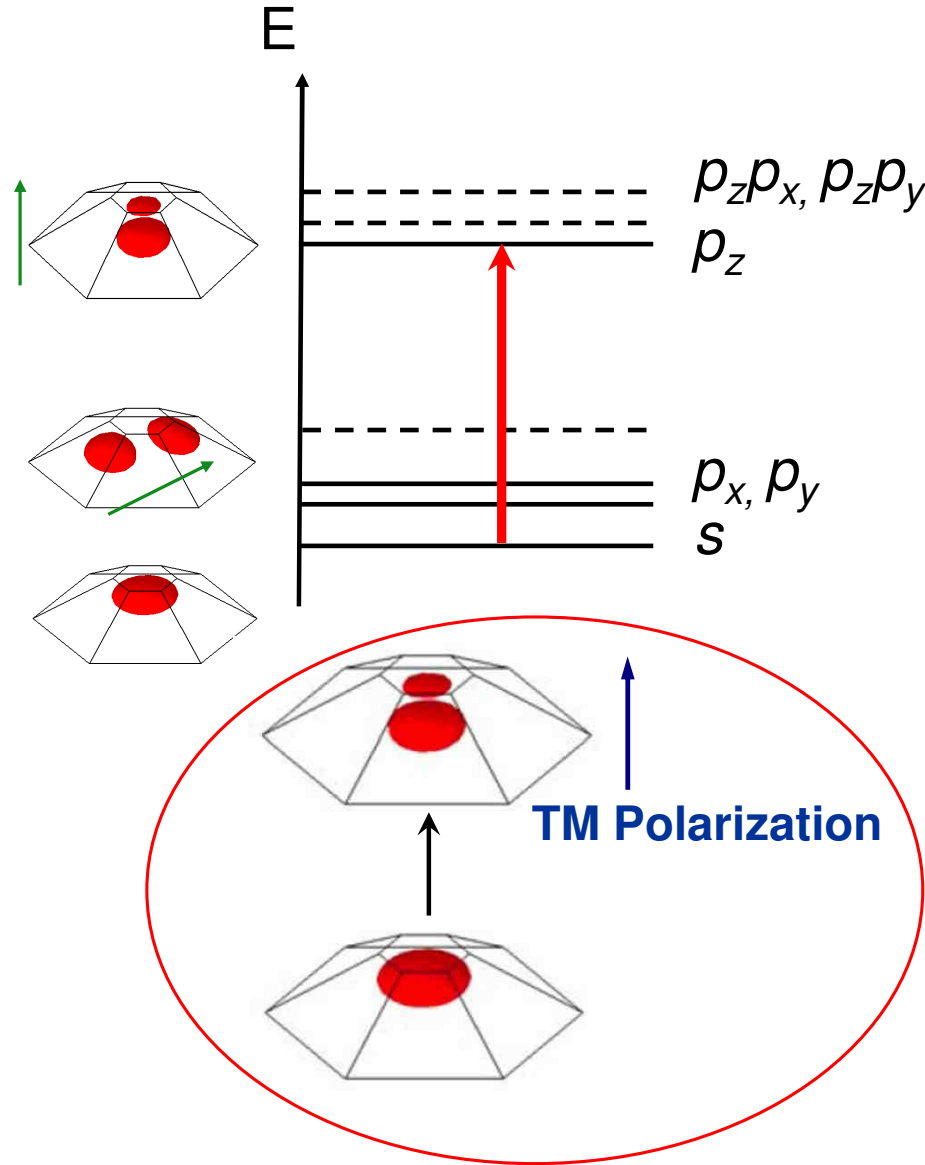


UNIVERSITÉ
PARIS-SUD 11

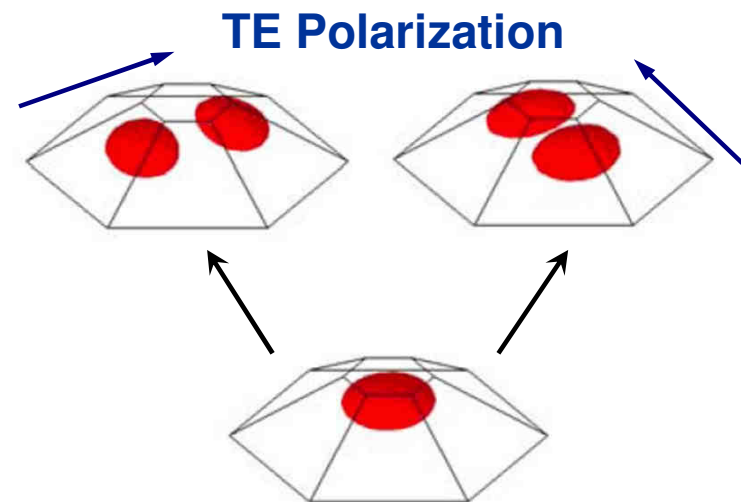


- ✓ PA-MBE growth N-rich $T = 700^\circ \text{ C}$
- ✓ Small QDs $h = 1\text{-}1.5 \text{ nm}$, $d = 6\text{-}15 \text{ nm}$
- ✓ High Si doping in QDs
- ✓ High density up to several 10^{12} cm^{-2}
- ✓ Homogeneous stack of QD planes can be achieved

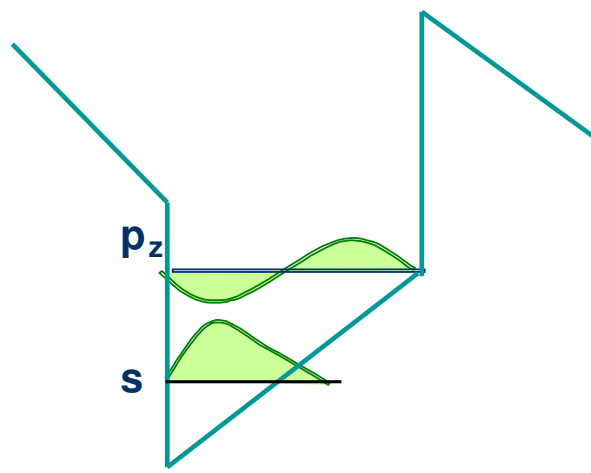
Quantum confinement in GaN/AlN QDs



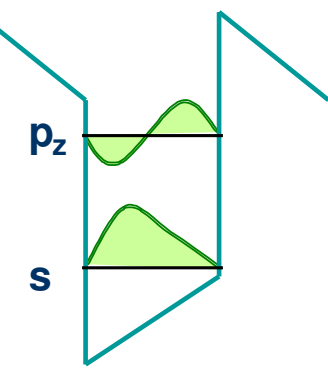
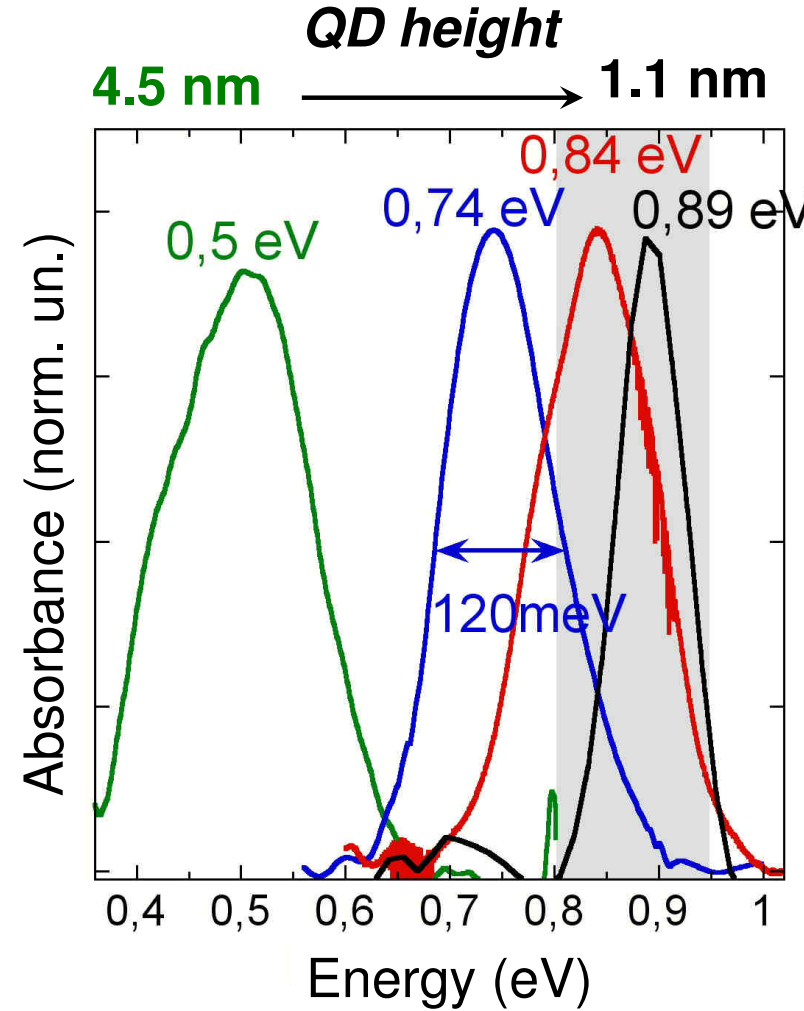
- ✓ Excited state both with in-plane and vertical confinement
- ✓ Strong TM-polarized *s*- p_z transition in the near-IR



$s-p_z$ intraband transition in GaN QDs



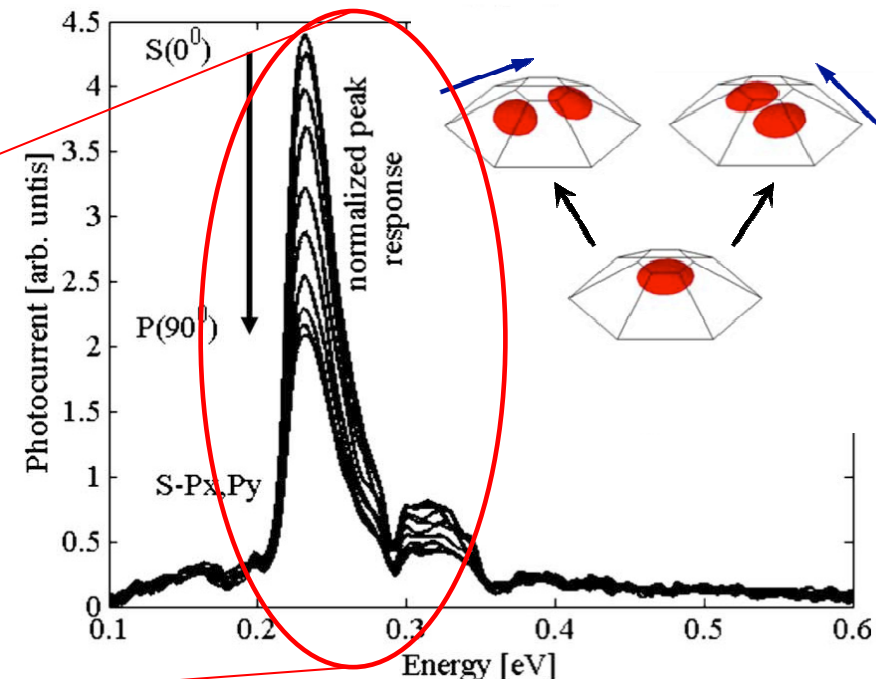
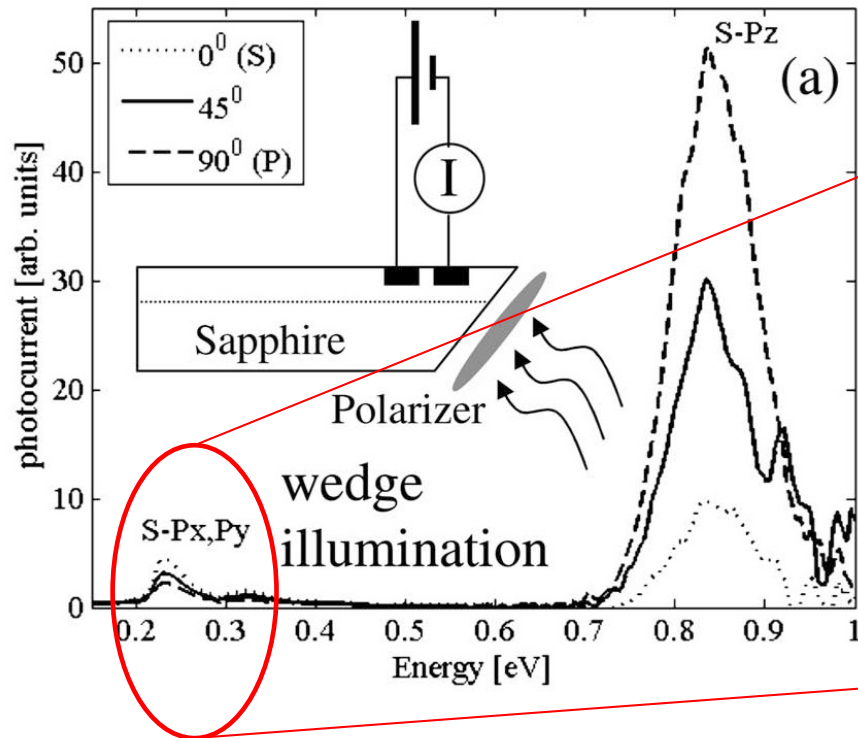
Big QD
Internal electric field



Small QD
QD height

- $s-p_z$ transition TM-polarized transition is tunable from 2.5 μm to 1.3 μm
- Gaussian lineshape due to the diameter fluctuations

In-plane intraband transitions in GaN QDs



- Photocurrent measurement to probe in-plane $s-p_x$ and $s-p_y$ transitions
- $s-p_x$ and $s-p_y$ TE-polarized transitions are detected at 0.15 - 0.25 eV depending on the dot diameter (10-16 nm)

Nitride near-IR ISB devices

- ✓ **IR photodetectors**
 - ✓ Quantum well IR photodetector
 - ✓ Quantum cascade detectors
 - ✓ Quantum dot IR photodetector
- ✓ Modulators
- ✓ Light emitters

Photodetectors: D. Hofstetter et al. APL 2006; Vardi et al. APL 2008

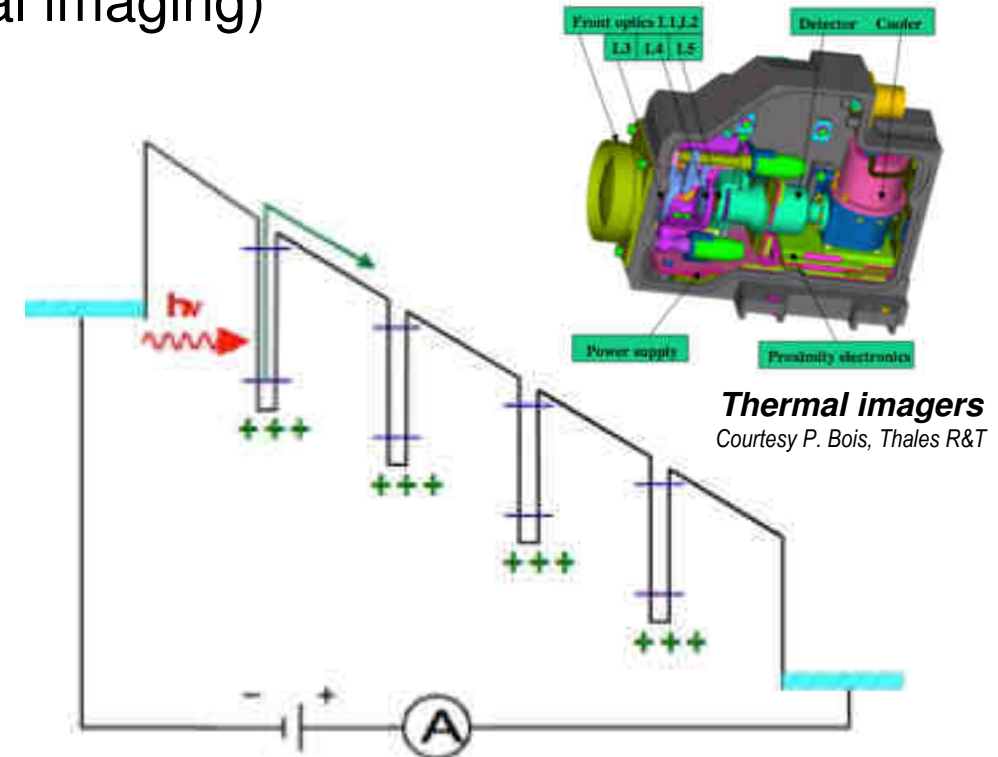
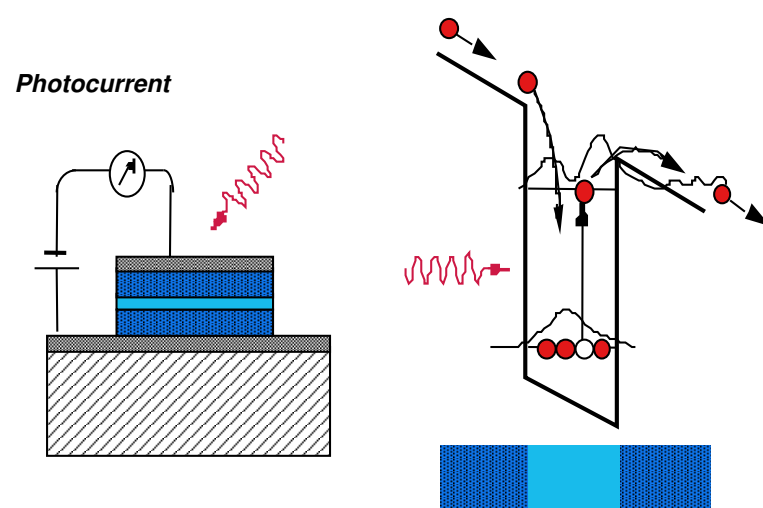
Fast electro-optical modulators: Bauman et al. APL 89, 101121 (2006); Nevou et al. APL 2007;
Kheiroudin et al. IEEE PTL 2008, Lupu et al., Optics Express (2012)

All-optical switches: Iizuka et al., Opt. Expr. 2005; Li et al., Opt. Expr. 2007

ISB light emission: Nevou et al., Electron. Lett. 2006, APL 2007; Driscoll et al. APL 2009

Quantum well infrared photodetectors

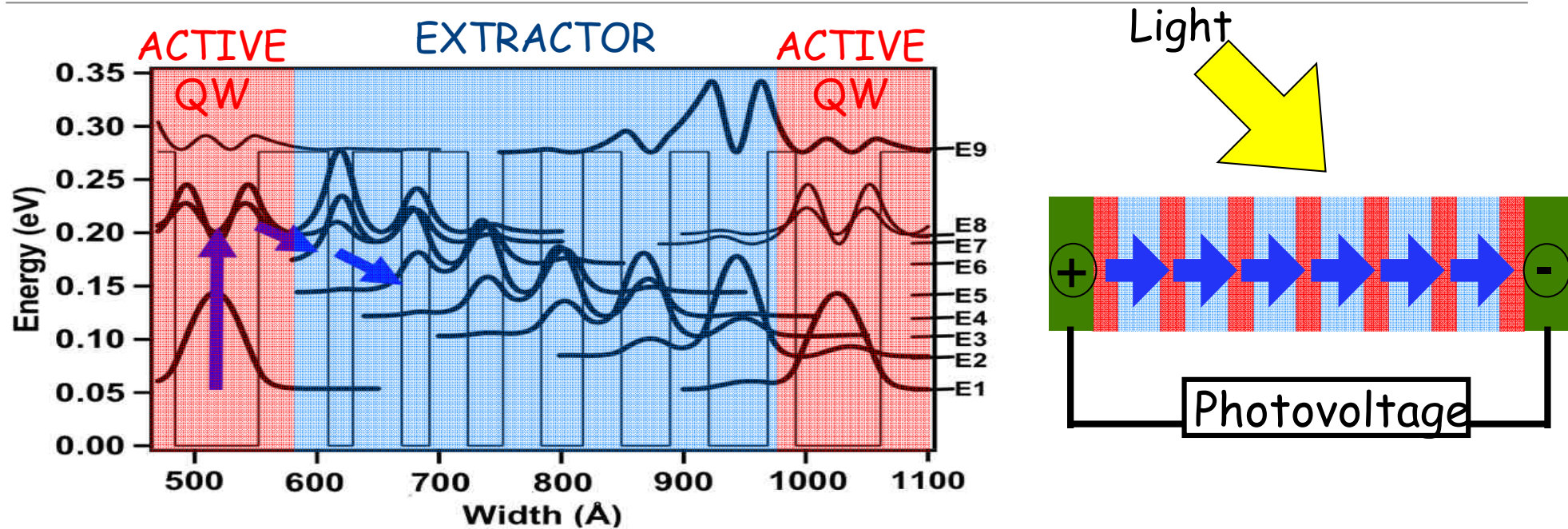
IR photoconductive detectors (QWIPs or QDIPs) in conventional III-V semiconductors (Mid-IR range, thermal imaging)



Electron is promoted to the excited state, tunnel to the continuum and creates the photocurrent

Commercial devices used for IR imaging

Quantum cascade detectors



- ✓ QCDs are photovoltaic devices operated at zero bias : **no dark current**
- ✓ QCDs rely on ISB absorption in an active QW and LO-phonon-assisted relaxation in an extractor region
- ✓ Electron transfer in each period results in a macroscopic photovoltage across the QCD stack
- ✓ Potentially extremely fast (low capacitance devices)

QWIPs versus QCDs

Photoconductive gain : $g = \frac{\tau_{capture}}{\tau_{transit}}$

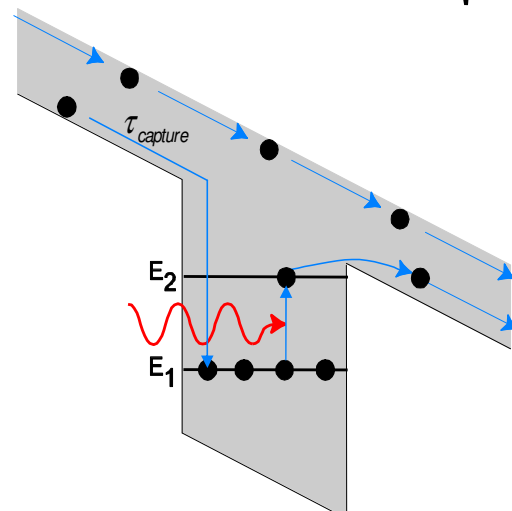
Quantum efficiency : η

Responsivity = $e \frac{\eta g}{h\nu}$

Thermally-limited detectivity :

$$D^* = \frac{\eta}{2h\nu} \sqrt{\frac{\tau_{capture}}{n_t L}}$$

BLIP detectivity : $D_{BLIP}^* = \frac{1}{2} \sqrt{\frac{\eta}{h\nu F_B}}$



Responsivity in A/W independent of number of periods (N):

$$R(\lambda) = a \times \eta \times \frac{1}{E(eV)}$$

a light absorption per period

η electron transfer efficiency per period

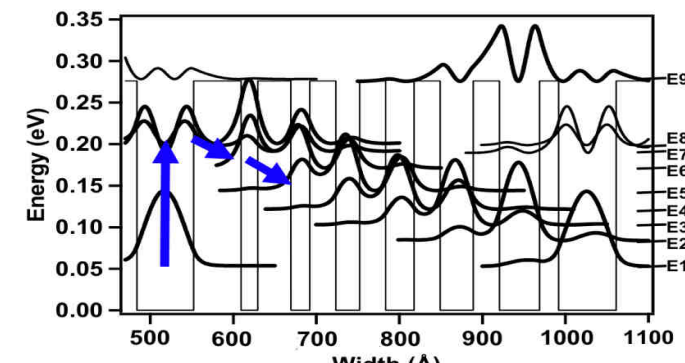
$E(eV)$ ISB transition energy in eV

Photoconductive gain = 1/N (≤ 1)

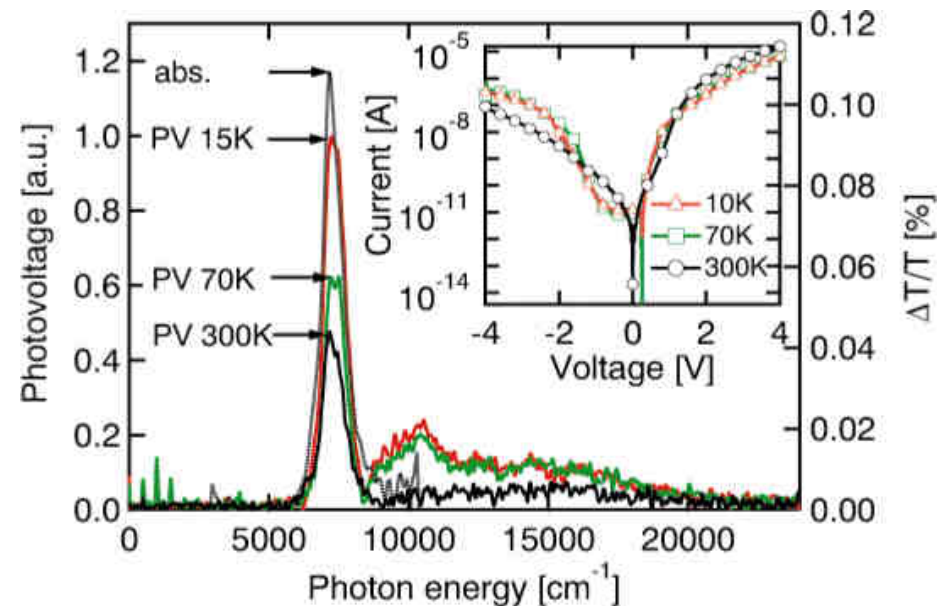
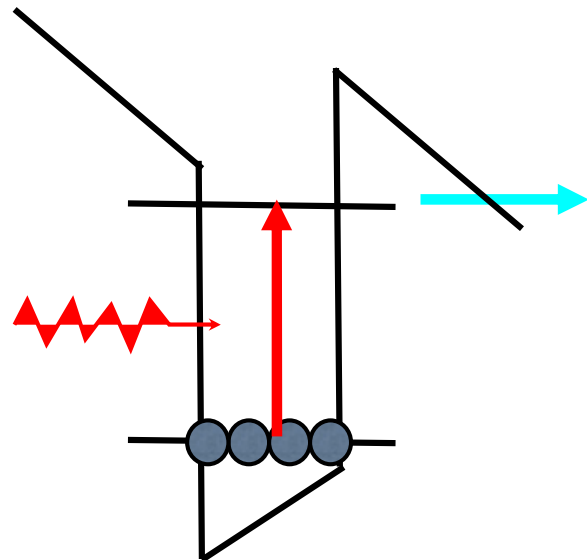
Detectivity limited by Johnson noise

$$D^* = R(\lambda) \sqrt{\frac{R_0 A}{4kT}}$$

R_0 internal resistance at zero bias, A device area



GaN/AlN QW infrared photodetectors

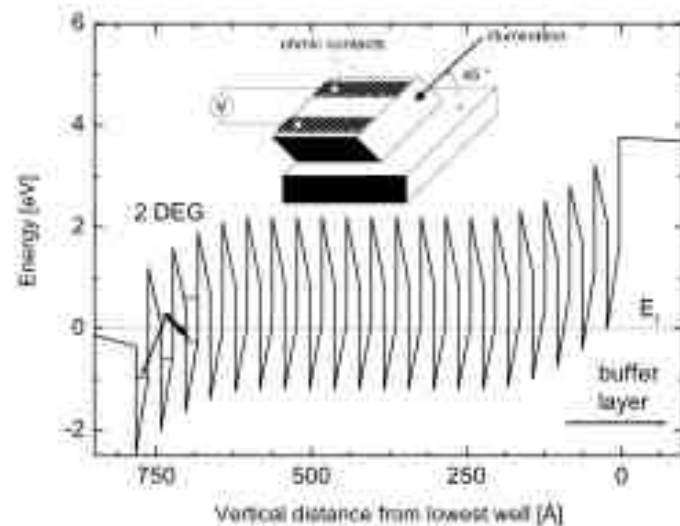


Photoconductive QWIP:

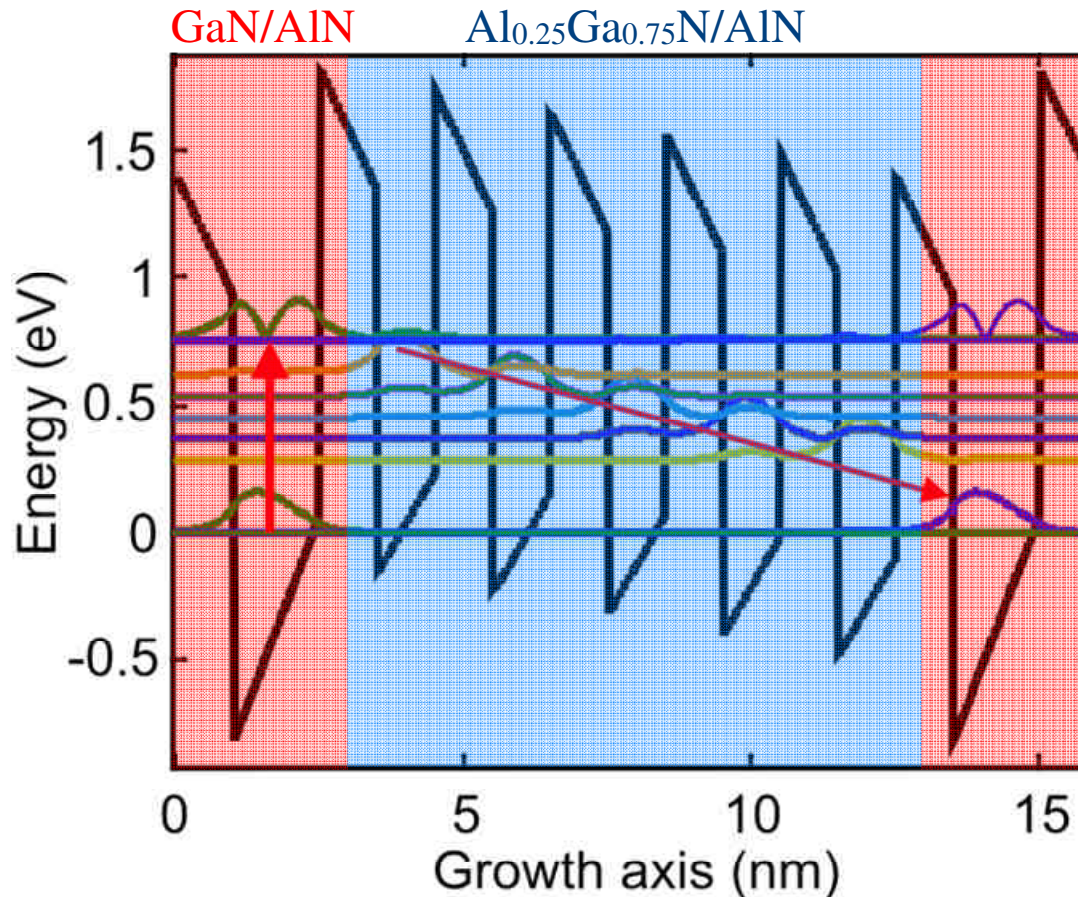
- excess dark current due to dislocations

Photovoltaic QWIP :

- Low responsivity (3 mV/W @ 150 K)

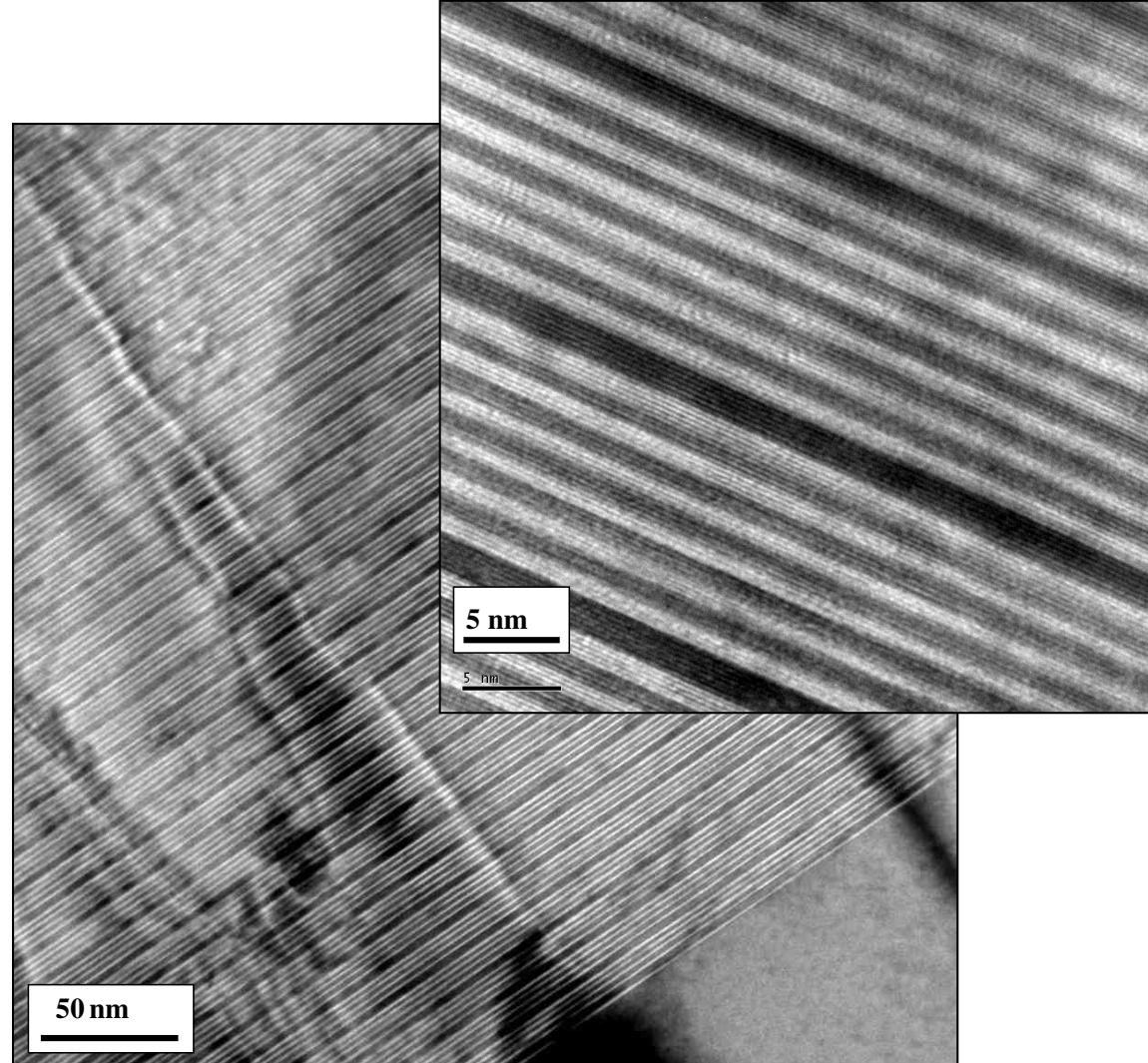
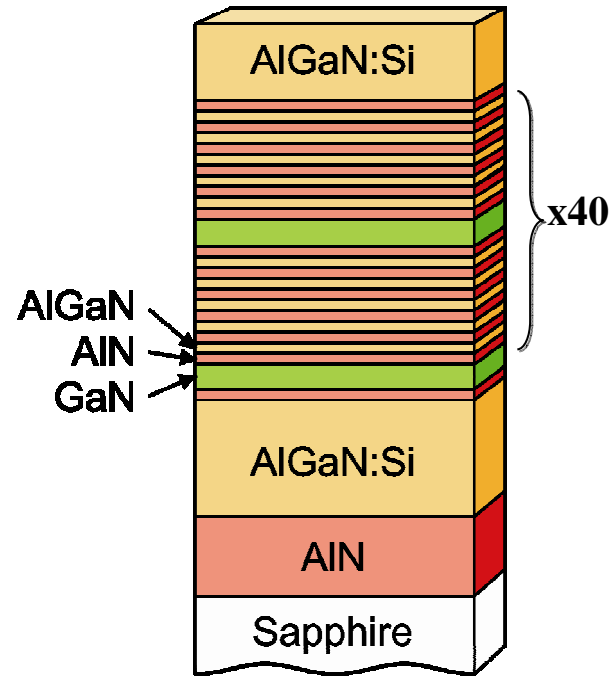


The GaN/AlGaN quantum cascade detector



- ✓ Design making use of spontaneous/piezoelectric polarization
- ✓ Active QW: 1.5 nm thick (6 ML) GaN/AlN QW
- ✓ Extractor region: 4 ML thick Al_{0.25}Ga_{0.75}N/4 ML thick AlN multiple QWs

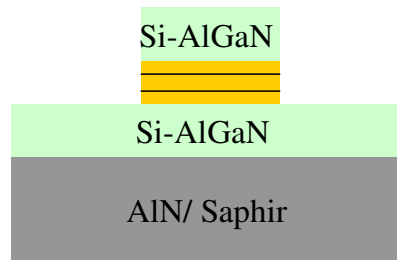
Nitride quantum cascade detector – sample structure



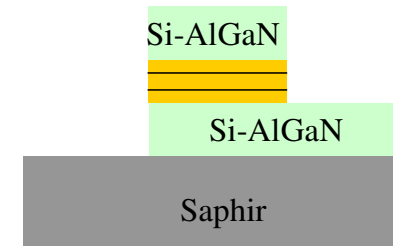
- ✓ Cascade structure with 40 periods
- ✓ $\text{Al}_{0.25}\text{Ga}_{0.75}\text{N}$ contact layers with $n = 1 \times 10^{19} \text{ cm}^{-3}$

Device processing

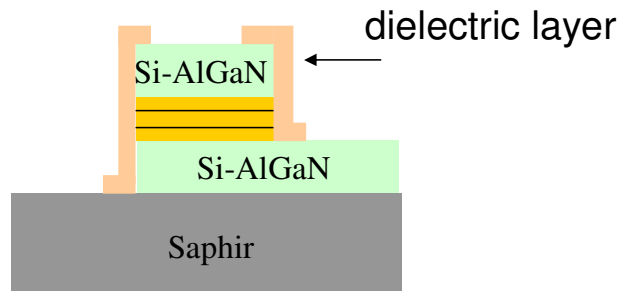
1. ICP mesa etching



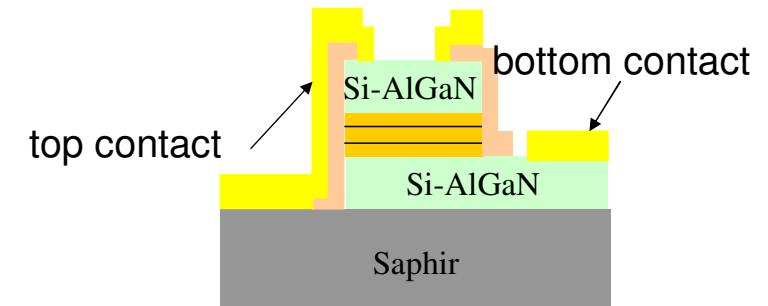
2. Second etching down to sapphire substrate



3. Dielectric ensulation



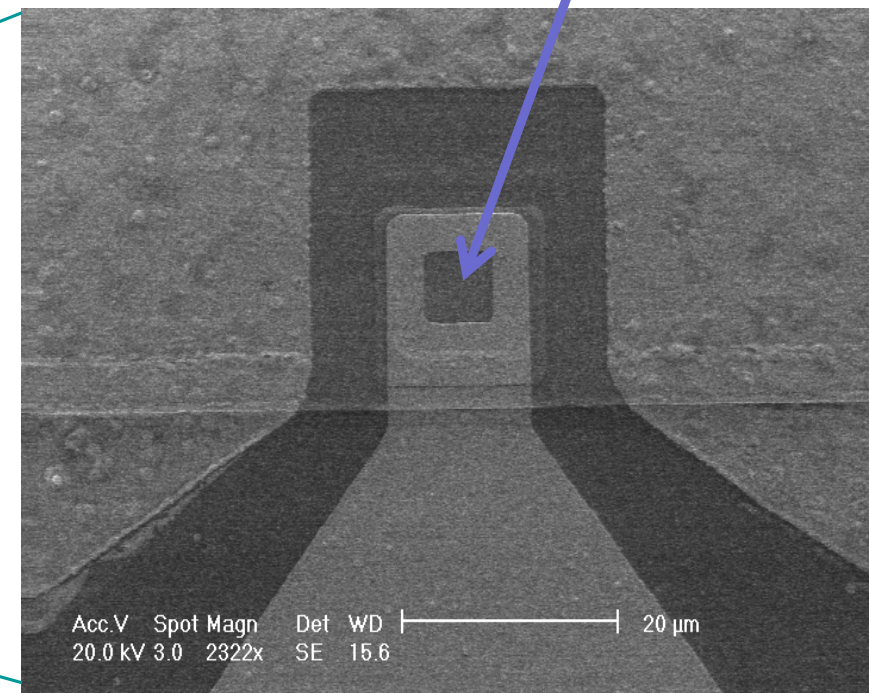
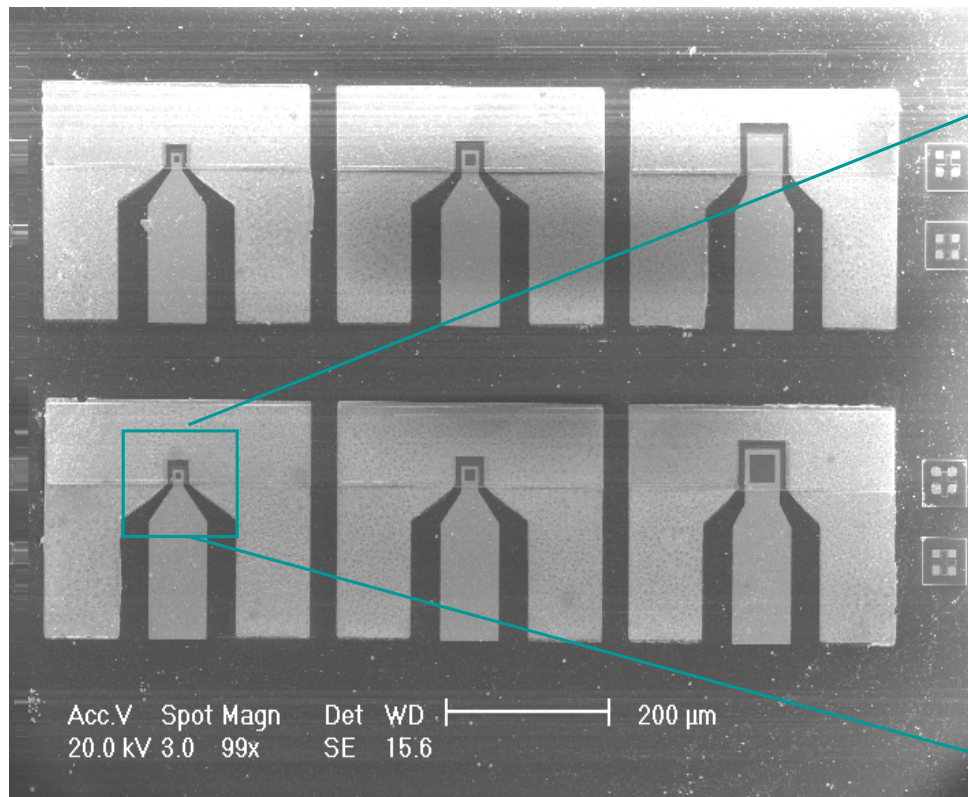
4. Bottom contact deposition + annealling
5. Top contact deposition (no annealing to avoid metal defusion)



Example of a QCD with RF contact lines

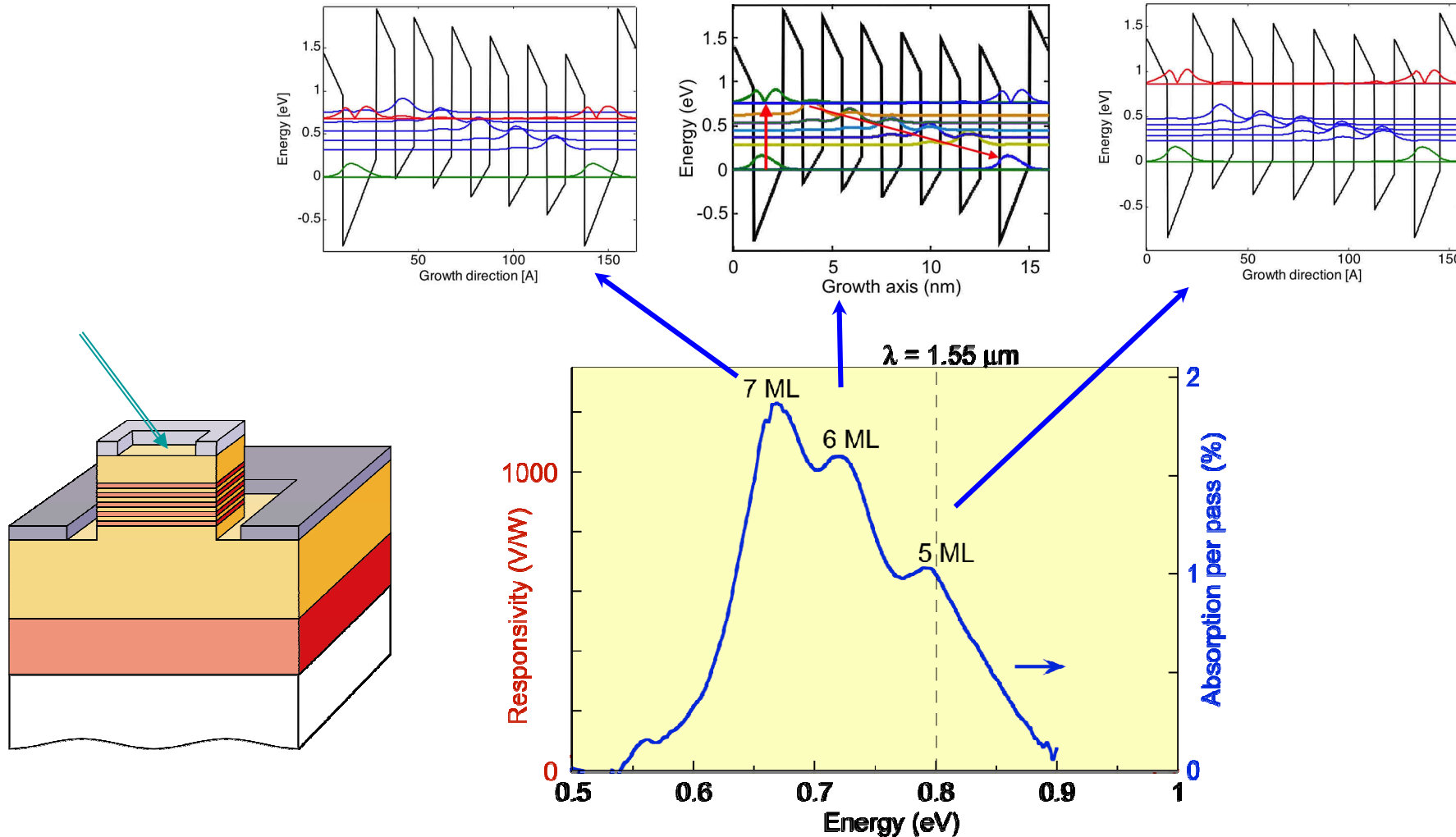


UNIVERSITÉ
PARIS-SUD 11



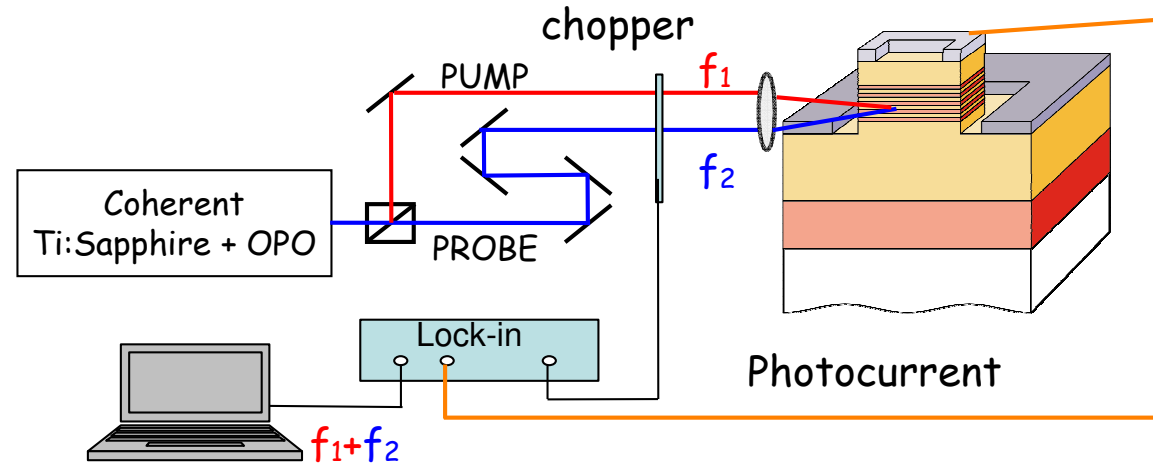
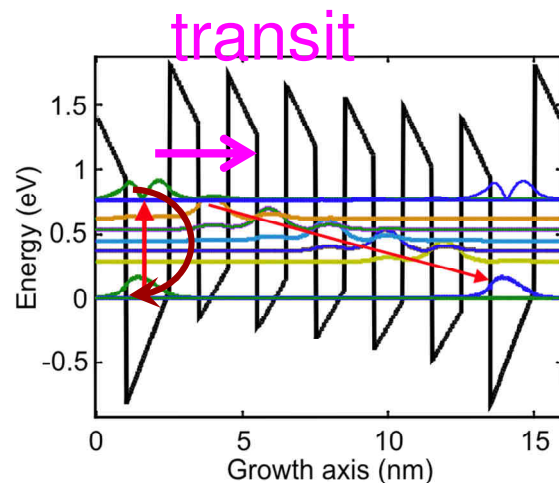
active device

Spectral response



- Peak responsivity at 300 K: 1000 V/W, 10 mA/W
- Internal quantum efficiency: number of electrons per absorbed photons 14%

Intrinsic speed of GaN QCD



$$R = \alpha \times \frac{\tau_{z1}}{\tau_{z1} + \tau_p} \times \eta \times \frac{1}{E_z}$$

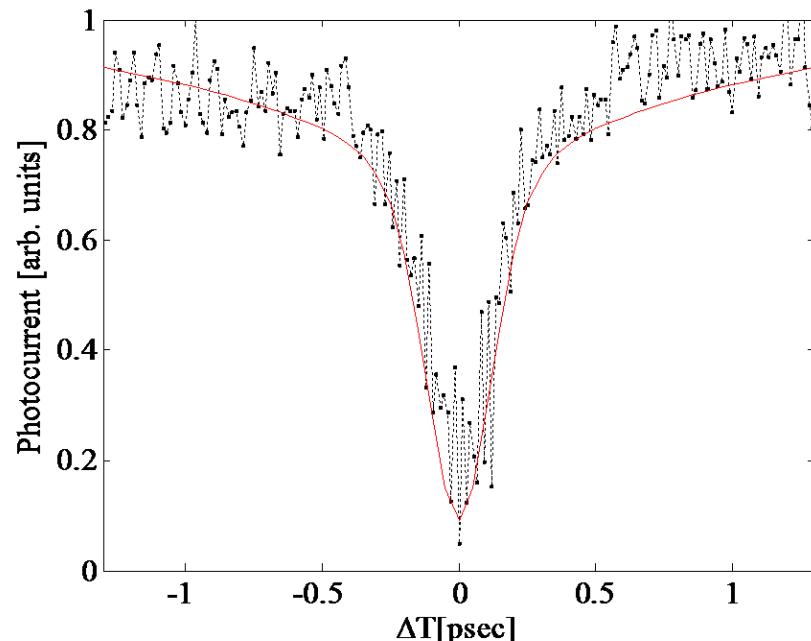
ISB relaxation time

τ_{z1}

τ_p

η extraction efficiency

Transit time (tunneling + cascade relaxation)

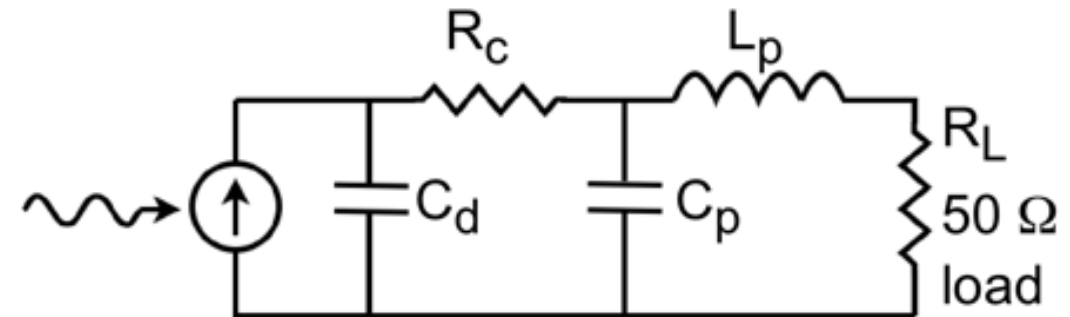
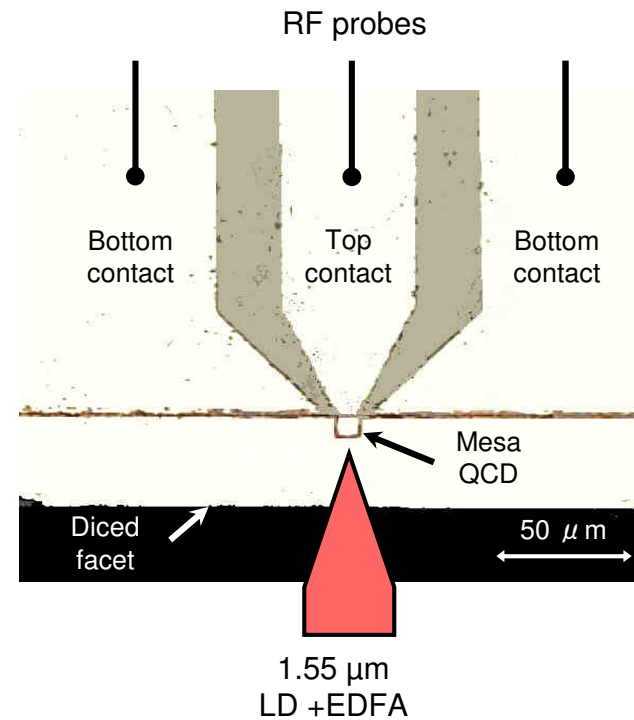


The transit time is the intrinsic speed and response limitation

Time-resolved measurements: transit time ≤ 1 ps

Available bandwidth above 100 GHz

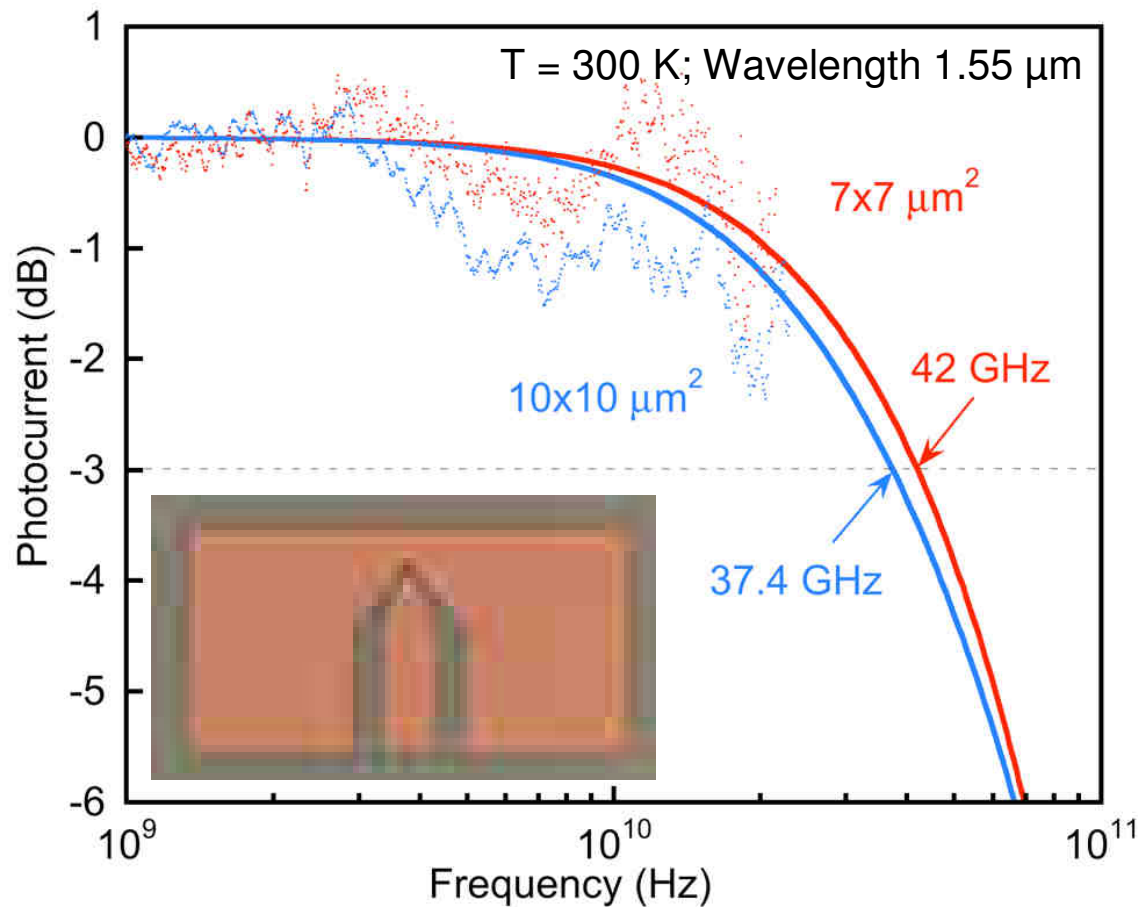
Frequency response of 1.55 μm GaN QCD



Mesa size	RC
25x25 μm^2	180 Ω 97 fF
17x17 μm^2	210 Ω 97 fF
10x10 μm^2	56 Ω 72 fF
7x7 μm^2	74 Ω 52 fF

- Impedance-matched RF access lines.
Top contact fully metallized
- Agilent component analyzer and S-parameter measurements at 300 K

Frequency response of 1.55 μm GaN QCD

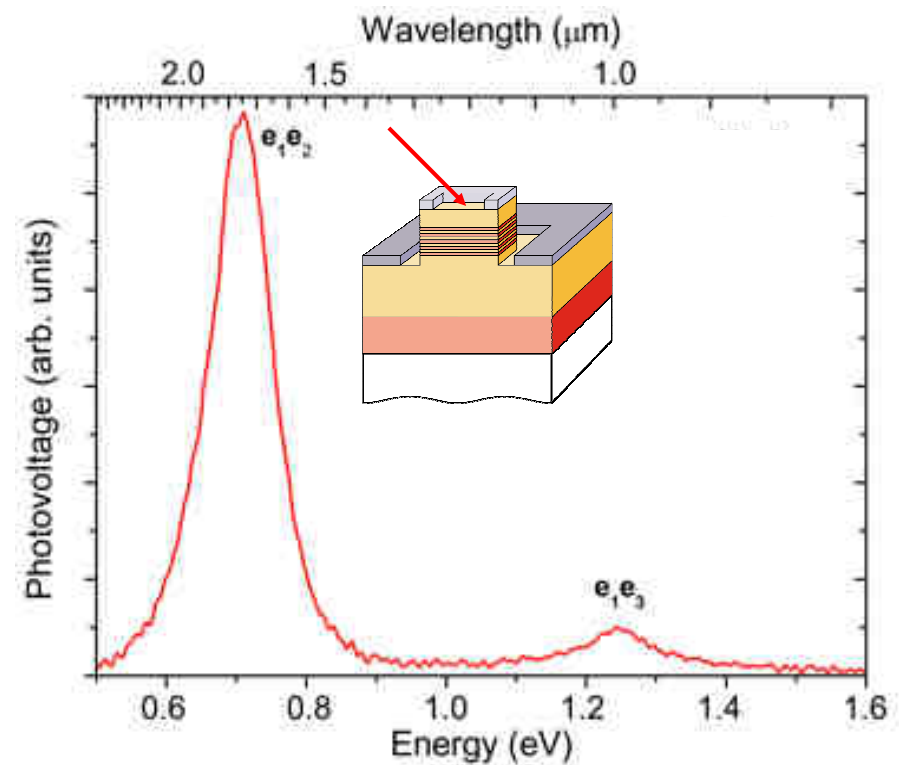
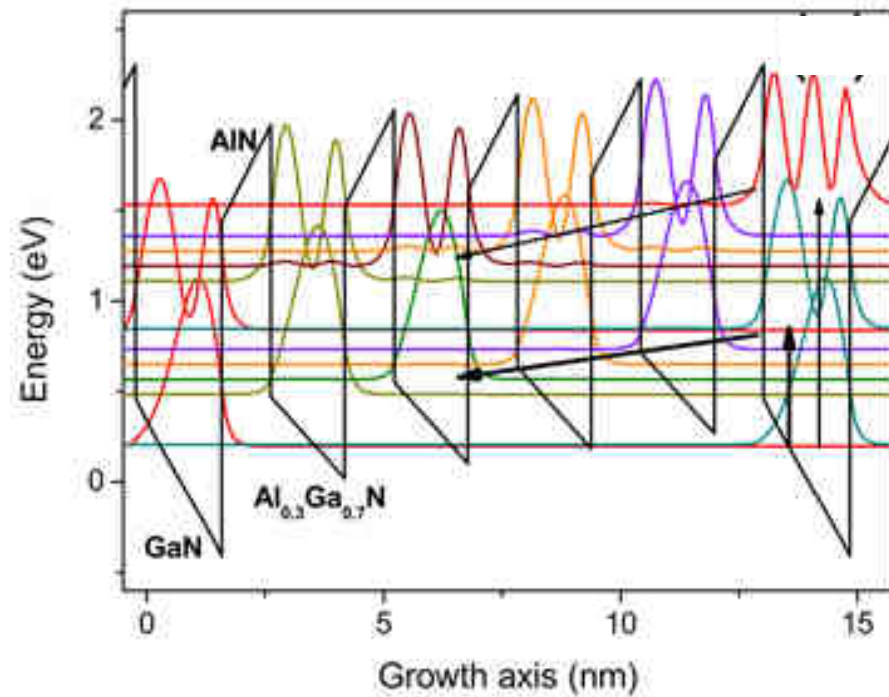


Mesa size	RC	- 3 dB frequency cut-off
25x25 μm^2	180 Ω 97 fF	6.5 GHz
17x17 μm^2	210 Ω 97 fF	11.4 GHz
10x10 μm^2	56 Ω 72 fF	38 GHz
7x7 μm^2	74 Ω 52 fF	42 GHz

Frequency response is RC limited

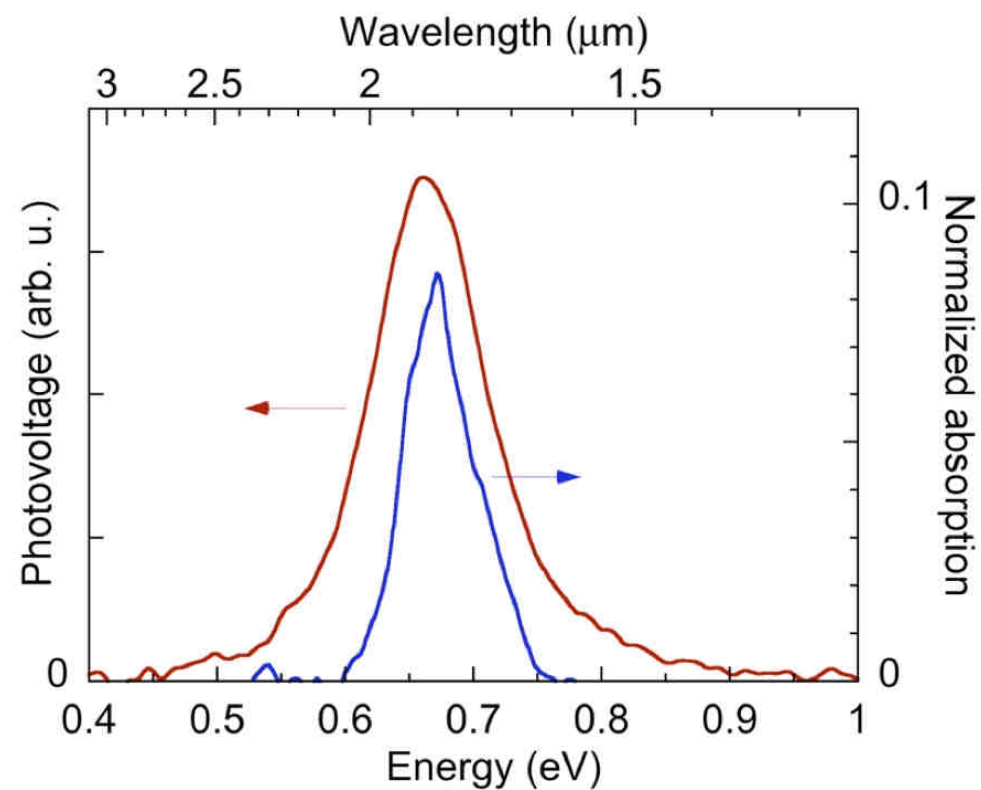
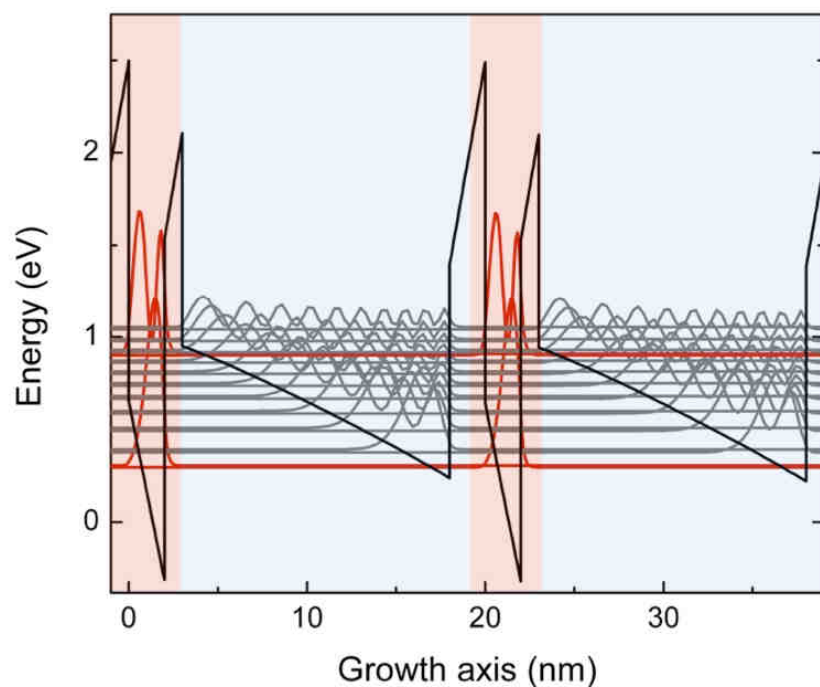
Bandwidth in excess of 40 GHz achievable

Other designs : two-color QCD



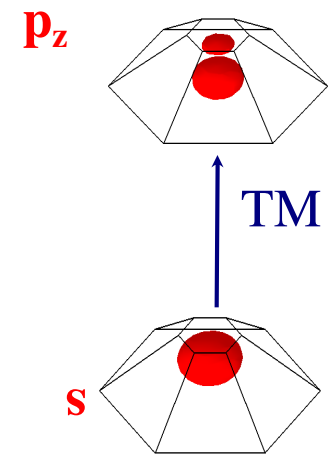
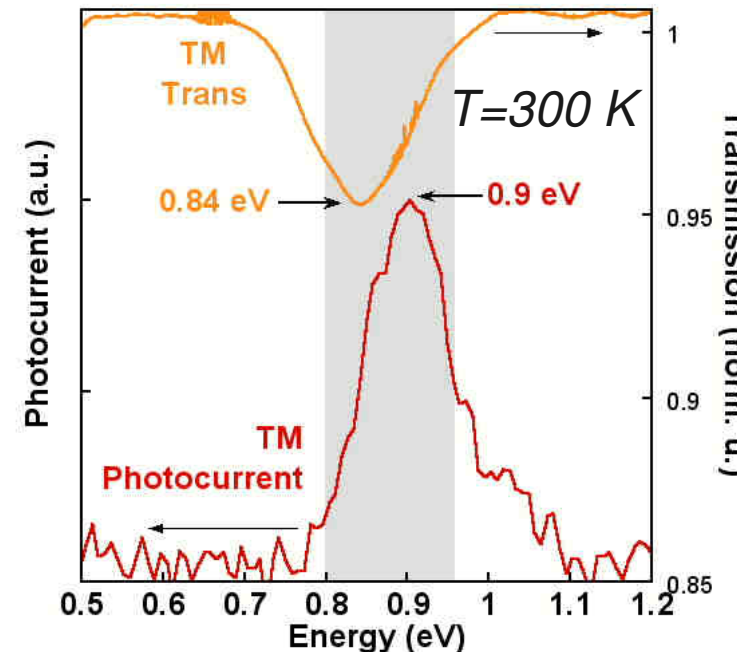
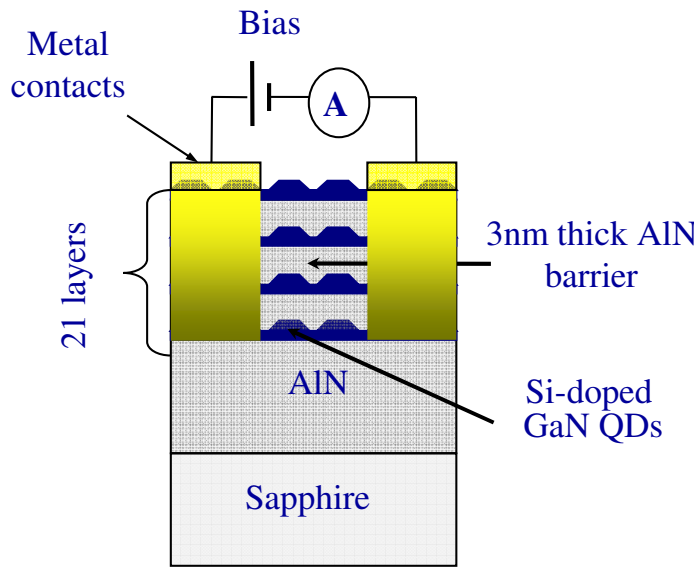
- Peak detection wavelength of 1.7 and 1 μm
- Shortest wavelength intersubband detector

Other designs : alloy extractor QCD



- Simplified and flexible design
- Interesting and robust design for GaN-based far infrared QCDs

Quantum dot intraband photodetector



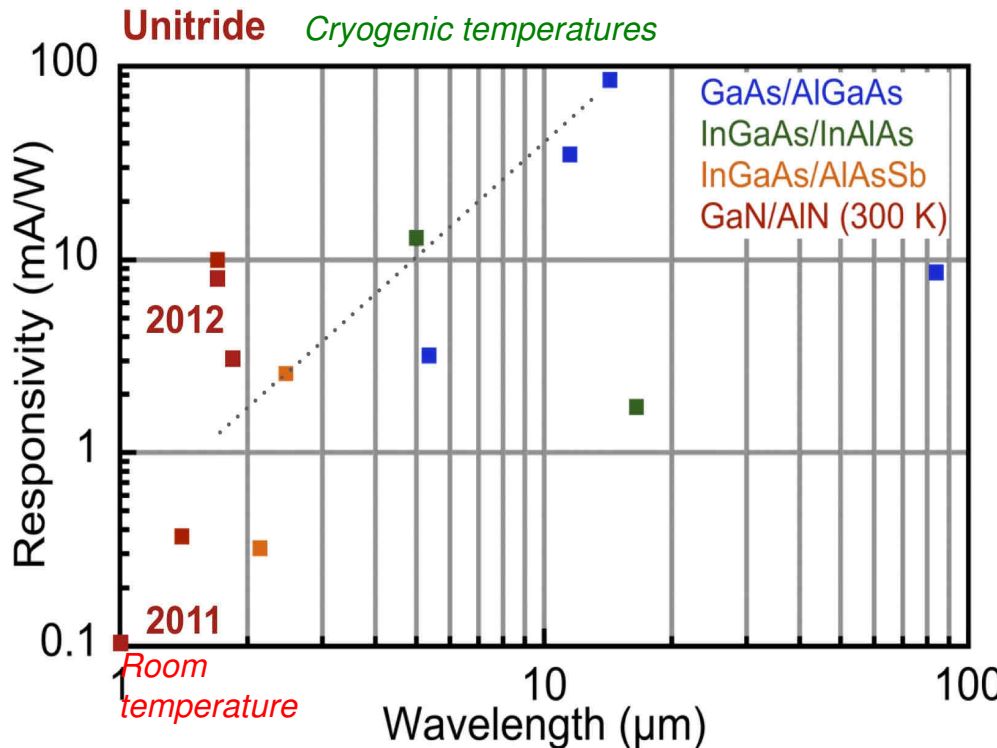
- ✓ Absorption involves the $s-p_z$ intraband transition
- ✓ p_z electrons transfer to the WL ground state via phonon absorption
- ✓ In-plane transport in the WL generates the photo-current.
- ✓ Responsivity 12 mA/W at 1.3 μ m at room temperature

L. Doyennette et al., Electron. Lett., 41, 1077, (2005)

A. Vardi et al., Appl. Phys. Lett., 88, 143101, (2006)

Comparison of nitride QCDs with state-of-the-art

- Infrared QCDs:



GaN/AlGaN QCDs offer superior responsivity at room temperature and allow for photodetection at record-short near-infrared wavelengths.

- High-speed telecom photodiodes:

Waveguide detectors at $\lambda=1.55 \mu\text{m}$	InGaAs photodiode	Ge/Si photodiode	Unitride GaN QCD
Size (μm^2)	60	78	49
$f_{-3\text{dB}}$ (GHz)	100 @ -1 V	42 @ -4 V	42 @ 0 V
Responsivity (A/W)	0.58	1	0.01
D^* (Jones)	5×10^{12}	1×10^{11}	$> 1 \times 10^{11}$

QCDs are the fastest ISB detectors developed so far, whatever the material system. The frequency performance of QCDs is comparable to that of current-technology waveguide InGaAs or Ge p-i-n photodiodes at $\lambda = 1.55 \mu\text{m}$ regarding the device size.

Nitride near-IR ISB devices

- ✓ IR photodetectors
- ✓ **Modulators**
 - ✓ Coupled QW modulator
 - ✓ Depletion modulator
 - ✓ All-optical switches
- ✓ Light emitters

Electro-optical modulators : Motivations

Potential advantages of ISB electro-optical modulators

- intrinsically very fast - large spectral bandwidth
- possibility to obtain negative chirp parameter
- insensitive to saturation
- potentially low drive voltage (symmetric around zero bias)

Theoretical paper by *P. Holmström, IEEE J Quant Elec, 42, 810 (2006)*

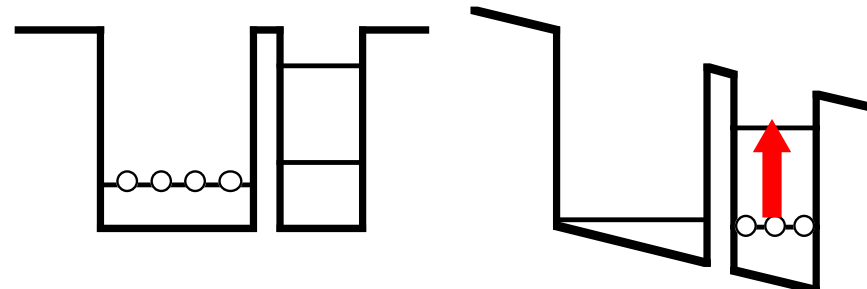
First proposal by *N. Vodjdani et al., APL 59, 555 (1991)* in GaAs/AlGaAs coupled quantum wells operating at $\sim 10 \mu\text{m}$

Further optimization in Mid-IR :

H. C. Liu, et al., J. Appl. Phys., 70, 7560 (1991)

E. Dupont, et al., Appl. Phys. Lett. 62, 1907 (1993)

J. Y. Duboz, et al., Appl. Phys. Lett. 70, 1569 (1997)

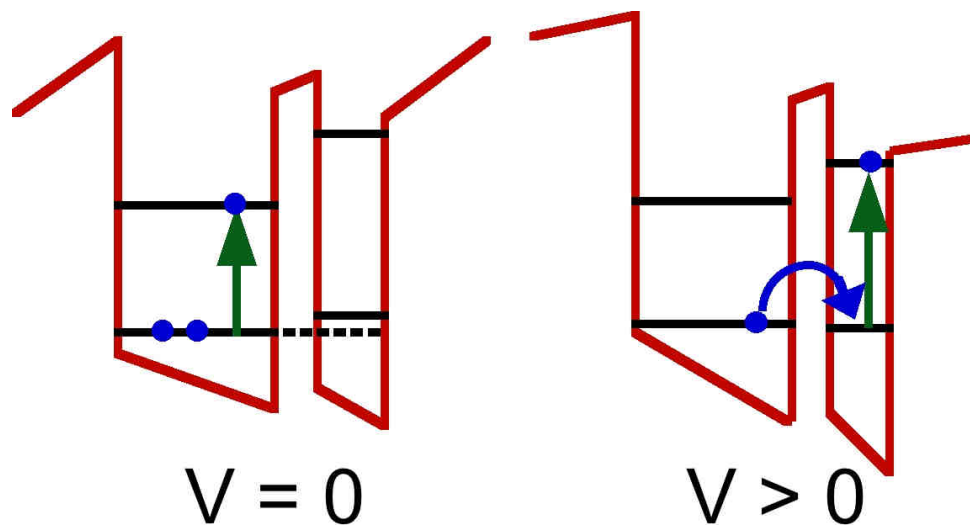


Charge-transfer electro-optical modulator based on GaN/AlN coupled QWs

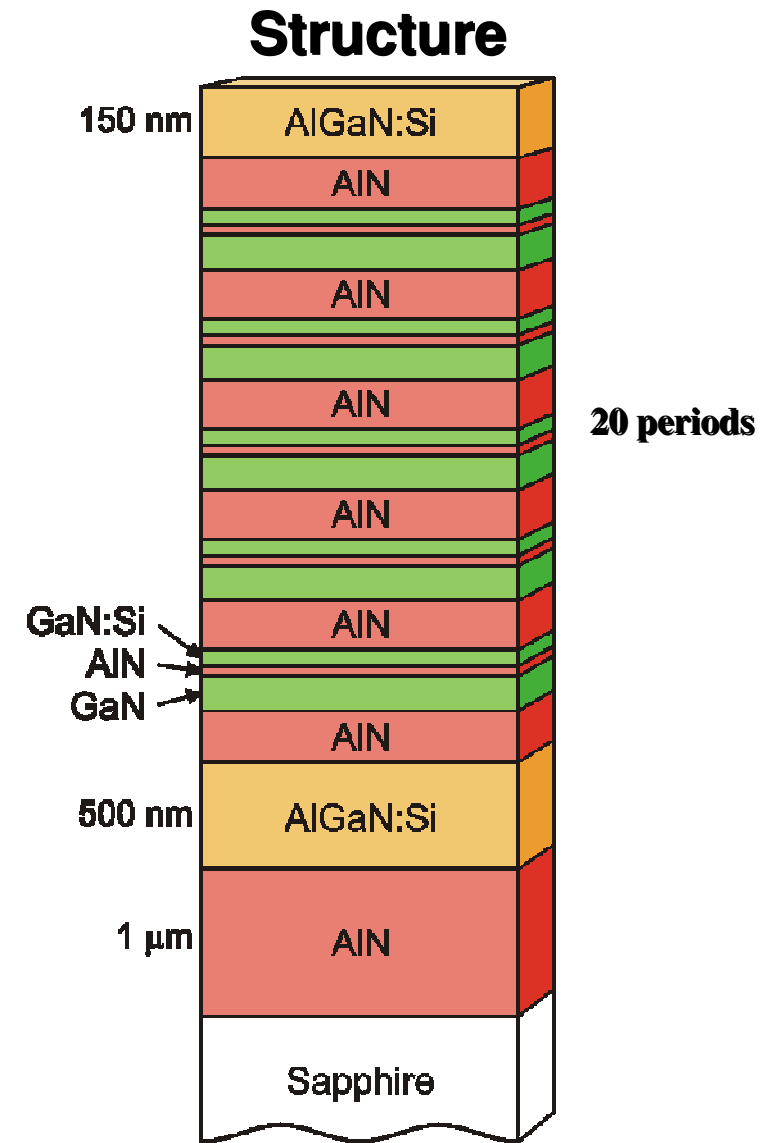


UNIVERSITÉ
PARIS-SUD 11

Operation principle

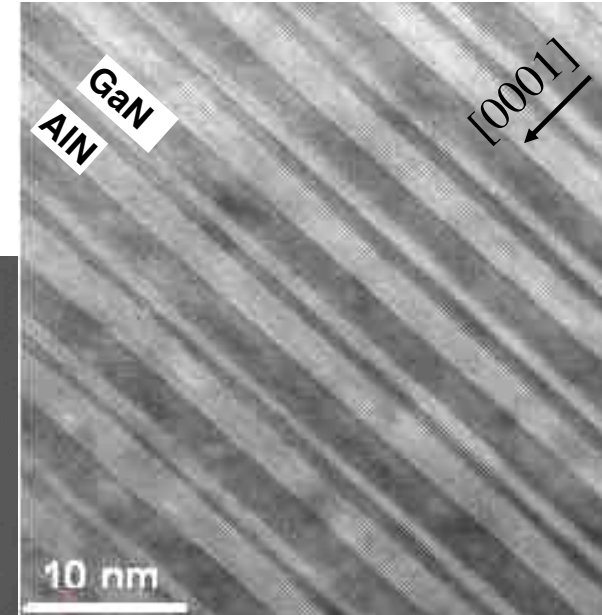
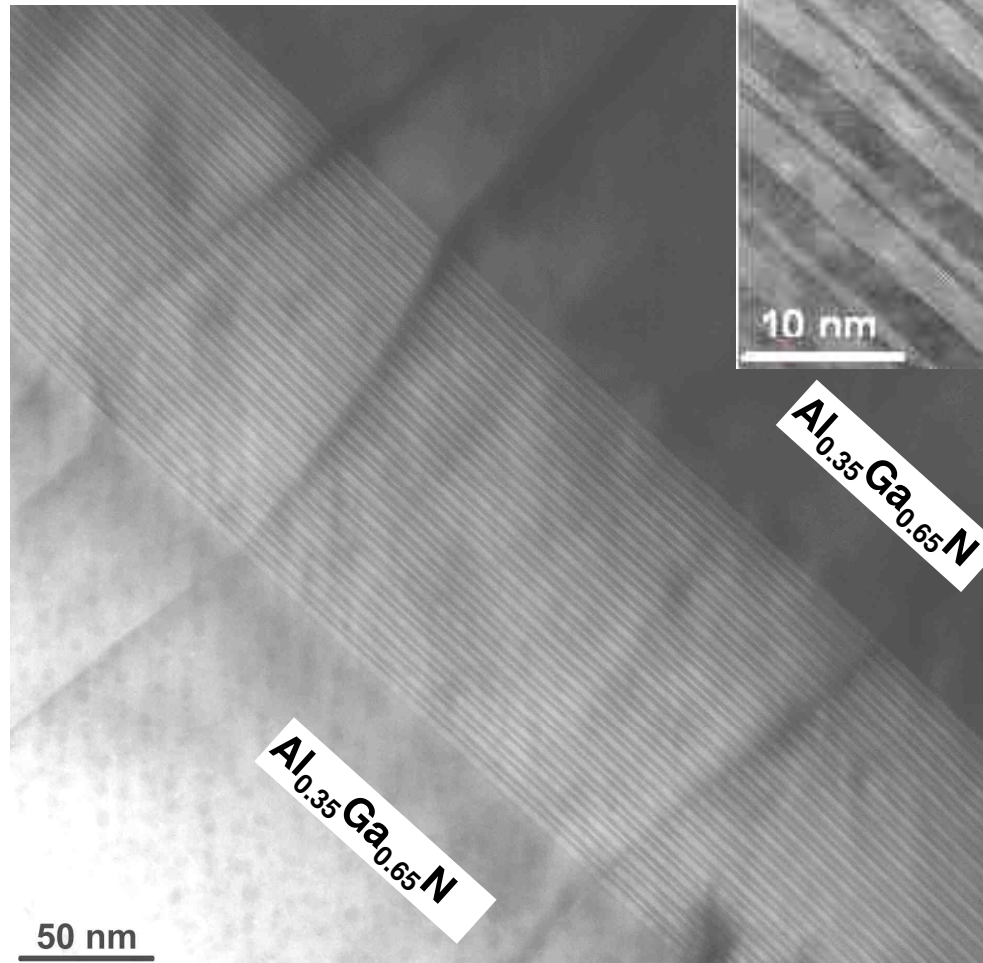


Electron transfer between two wells



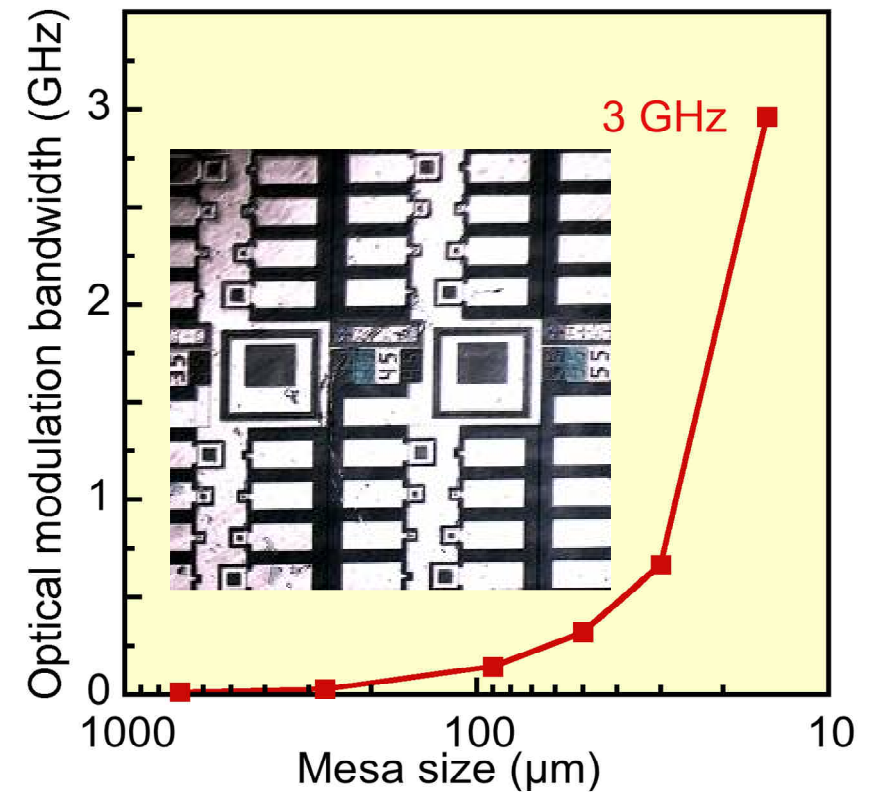
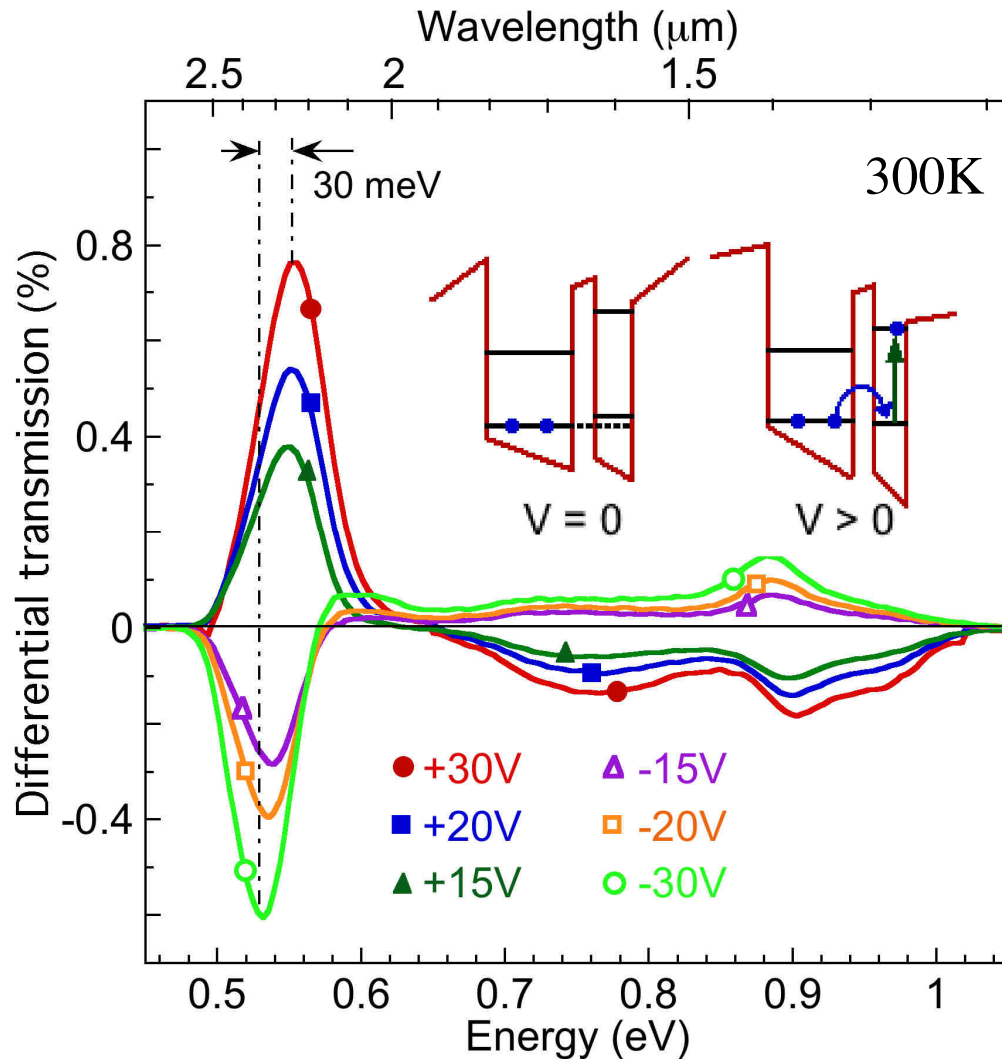
Structural characterization

- ✓ No cracks
- ✓ Sharp GaN/AlN interfaces
- ✓ Good periodicity



*PA-MBE E Monroy CEA,
HRTEM images by M. Albrecht*

Spectroscopy and bandwidth



L. Nevou et al., *APL* **90**, 121106 (2007)

N. Kheiroudin et al., *IEEE PTL* **20**, 724 (2008)

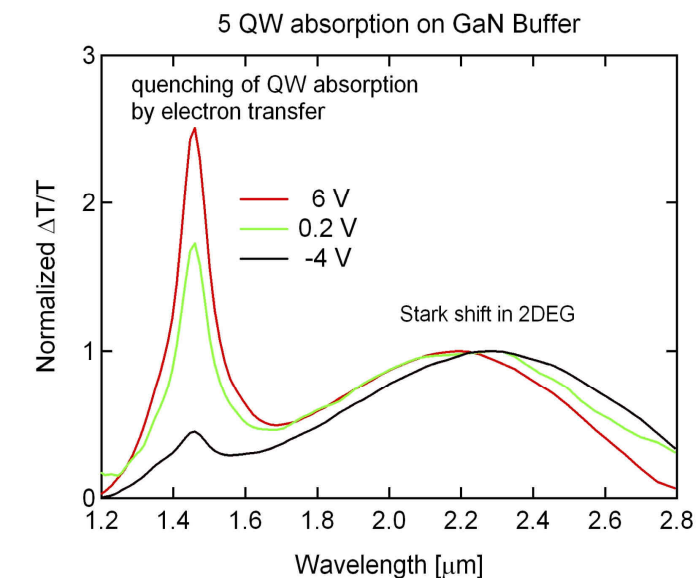
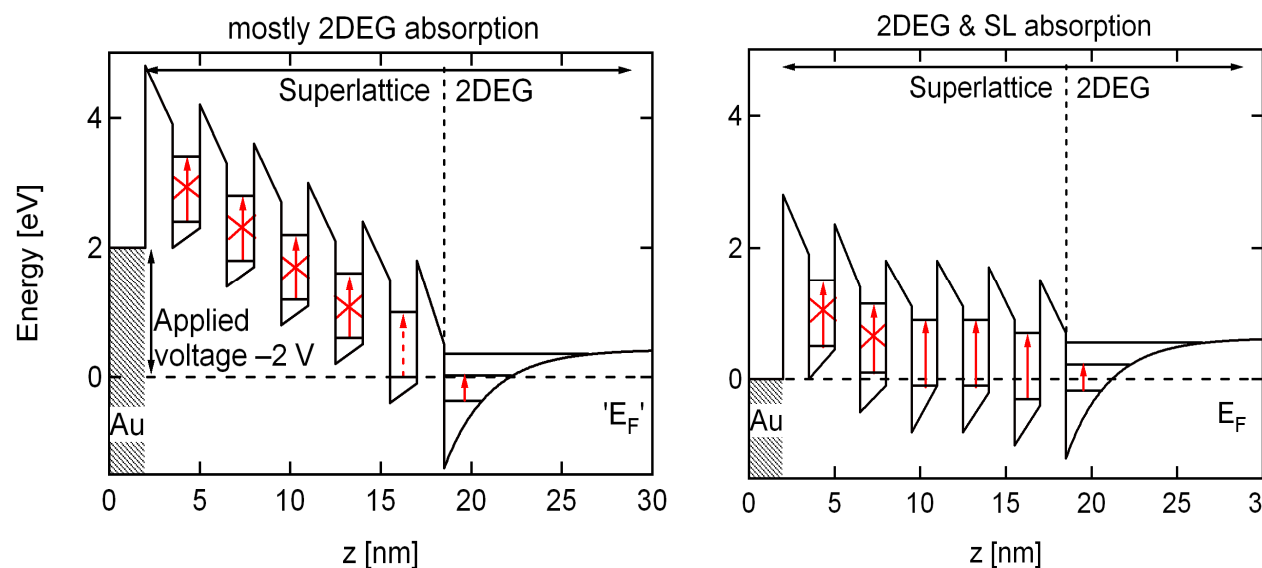
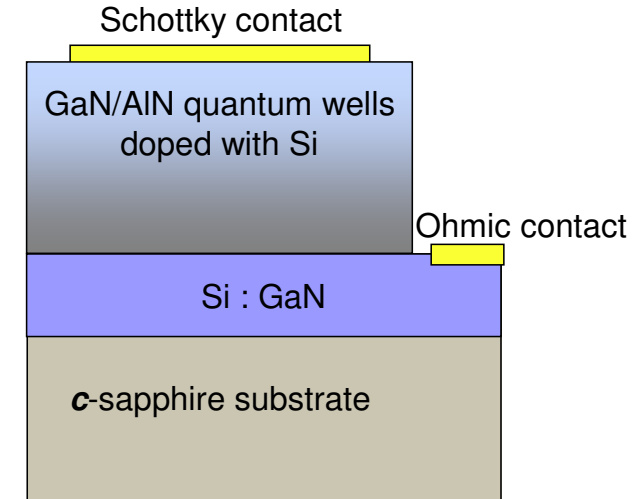
✓ Optical modulation bandwidth 3GHz @ 1.55 μm limited by RC constant

GaN/AlN depletion modulator

Depletion of quantum wells by applying bias to the Schottky contact

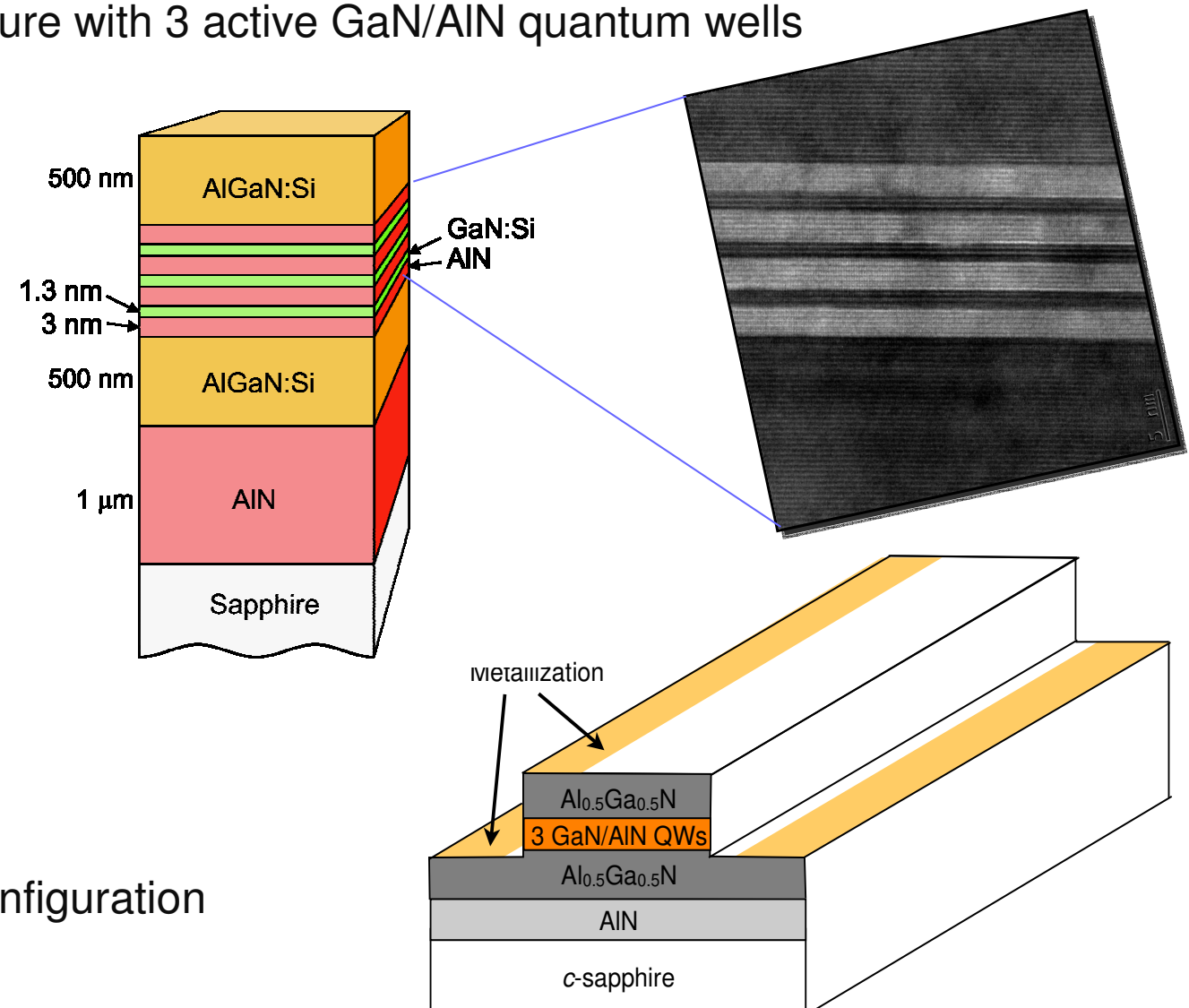
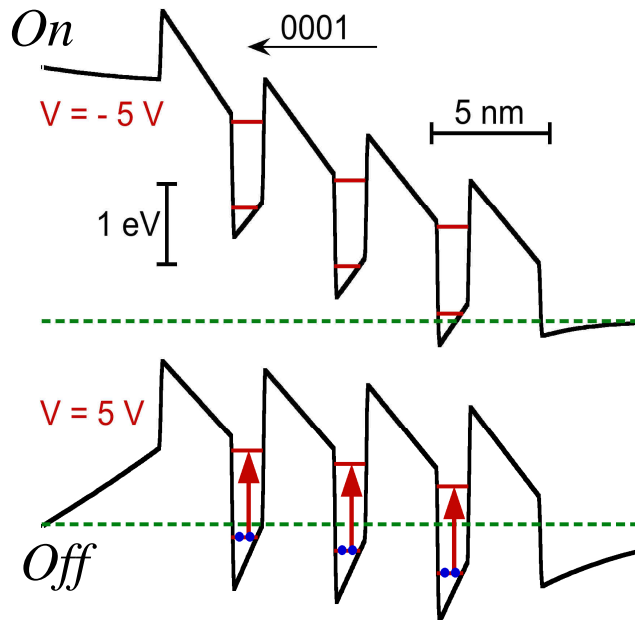
Quenching of the QW absorption

Stark shift of the 2DEG absorption



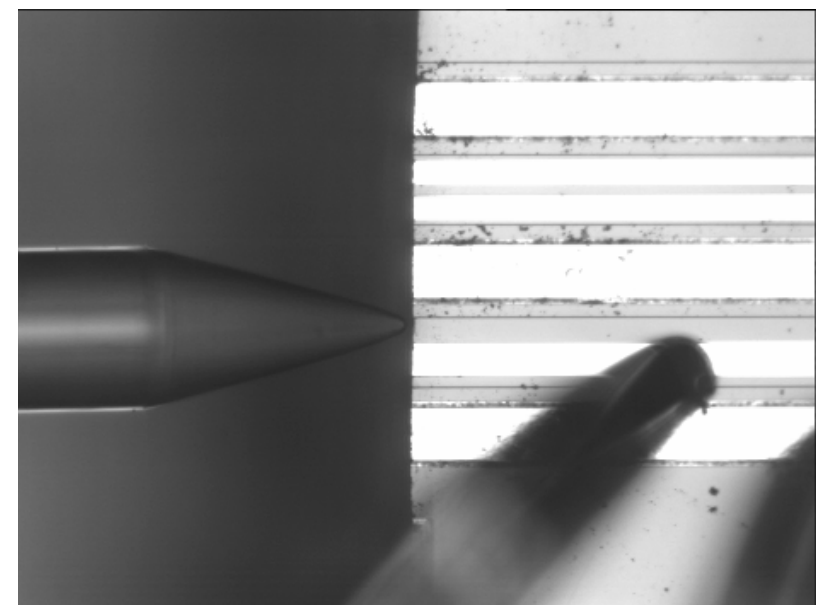
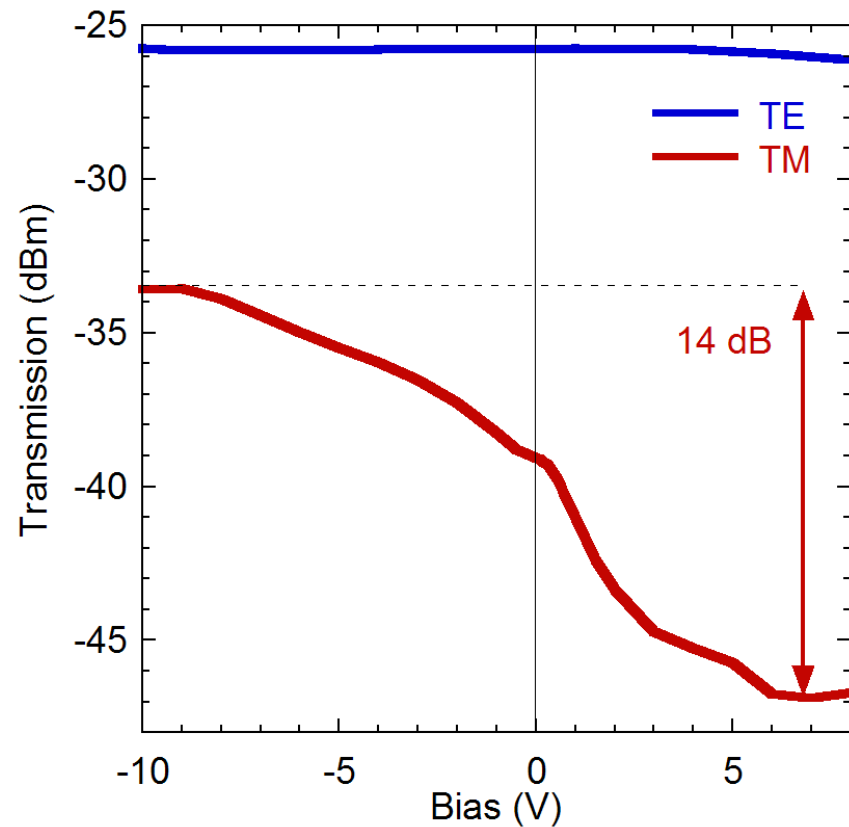
GaN/AlN waveguide depletion modulator

Depletion modulator structure with 3 active GaN/AlN quantum wells



Waveguide coupling configuration

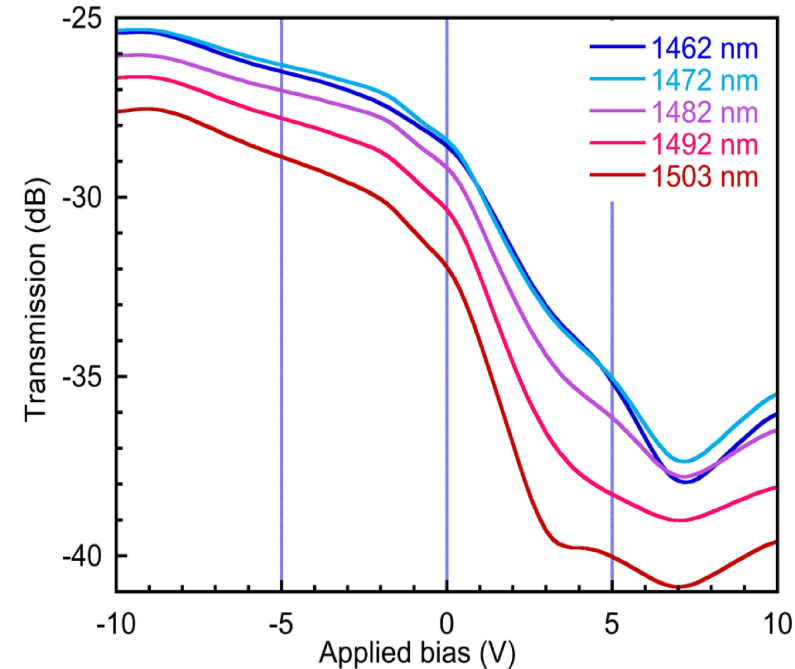
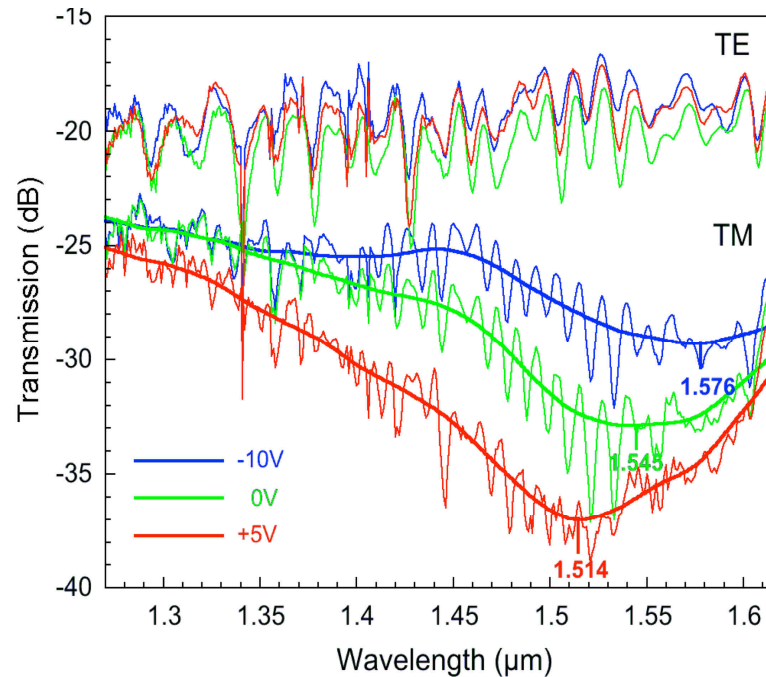
Modulation depth



- ✓ Modulation depth at $\lambda = 1.5 \mu\text{m}$ of 14 dB (10^{-14} bit error rate)
- ✓ Wide spectral width: 1.35 to 1.6 μm

Demonstration of waveguide amplitude and phase modulation

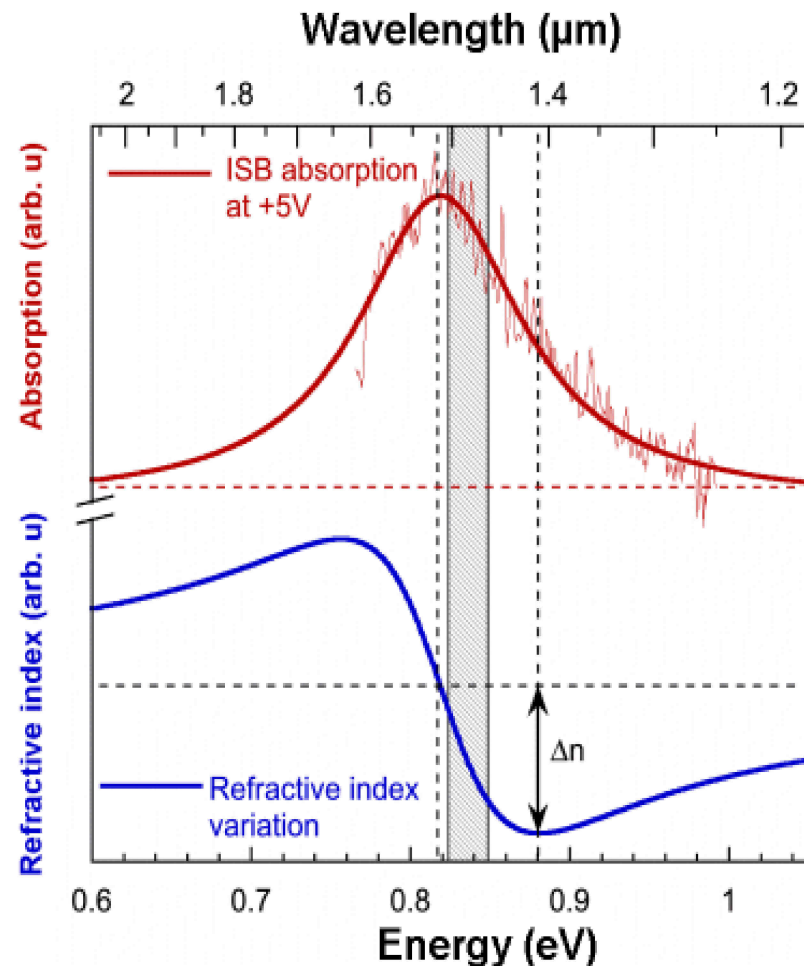
- Waveguide depletion modulator transmission at RT versus wavelength and bias.



- Demonstration of ISB absorption modulation due to population/depletion of active QWs and to the quantum confined Stark effect.
- Modulation depth as large as 14 dB.

Phase modulation with ISB transitions

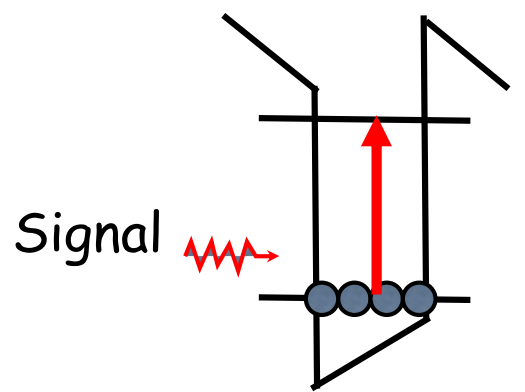
PM is directly used for phase shift encoding or can be converted to amplitude modulation with a Mach-Zehnder interferometer



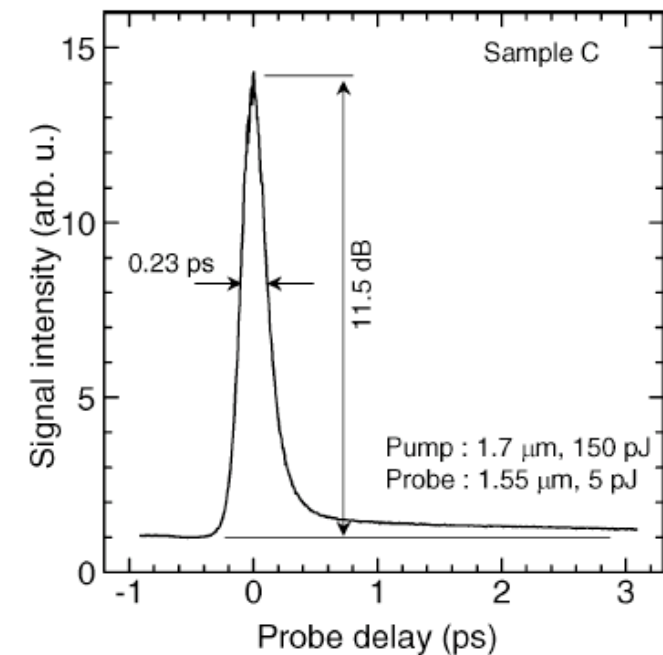
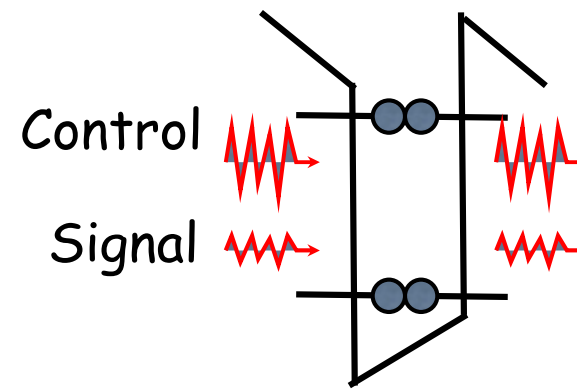
- Fourier analysis of mode beating interferences in the transmission spectrum.
- The maximum refractive index variation in the –5 V to 5 V bias range is found to be : $\Delta n/n \sim 5 \times 10^{-3}$ at 1.46 μm .
- This value achieved with only 3 QWs is comparable to the state-of-the-art value reported for InP-based phase modulators

@ 10 μm – E. Dupon et al., *APL* 62, 1907 (1993)
@ 1.5 μm – A. Lupu et al., *Optics Express* (2012)

Ultrafast all-optical switches based on GaN/AlN quantum wells



Absorption saturation



- ✓ Absorption recovery time 150-400 fs @ 1.5 μ m
- ✓ Key device for multi-Tbit/s all-optical processing
- ✓ Intense work dedicated to GaN/AlN QWs
- ✓ Switching energy 20-150 pJ

Iizuka et al., IEEE JQE 42, 765 (2006).

N. Iizuka et al., Appl. Phys. Lett. 77, 648 (2000)

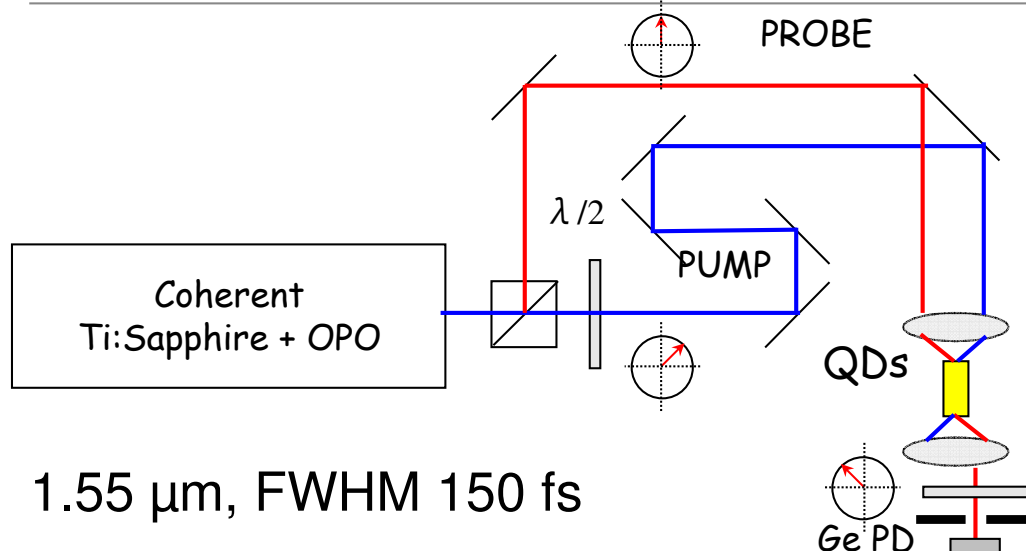
J. D. Heber et al., Appl. Phys. Lett. 81, 1237 (2002)

J. Hamazaki et al., Appl. Phys. Lett. 84, 1102 (2004)

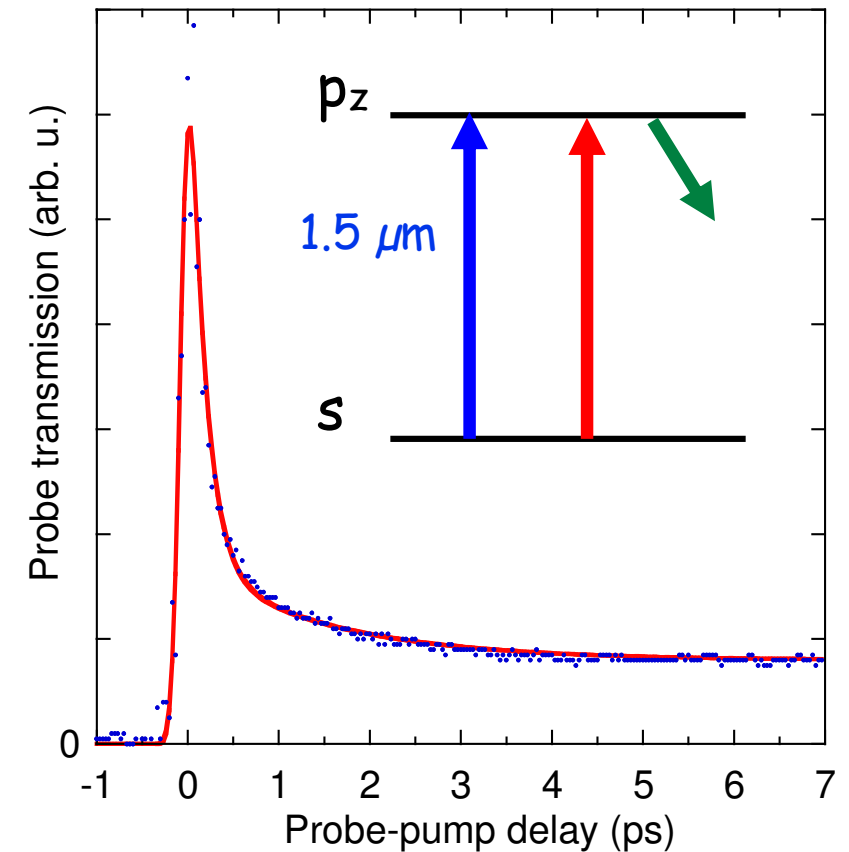
N. Iizuka et al., J. Appl. Phys. 99, 093107 (2006)

Yang Li et al., Optics Express, 15, 17922 (2007)

Carrier relaxation in GaN/AlN QDs



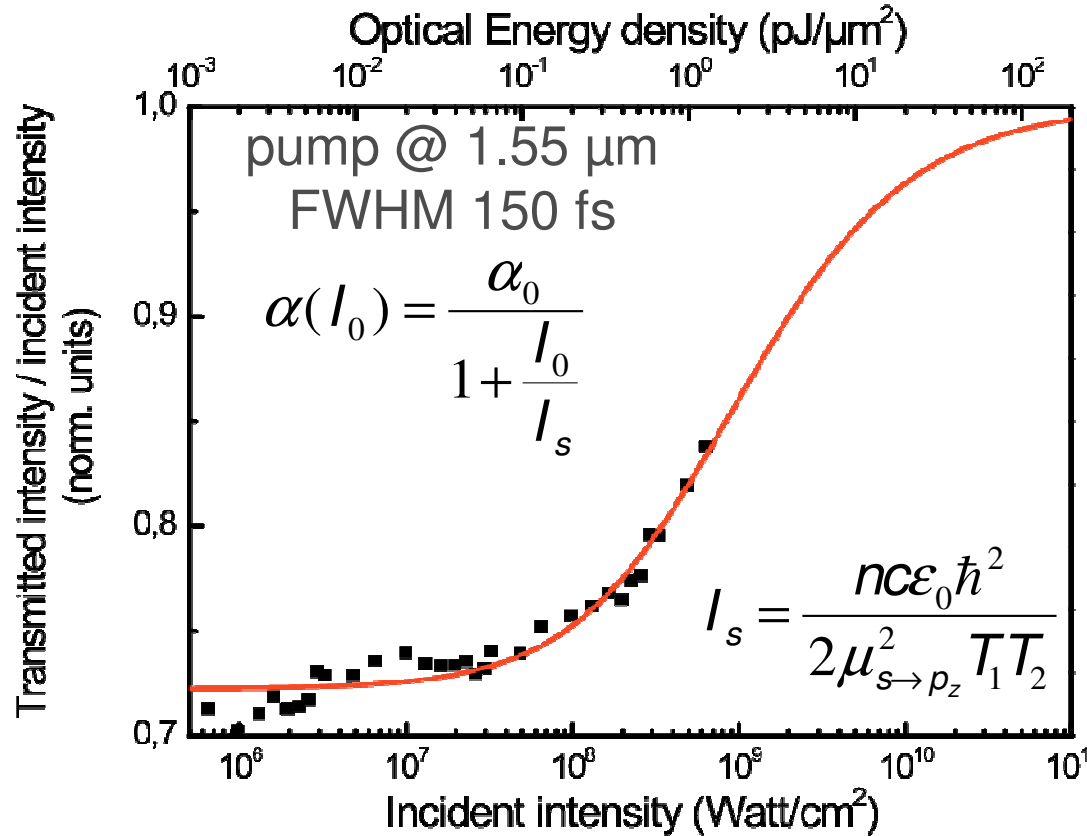
1.55 μm , FWHM 150 fs



Intraband absorption recovery exhibits two-exponential decay

- ✓ Electron lifetime in p_z state $T_1=165$ fs
- ✓ Thermalisation of electrons in the ground state 1.5 ps

Intraband absorption saturation of GaN/AlN QDs



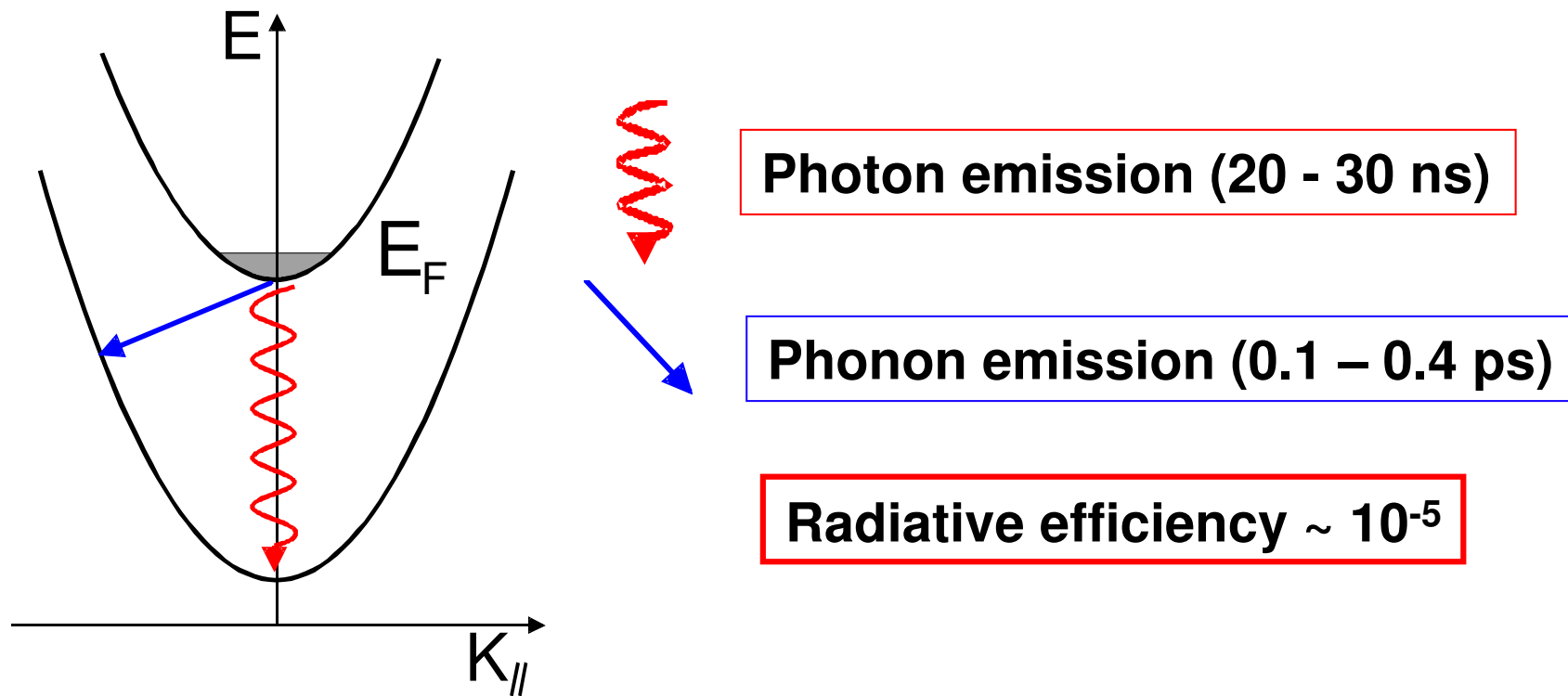
- ✓ Saturation intensity < 130 MWatt/cm² (saturation energy density < 0.27 pJ/µm²) is smaller than for QWs and comparable with IB devices on InP
- ✓ Simulation for a single quantum dot $I_s = 9 \text{ MW}/\text{cm}^2$
- ✓ QD-based all-optical switches: as fast as QWs, but with low control energy

Nitride near-IR ISB devices

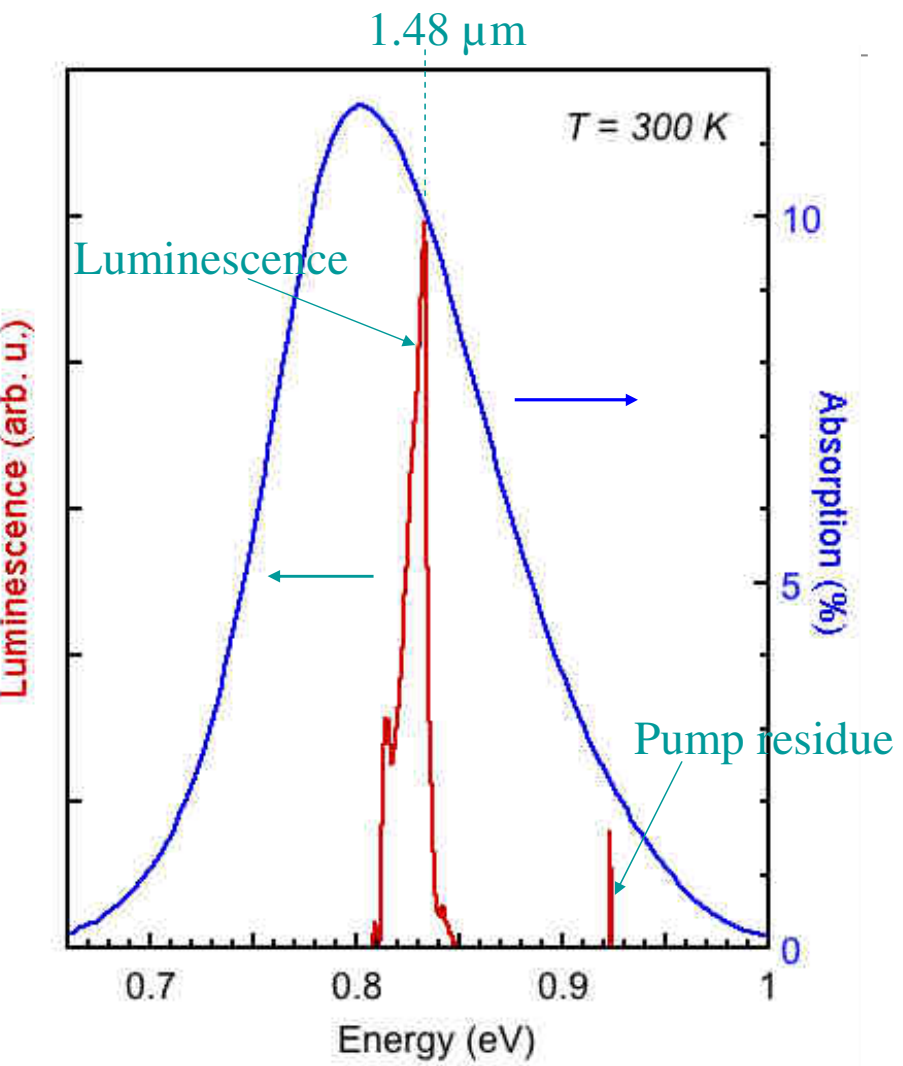
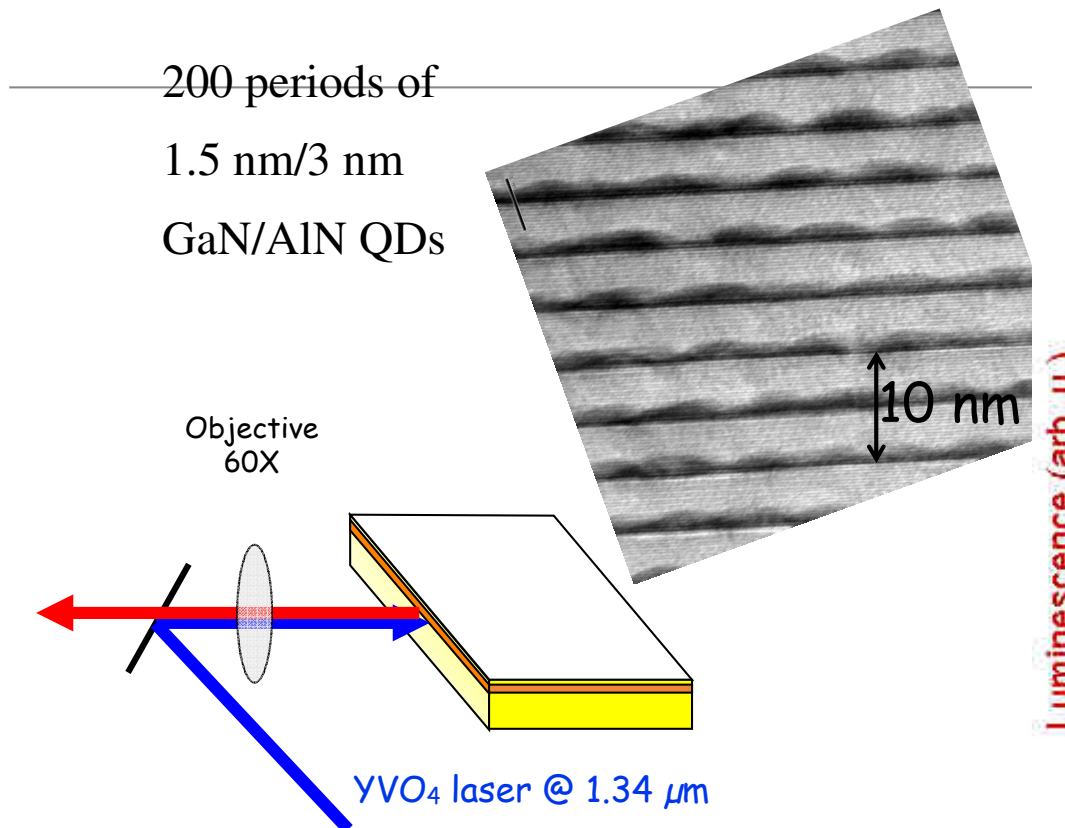
- ✓ IR photodetectors
- ✓ Modulators
 - ✓ Coupled QW modulator
 - ✓ Depletion modulator
 - ✓ All-optical switches
- ✓ **Light emitters**

ISB light emission in nitrides

- ✓ Internal quantum efficiency τ_{nr}/τ_r is very weak (radiative lifetime $\tau_r \sim 20-30$ ns, non-radiative scattering time $\tau_{nr} \sim 100-400$ fs)
- ✓ ISB transitions make bad LEDs but good lasers (high oscillator strength → high gain)

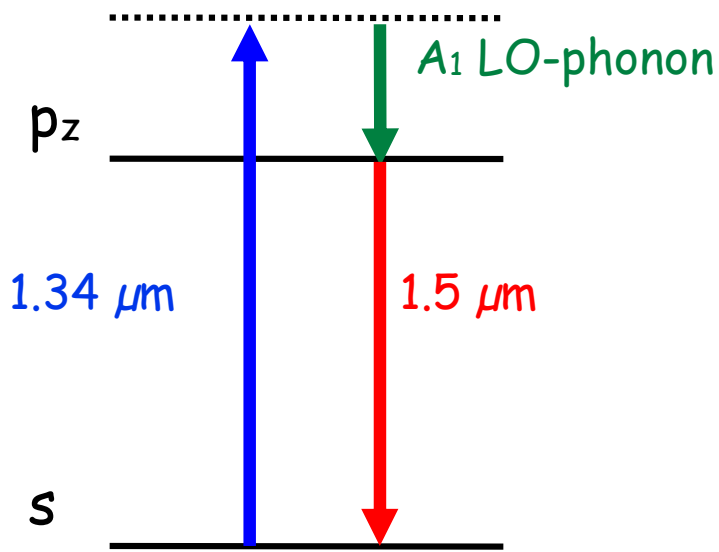
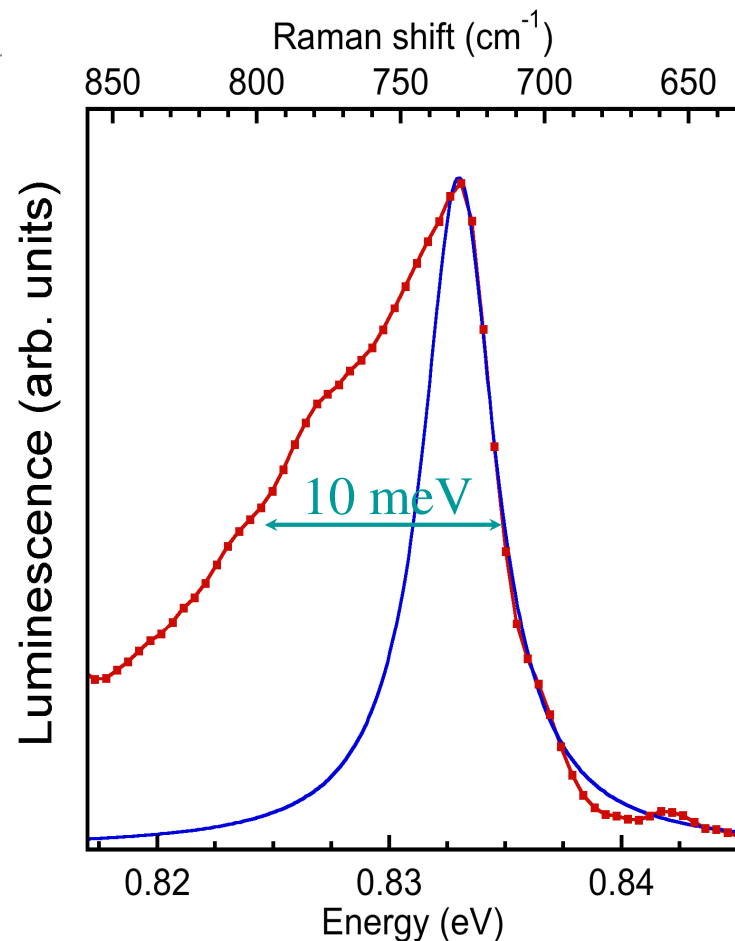


GaN/AlN quantum dot intraband emission



- ✓ TM-polarized p_z-s emission at **1.48 μm** only under TM-polarized excitation
- ✓ Energy shift 90 meV - GaN LO phonon
- ✓ T = 300 K

Intraband emission mechanism

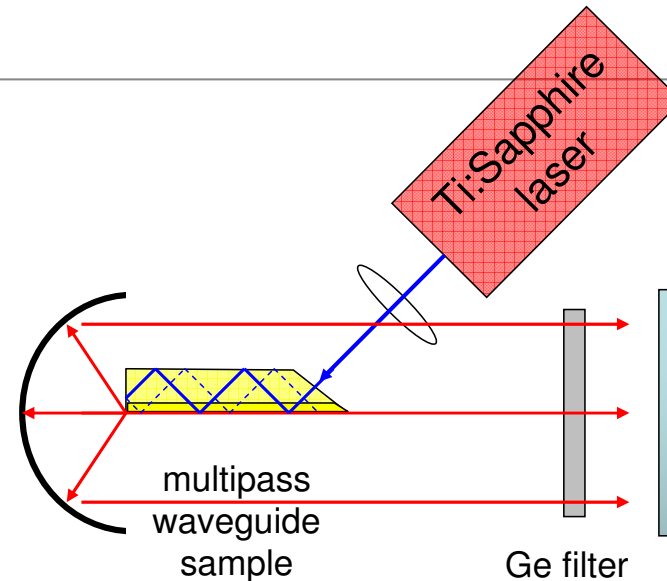
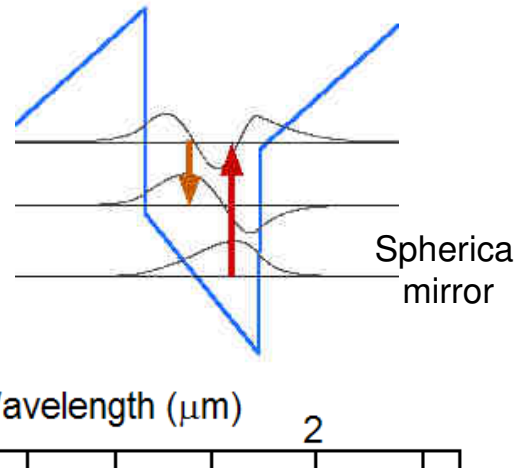


- ✓ Emission process is selective in terms of dot size
- ✓ FWHM for a single GaN QD < 10 meV (hole-burning experiments by *G. Cassabois et al.* ~15 meV at 300K, FWHM QWs 40 meV)
- ✓ Population inversion is achievable

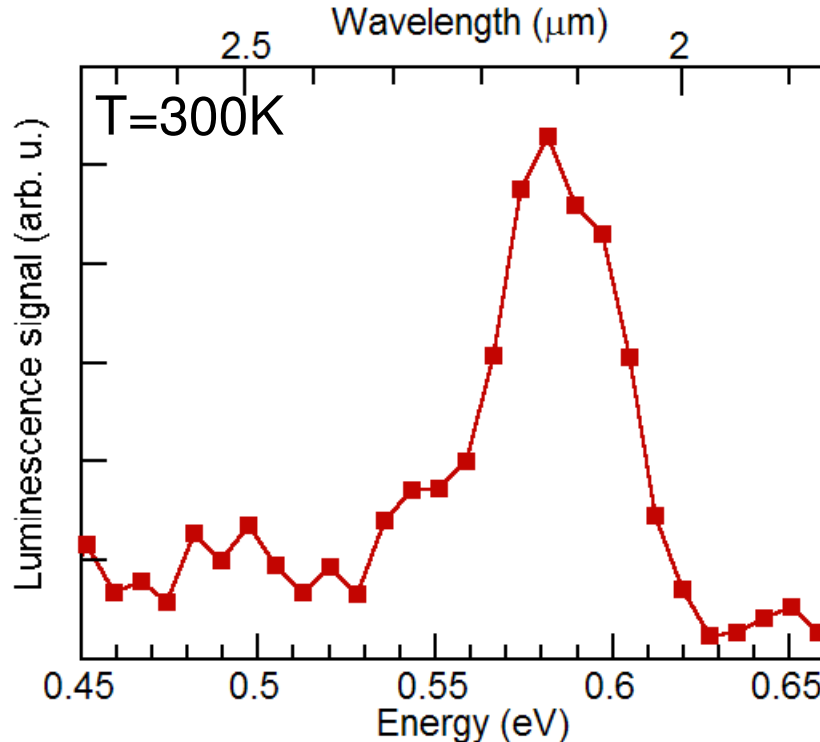
ISB luminescence from GaN/AlN QWs



200 periods 2nm
GaN / 3 nm AlN
1 μ m AlN
c-sapphire



FTIR
Spectrometer
InAs Detector



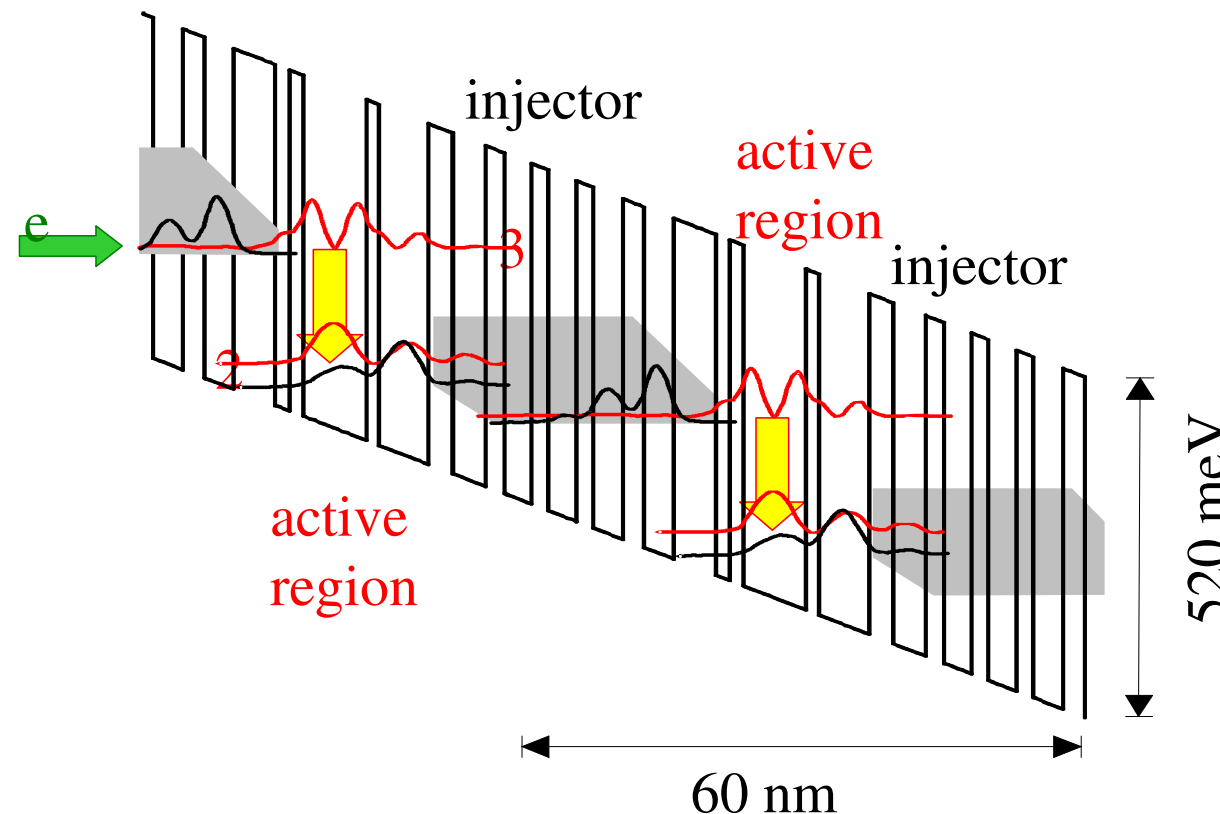
- ✓ Excitation resonant with e_1e_3 ISB absorption
- ✓ ISB emission at record short wavelength 2.13 μ m
- ✓ Room temperature
- ✓ Internal quantum efficiency 0.3 μ W /Watt of pump power

Why nitrides can make high temperature THz Quantum Cascade Lasers ?

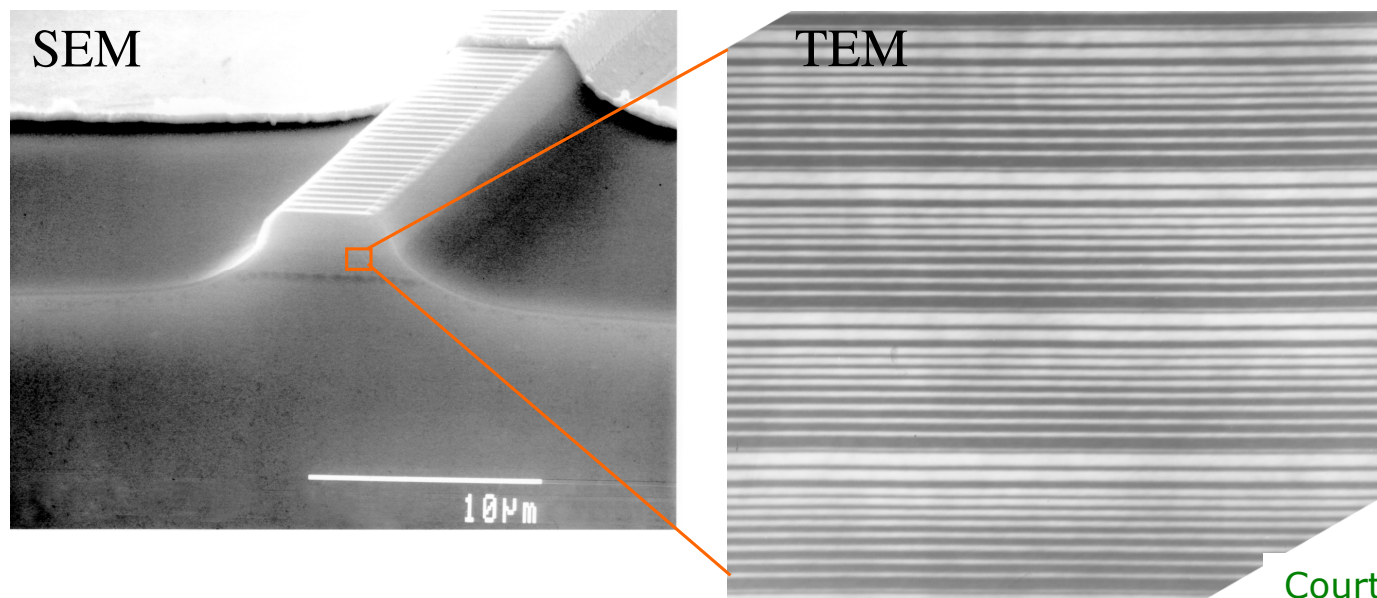
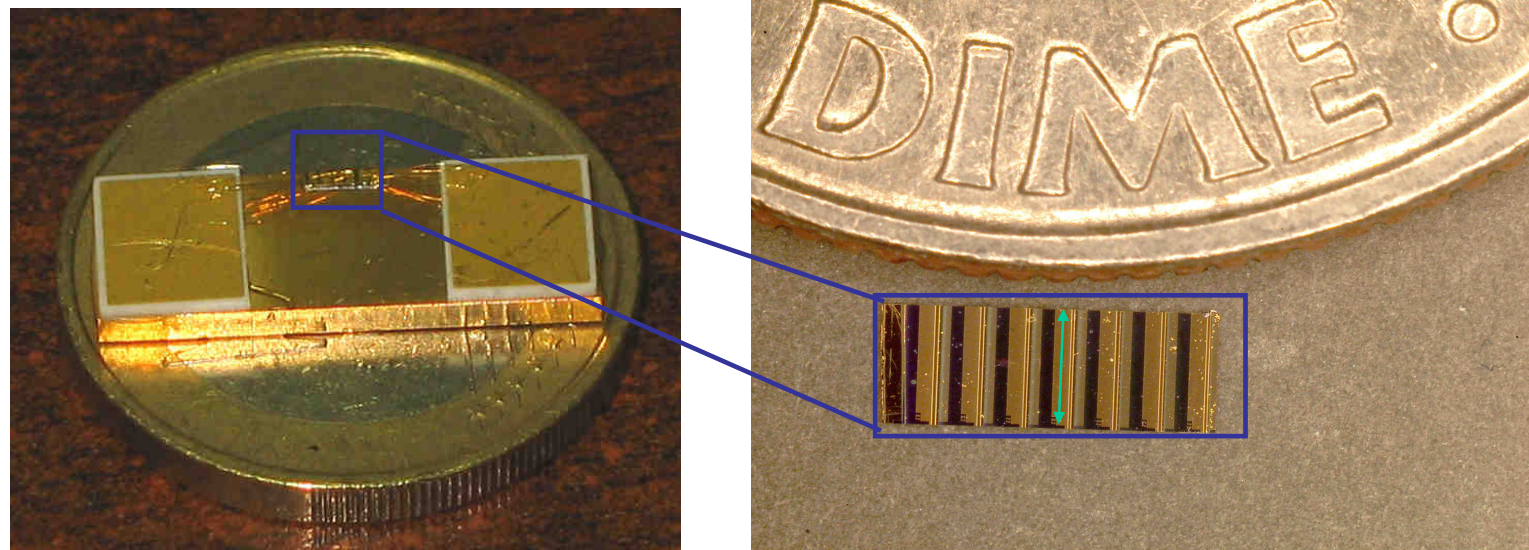
Quantum cascade laser

QCL materials: InGaAs/AlInAs on InP and GaAs/AlGaAs on GaAs

Operating λ : mid-IR ($\lambda \approx 3.5 - 24 \mu\text{m}$) and THz ($\lambda \approx 60 - 160 \mu\text{m}$)

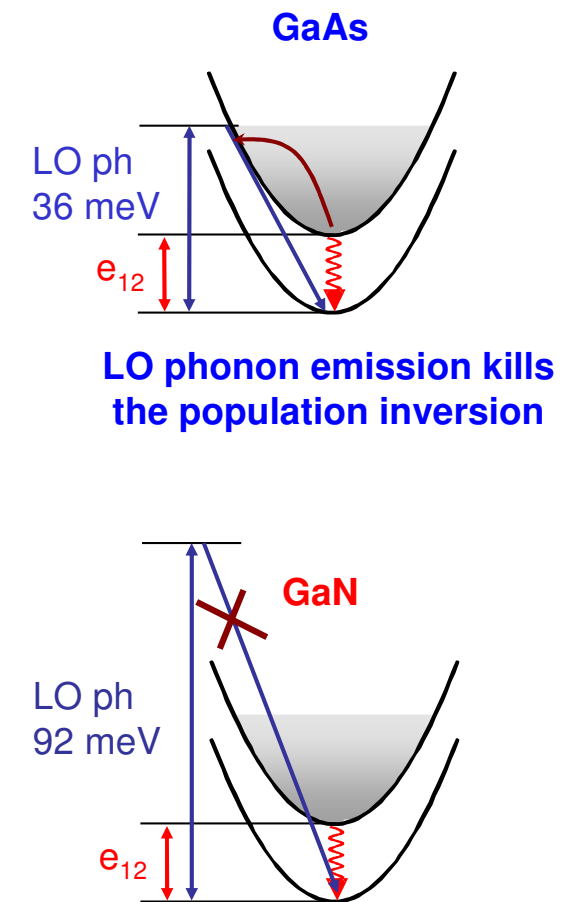
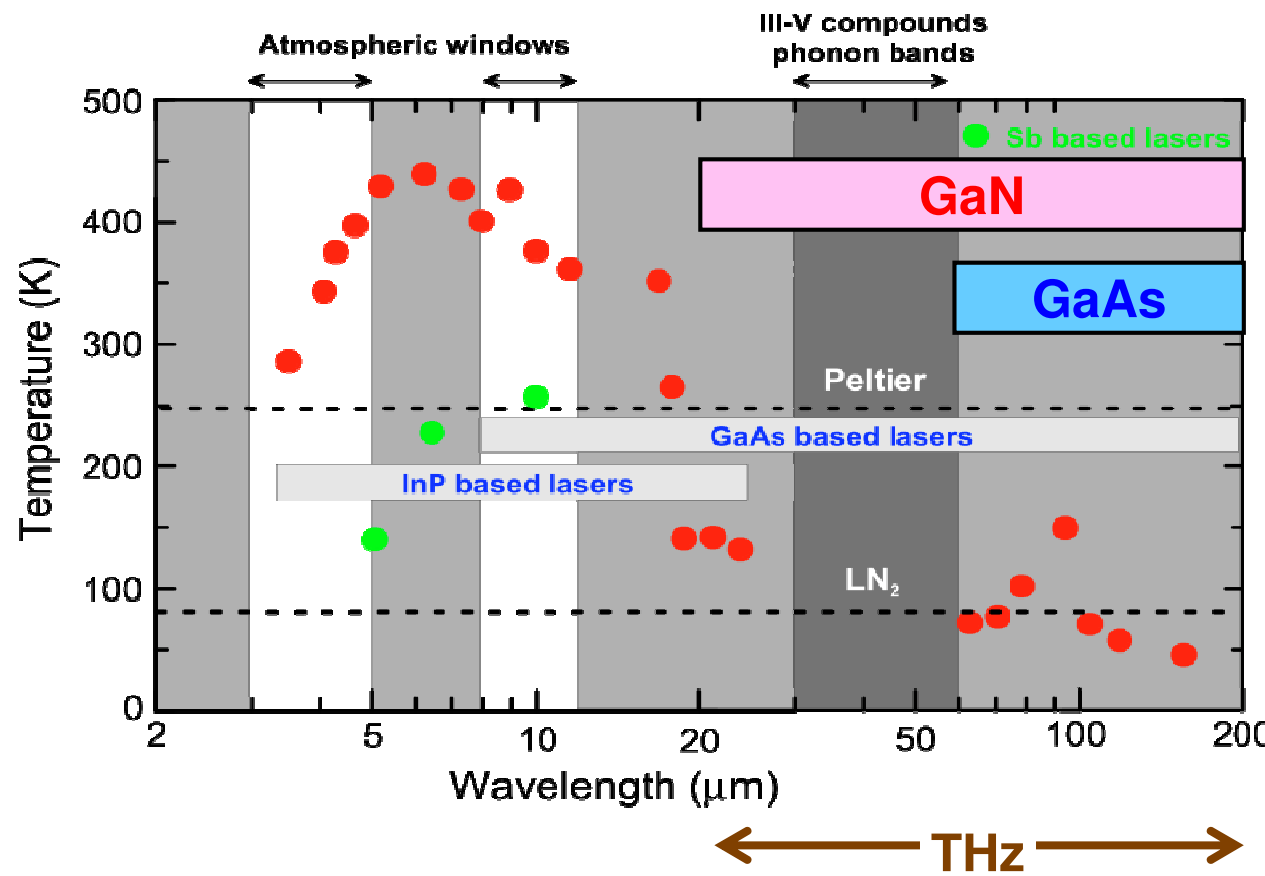


Quantum cascade lasers



Courtesy: R. Colombelli

Why GaN THz QC lasers



Taking benefit from the large LO-phonon energy

- ✓ Lasers at wavelengths inaccessible to GaAs-based QCLs
- ✓ Increase operating temperature above 300 K

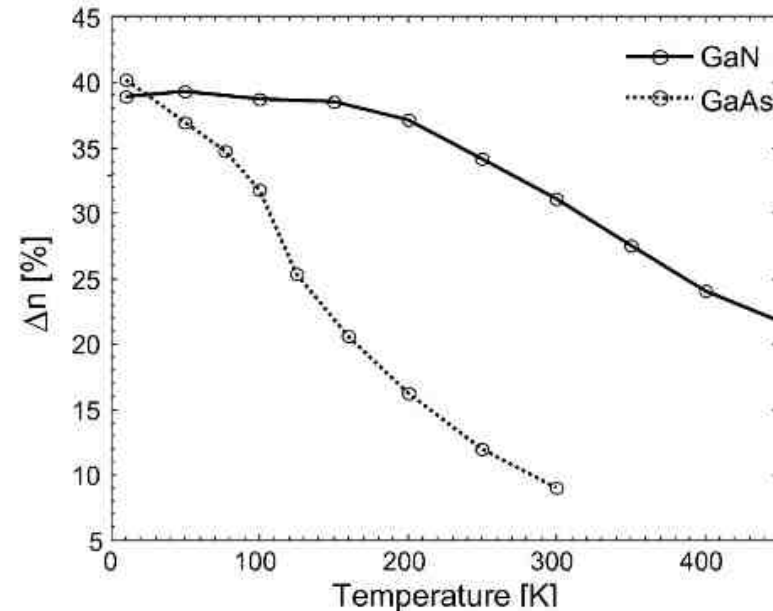
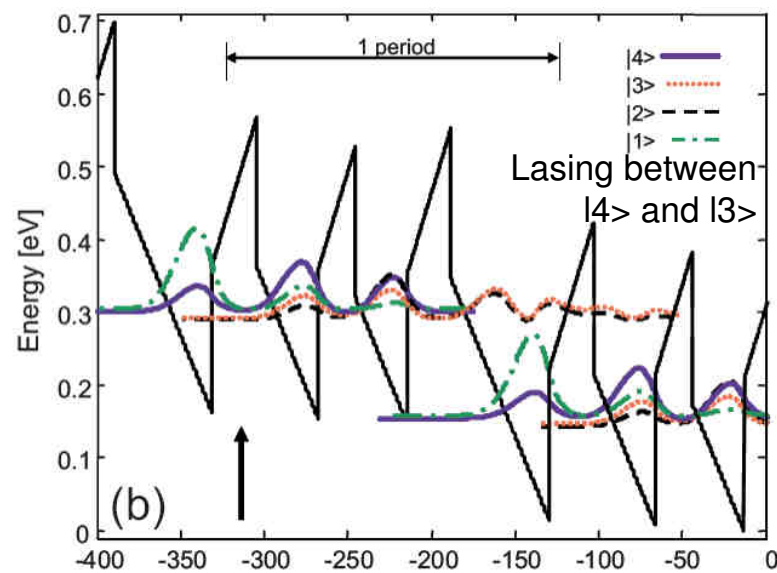
**THz QC lasers
above 300 K**

Nitride THz QCLs – theoretical proposals

Only theoretical proposals

Bellotti et al., "Monte Carlo study of GaN versus GaAs THz QCL structures", *Appl Phys Lett* 92, 101112 (2008)

Bellotti et al., "Monte Carlo simulations of THz QCL structures based on wide-bandgap semiconductors", *J. Appl Phys* 105, 113103 (2009)

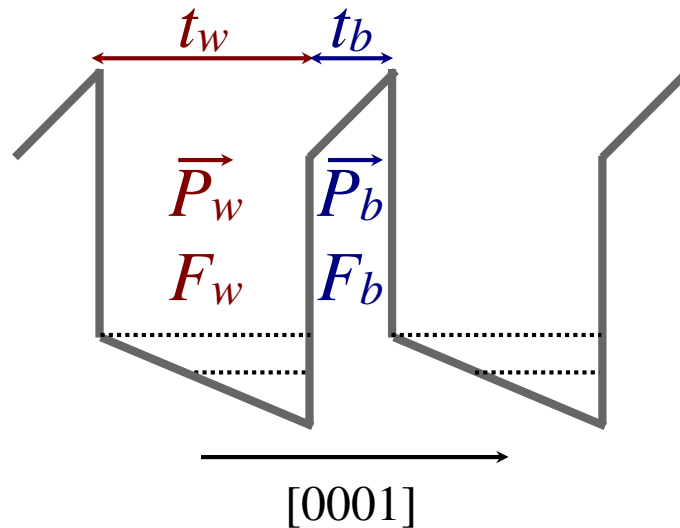


Present challenges

- ✓ to control resonant tunelling (injector fabrication)
- ✓ to tune the ISB absorption to the THz region

How to increase the ISB wavelength?

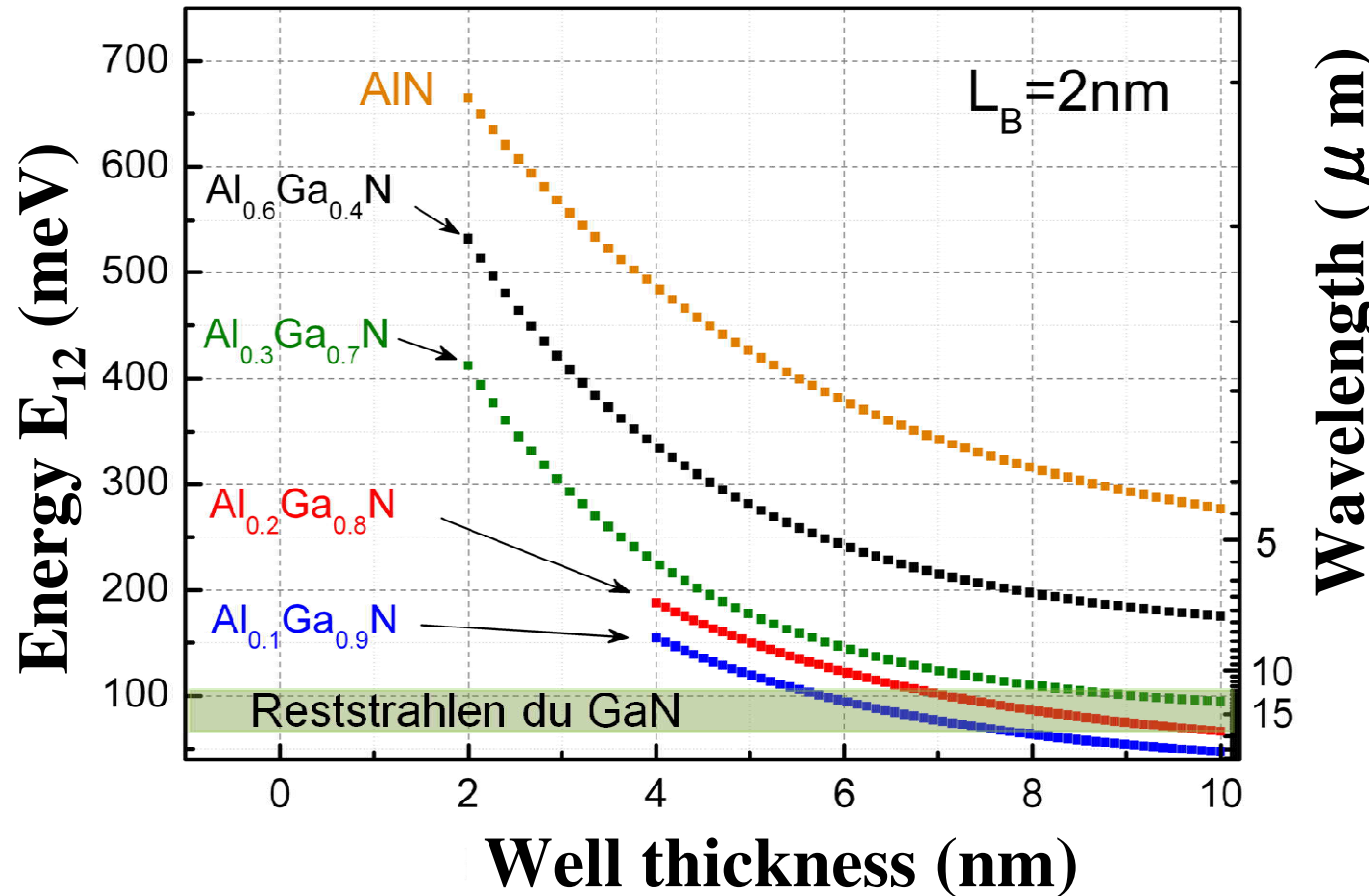
Reduce the internal electric field in the GaN well



$$\begin{aligned} F_w &= \frac{P_b - P_w}{\epsilon_0} \frac{L_b}{L_b \epsilon_w + L_w \epsilon_b} \\ F_b &= - \frac{P_b - P_w}{\epsilon_0} \frac{L_w}{L_b \epsilon_w + L_w \epsilon_b} \end{aligned}$$

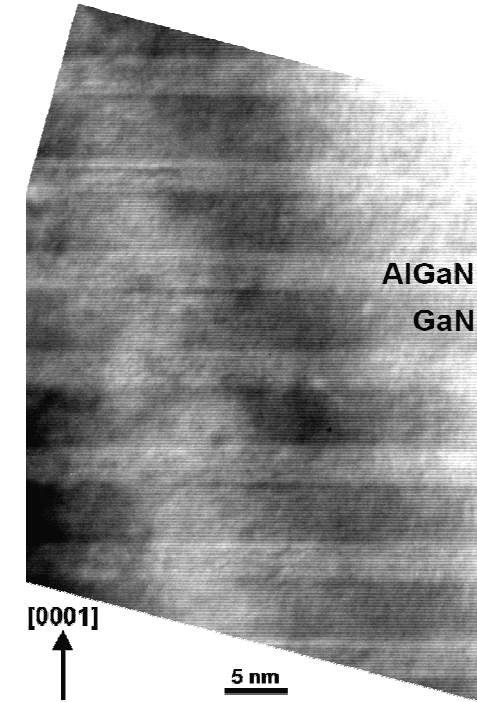
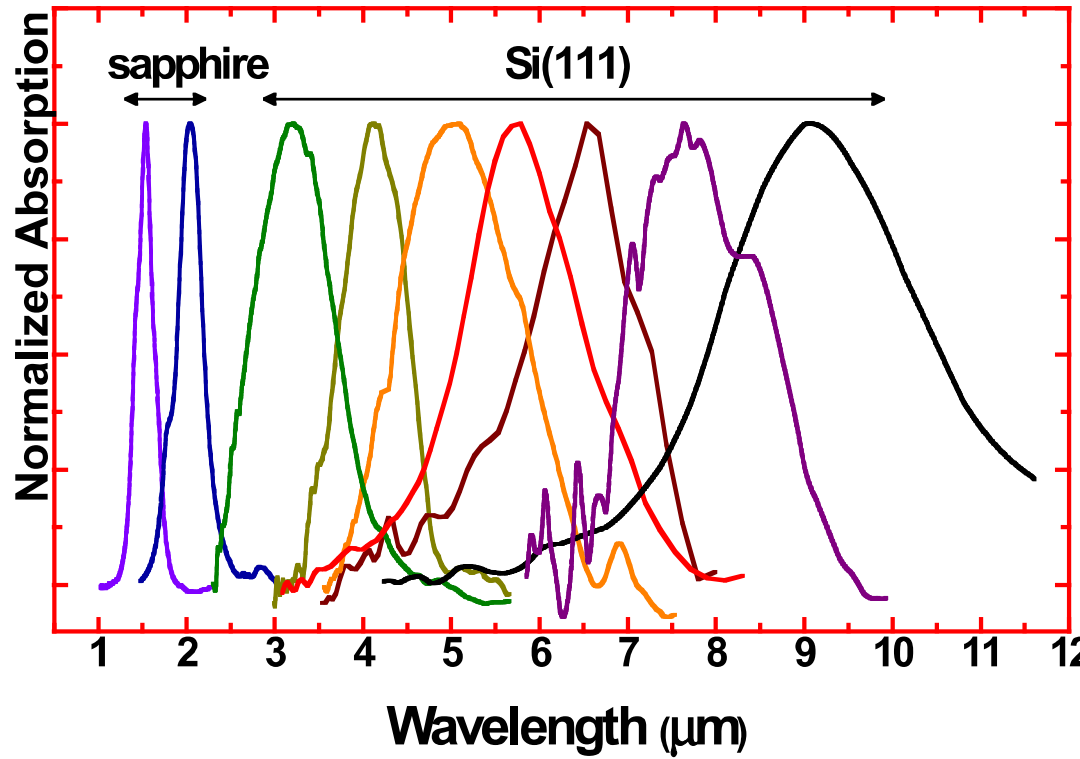
- ✓ Reducing the Aluminium content in the barrier
- ✓ Decreasing the barrier thickness
- ✓ Increasing the well thickness

Tunability in the mid-infrared spectral range



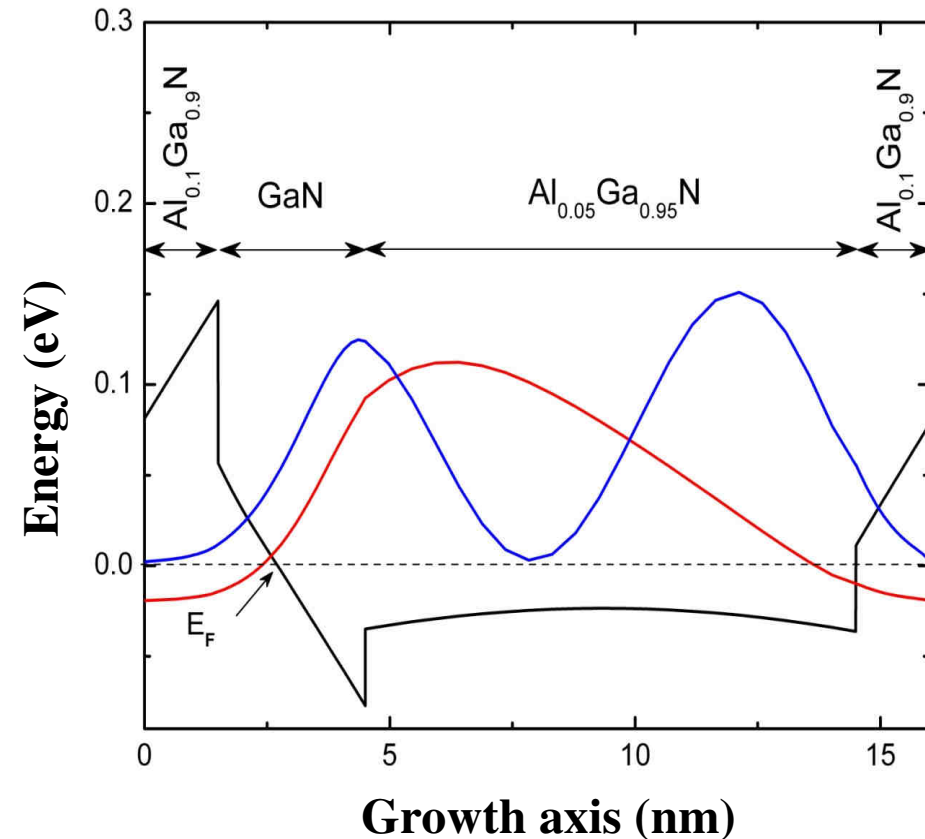
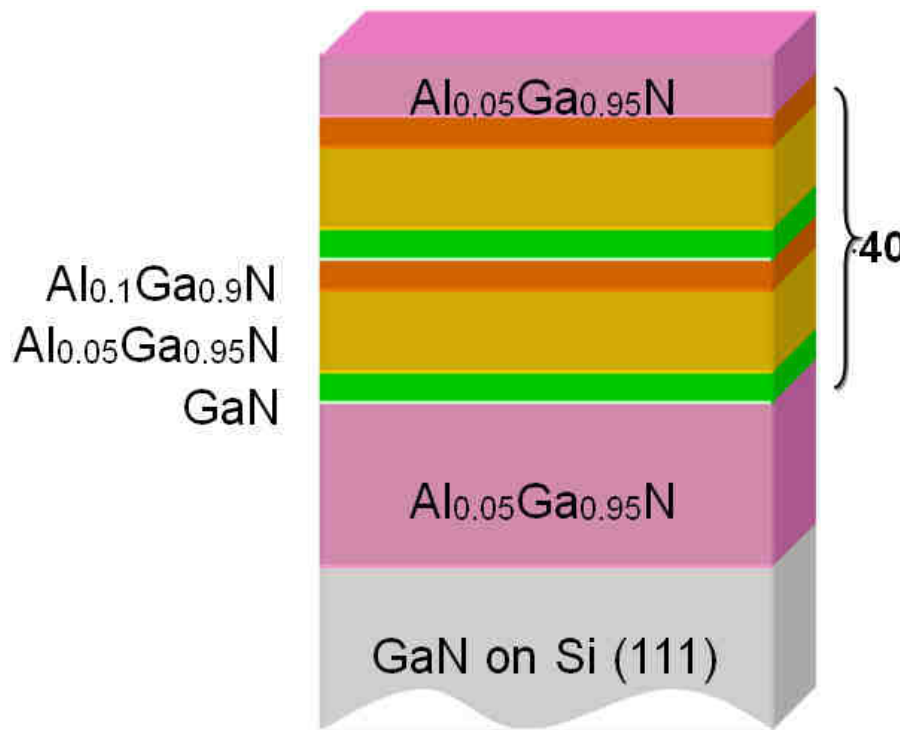
- ISB absorption can be easily tuned in the MIR
- ISB can go below the GaN Reststrahlen band for $\text{Al}_{0.1}\text{Ga}_{0.9}\text{N}/\text{GaN}$ QWs with thickness > 9 nm

MID-IR absorption in GaN/AlGaN QWs



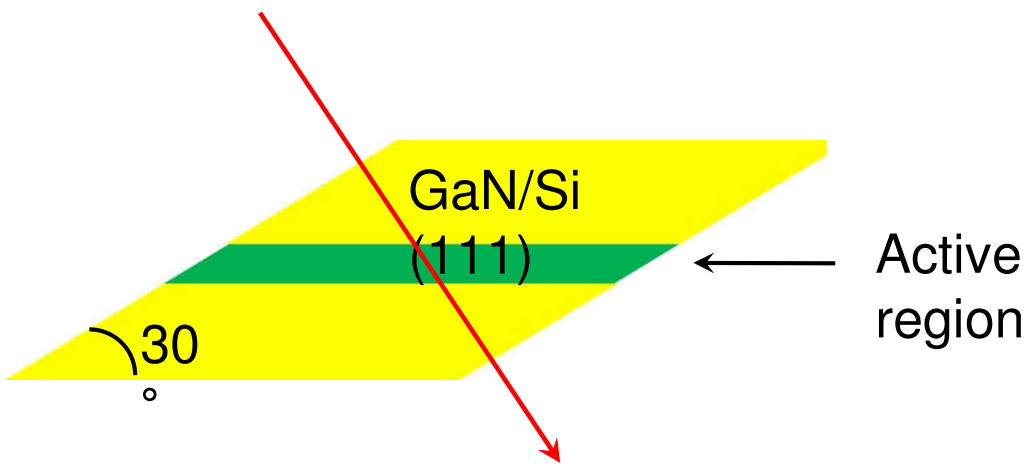
- ✓ Room-temperature ISB absorptions up to $\sim 9.5 \mu\text{m}$
- ✓ Parameters: barrier Al content (**10-100%**), barrier width ($\sim 3 \text{ nm}$)
well width (**1.5-8 nm**), doping ($1 \times 10^{19} \text{ cm}^{-3}$)

Going to far-infrared – step quantum well



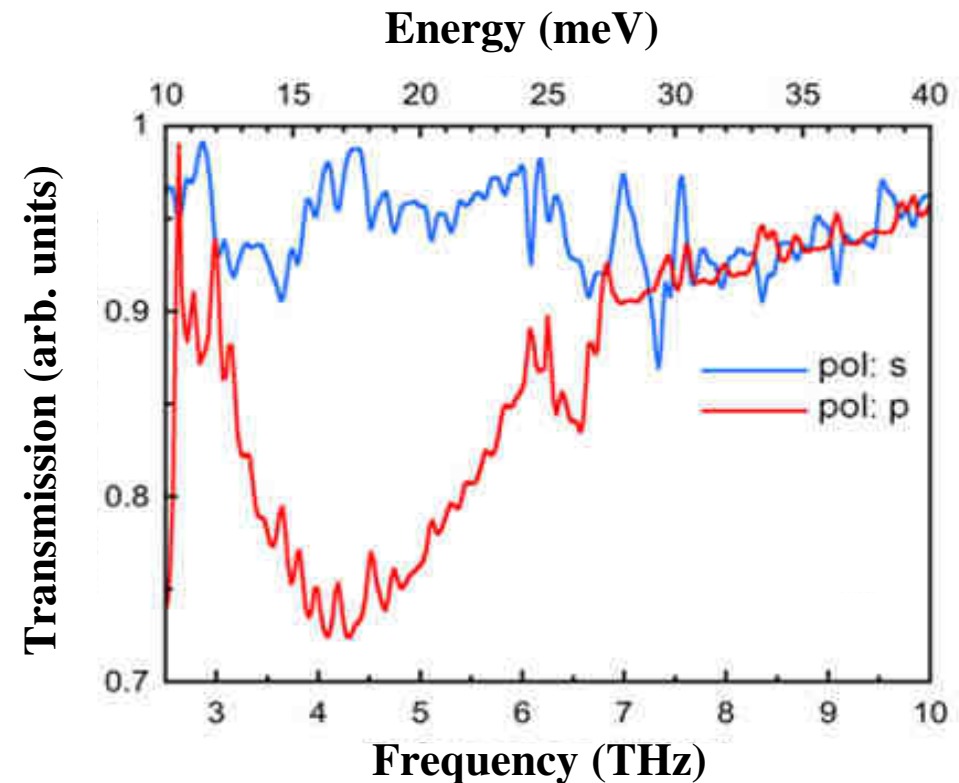
- ✓ Design of a step quantum well with an AlGaN insertion having an intermediate Al content
- ✓ Almost flat potential profile in the AlGaN step

Observation of far - IR absorption in GaN quantum wells

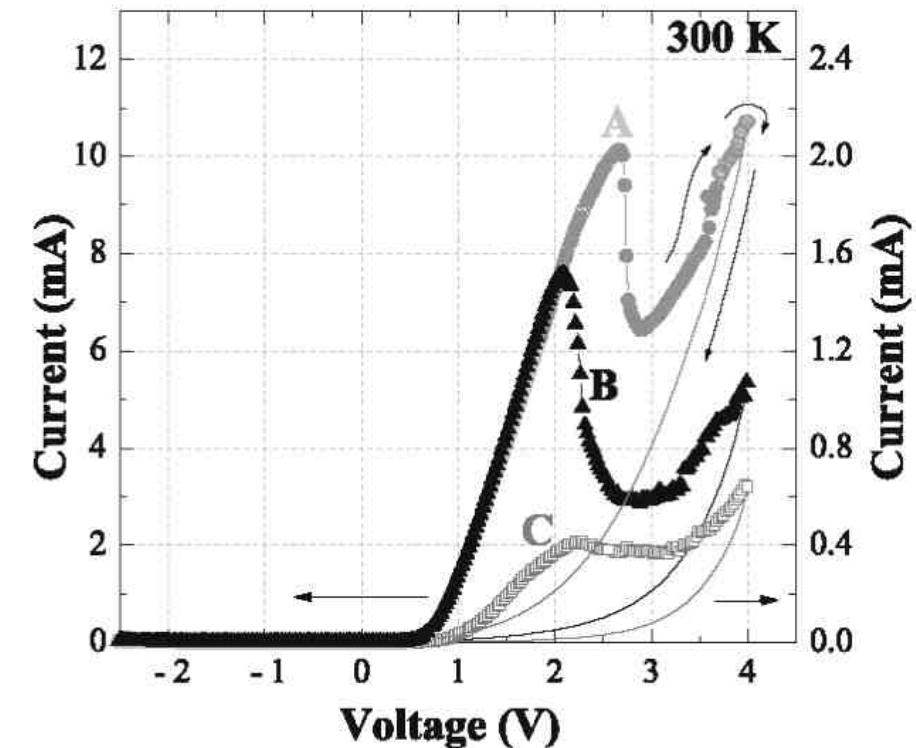
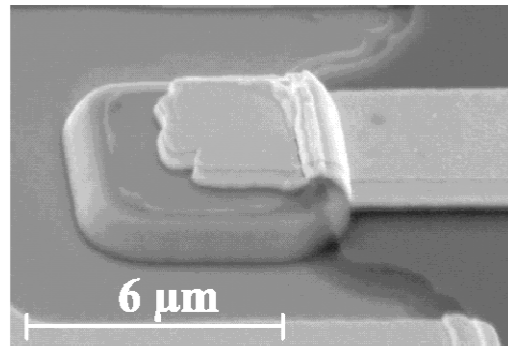
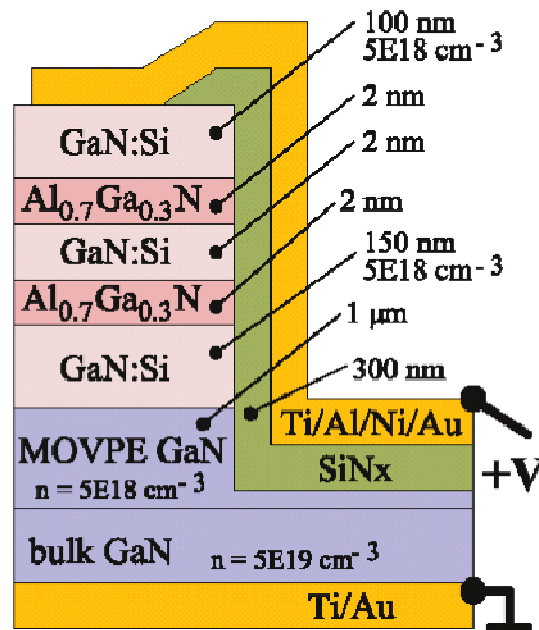


Low temperature (4K) transmission
measurements

Step 10 nm : $e_1 - e_2 = 17$ meV (4.2 THz)

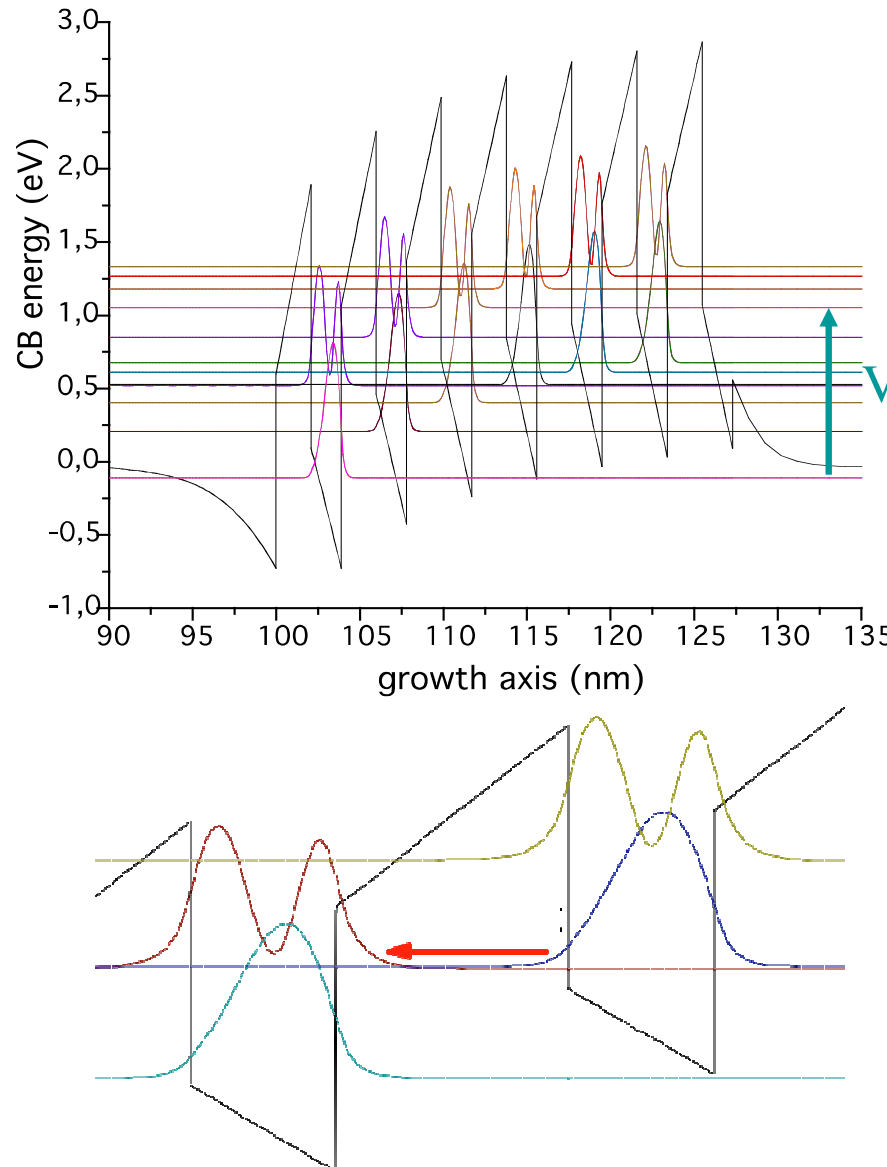


Tunneling in III-N thin film heterostructures

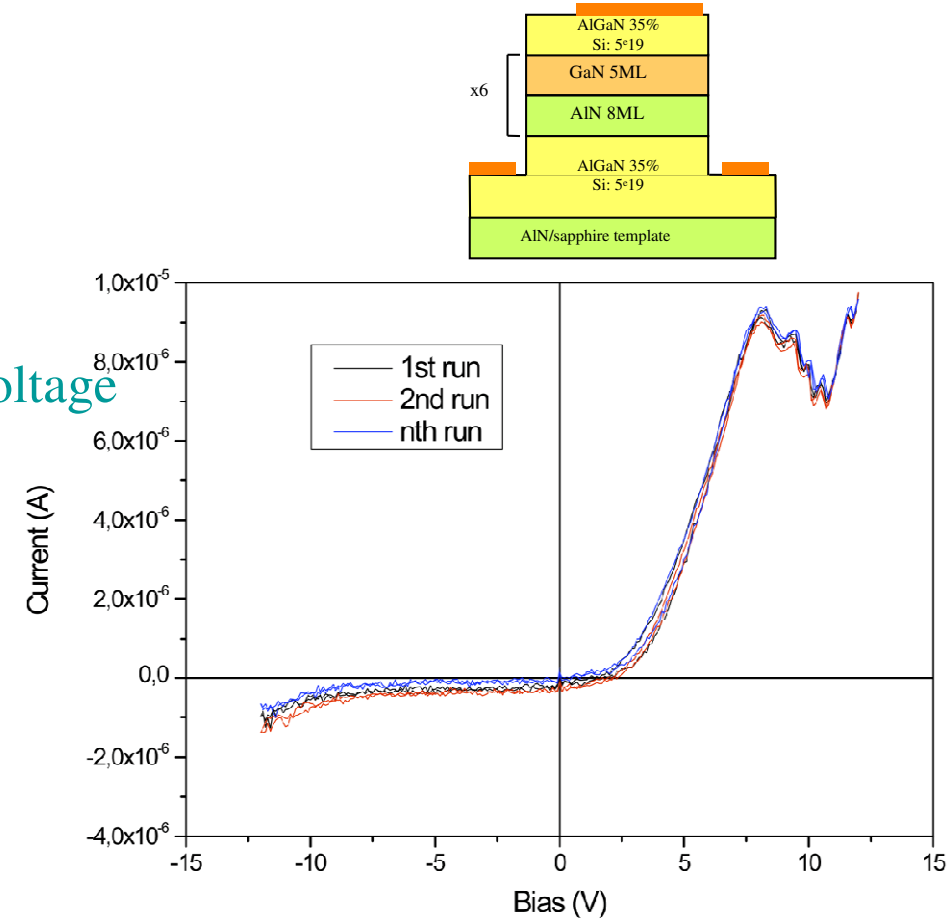


Negative differential resistance observed in I-V characteristics at 300K
But appears only once for forward bias scan
Problem of non-reproducibility attributed to material defects

Resonant tunneling in a GaN/AlN superlattice



S. Sakr et al. APEX 5, 052203 (2012)



Reproducible resonant tunneling in a
GaN/AlN superlattice
Attributed to the consecutive alignment of
e₁ and e₂ levels of adjacent QWs

Conclusions and prospects

- Nitride semiconductors present numerous advantages for near IR and THz spectral ranges
- Huge progress in crystal growth has made possible III-nitride ISB devices such as electro-optical modulators and cascade photodetectors
- Next route is to achieve ISB laser emission ... Only spontaneous emission has been observed so far
- III-nitride are expected to outperform quantum cascade lasers in the THz frequency range because of the large LO-phonon energy

Acknowledgements

- IEF:
PhDs: S. Sakr, : H. Macchadani, L. Nevou, L. Doyennette.
Post-doc: L. Rigutti, A. Bousseksou, J.R. Coudeville
Staff: F. H. Julien, E. Warde, N. Isac, A. Lupu, R. Colombelli, L. Vivien, J. Mangeney, P. Crozat.
- INAC-CEA Grenoble: P. Kandaswamy, Y. Kotsar, A. Wirtmuller, F. Guillot, I. Sarigiannidou, C. Bougerol, E. Monroy
- EPFL Lausanne, Switzerland: A. Dussaigne, E. Giraud, N. Grandjean
- Technion Institute, Israel: A. Vardi, G. Bahir
- Technische Universität Wien, Austria: G. Pozzovivo, G. Strasser
- IKZ Berlin: M. Albrecht

This work was supported by European FP7 IST Fet-Open program “Unitride” under grant agreement #233950